Université de Montréal

Characterization of Carotid Plaques with Ultrasound Non-Invasive Vascular Elastography (NIVE): Feasibility and Correlation with High-Resolution Magnetic Resonance Imaging

par

Cyrille Naïm

Programme de Sciences biomédicales

Faculté de médecine

Mémoire présenté à la Faculté de médecine

en vue de l'obtention du grade de

Maîtrise en Sciences biomédicales, option recherche

Mars, 2013

Université de Montréal
Faculté des études supérieures et postdoctorales

Ce mémoire intitulé :

Characterization of Carotid Plaques with Ultrasound Non-Invasive Vascular Elastography (NIVE): Feasibility and Correlation with High-Resolution Magnetic Resonance Imaging

présenté par :
Cyrille Naïm

a été évalué par un jury composé des personnes suivantes :

Alain Rivard, président-rapporteur
Gilles Soulez, directeur de recherche
Guy Cloutier, co-directeur
Oury Monchi, membre du jury

RÉSUMÉ

L'accident vasculaire cérébral (AVC) est une cause principale de décès et de morbidité dans le monde; une bonne partie des AVC est causée par la plaque d'athérosclérose carotidienne. La prévention de l'AVC chez les patients ayant une plaque carotidienne demeure controversée, vu les risques et bénéfices ambigus associés au traitement chirurgical ou médical. Plusieurs méthodes d'imagerie ont été développées afin d'étudier la plaque vulnérable (dont le risque est élevé), mais aucune n'est suffisamment validée ou accessible pour permettre une utilisation comme outil de dépistage. L'élastographie non-invasive vasculaire (NIVE) est une technique nouvelle qui cartographie les déformations (élasticité) de la plaque afin de détecter les plaque vulnérables; cette technique n'est pas encore validée cliniquement. Le but de ce projet est d'évaluer la capacité de NIVE de caractériser la composition de la plaque et sa vulnérabilité in vivo chez des patients ayant des plaques sévères carotidiennes, en utilisant comme étalon de référence, l'imagerie par résonance magnétique (IRM) à haute-résolution. Afin de poursuivre cette étude, une connaissance accrue de l'AVC, l'athérosclérose, la plaque vulnérable, ainsi que des techniques actuelles d'imagerie de la plaque carotidienne, est requise.

Trente-et-un sujets ont été examinés par NIVE par ultrasonographie et IRM à haute-résolution. Sur 31 plaques, 9 étaient symptomatiques, 17 contenaient des lipides, et 7 étaient vulnérables selon l'IRM. Les déformations étaient significativement plus petites chez les plaques contenant des lipides, avec une sensibilité élevée et une spécificité modérée. Une association quadratique entre la déformation et la quantité de lipide a été trouvée. Les déformations ne pouvaient pas distinguer les plaques vulnérables ou symptomatiques.

En conclusion, NIVE par ultrasonographie est faisable chez des patients ayant des sténoses carotidiennes significatives et peut détecter la présence d'un cœur

lipidique. Des études supplémentaires de progression de la plaque avec NIVE sont requises afin d'identifier les plaques vulnérables.

Mots-clés : Accident vasculaire cérébral (AVC), Plaque de l'artère carotidienne, Plaque d'athérosclérose, Élastographie, Ultrasonographie, Élastographie Non-invasive Vasculaire (NIVE), Imagerie par résonance magnétique (IRM), cœur lipidique.

ABSTRACT

Stroke is a leading cause of death and morbidity worldwide, and a significant proportion of strokes are caused by carotid atherosclerotic plaque rupture. Prevention of stroke in patients with carotid plaque poses a significant challenge to physicians, as risks and benefits of surgical or medical treatments remain equivocal. Many imaging techniques have been developed to identify and study vulnerable (high-risk) atherosclerotic plaques, but none is sufficiently validated or accessible for population screening. Non-invasive vascular elastography (NIVE) is a novel ultrasonic technique that maps carotid plaque strain (elasticity) characteristics to detect its vulnerability; it has not been clinically validated yet. The goal of this project is to evaluate the ability of ultrasound NIVE strain analysis to characterize carotid plaque composition and vulnerability in vivo in patients with significant plaque burden, as determined by the reference standard, high resolution MRI. To undertake this study, a thorough understanding of stroke, atherosclerosis, vulnerable plaque, and current non-invasive carotid plaque imaging techniques is required.

Thirty-one subjects underwent NIVE and high-resolution MRI of internal carotid arteries. Of 31 plaques, 9 were symptomatic, 17 contained lipid and 7 were vulnerable on MRI. Strains were significantly lower in plaques containing a lipid core compared to those without lipid, with high sensitivity and moderate specificity. A quadratic fit was found between strain and lipid content. Strains did not discriminate symptomatic patients or vulnerable plaques.

In conclusion, ultrasound NIVE is feasible in patients with significant carotid stenosis and can detect the presence of a lipid core. Further studies of plaque progression with NIVE are required to identify vulnerable plaques.

Keywords: Stroke, Carotid Artery Plaque, Atherosclerotic Plaque, Elastography, Ultrasound, Non-Invasive Vascular Elastography (NIVE), Magnetic Resonance Imaging (MRI), lipid core.

TABLE OF CONTENTS

LIST OF TABLES

LIST OF FIGURES

images adapted from: Chen, Pope and Ott. Basic Radiology, 2nd edition, Chapter 12.

Figure 1.10: CT scan of a cerebral infarction in a 56 year old hypertensive and diabetic male who presented with left hemiparesis in the emergency department. A and B. Axial CT at 2 different levels without contrast injection showing a well-defined hypodense area in the right MCA territory (between white arrows) and a mass effect on the surrounding brain tissue (compression of right ventricle). The right MCA is brighter than the left (large white arrow head on B) and corresponds to an occluding thrombus. C. A 3-D volume rendering CT angiogram shows the occlusion in the superior branch of the right MCA. D. Axial CT with contrast injection shows decreased filling of blood vessels in the right MCA territory (between white arrows) compared to the left (black arrows). Images adapted from: Chen, Pope and Ott. Basic Radiology, 2nd edition, Chapter 12.

Figure 1.11: Axial CT scan without contrast of a 68 year old hypertensive female who was found unresponsive. There is a large bright (hyperdense) area consistent with hemorrhage in the right basal ganglia (black arrow), mass effect (small white arrows), bleeding into the ventricles (arrowheads), and entrapment of the left ventricle (large white arrow). This bleed is probably due to a vascular defect induced by chronic hypertension. Thrombolysis is contra-indicated, and immediate neurosurgical consultation is required for surgical decompression. Image adapted from: Chen, Pope and Ott. Basic Radiology, 2nd edition, Chapter 12.

Figure 1.12: Axial MR images of the patient with right MCA territory infarction shown in Figure 1.10. Images are at the same anatomic level. A. DWI demonstrating restricted movement of water in the infarcted area (increased signal intensity between white arrows). B. T2-weighted image demonstrating area of hyperintensity and

axial strain is obtained from the strain difference between two consecutive image frames, thus representing the variation of mean axial strain over time. Peak systolic compression is denoted by red circles. Mean Strain at Peak Systolic Compression (MSPSC) is the average of these peak values over the number of cardiac cycles. Dotted vertical lines represent end-diastole, estimated from B-mode videos and M-mode images. (c) Strain Rate is the slope of the instantaneous strain in (b). Maximum Strain Rate (MaxSR) is the mean of the greatest strain rate occurring at end-diastole (green circles). Minimum Strain Rate (MinSR) is the mean of the lowest strain rate, occurring at the onset of diastole (purple circles). In other words, MaxSR represents greatest tissue compression over time, and MinSR represents greatest tissue dilation over time, which explains why MinSR is a negative value. (d) A graph of cumulated mean axial strains is derived from (b). Double-sided blue arrows represent strain amplitude for each cardiac cycle. Mean Strain Amplitude (MSA) is the average of these three amplitudes. The peak of the third cardiac cycle corresponds to the elastogram in (a).

Figure 4.3: High-resolution MRI of the left internal carotid artery plaque of a 65 year old man who presented with a left hemispheric stroke (axial view). This is a vulnerable-appearing lipid-rich hemorrhagic plaque. The external and internal carotid arteries are indicated with a white and black arrow, respectively. The segmentation using the QPlaque software is shown superimposed on the T1-weighted image (framed inset at the center). The green and red contours designate the outer and inner vascular wall contours of the internal carotid artery. Yellow represents lipid, pink represents hemorrhage, and purple represents inflammation. T1W = T1-weighted; T2W = T2-weighted; PDW = Proton Density-weighted; T1WC+ = T1-weighted post-contrast injection.

LIST OF ABBREVIATIONS

%Calcium volume, calcium percentage of total plaque volume
%Lipid volume, lipid percentage of total plaque volume
2D, two-dimensional
3D, three-dimensional
ACA, anterior cerebral artery
ACAS, Asymptomatic Carotid Artery Trial
ACE-inhibitors, angiotensin-converting-enzyme inhibitors,
ACST, Asymptomatic Carotid Stenosis Trial
ANS, Autonomic nervous system
ARBs, angiotensin II receptor blockers
ARFI, acoustic radiation force imaging
ARIC, Atherosclerosis Risk in Communities
ATP, adenosine triphosphate
AVC, Accident Vasculaire Cérébral
CAT, computed axial tomography
CBC, complete blood count
CCA, common carotid artery
CEA, Carotid Endarterectomy
CEUS, contrast-enhanced ultrasound
CHD, coronary heart disease
CI, confidence interval
CNR, contrast-to-noise ratio
CNS, Central nervous system
cont'd, continued
CRP, C-reactive protein
CT, computed tomography
CTA, computed tomography angiography
CVA, Cerebrovascular accident

dBP, diastolic blood pressure

DWI, Diffusion-Weighted Imaging

E, Young's elastic modulus

ECG, electrocardiogram

ECM, extracellular matrix

ECST, European Carotid Surgery Trial

FGF, Fibroblast growth factor

GSM, gray-scale median

HDL, high-density lipoprotein

HU, Hounsfield unit

Hz, Hertz

IBS, integrated backscatter

ICA, internal carotid artery (ICA)

ICC, intraclass correlation coefficient

ICP, intracranial pressure

IPH, intraplaque hemorrhage

IRM, Image par résonance magnétique

IVUS, intravascular ultrasound

LDL, low-density lipoprotein

LSME, Lagrangian Speckle Model Estimator

MaxSR, Maximal Strain Rate

MCA, middle cerebral artery

M-CSF, macrophage colony-stimulating factors

MDCTA, multidetector computed tomography angiography

MHz, megahertz

MinSR, Minimal Strain Rate

MMP, matrix metalloproteinase

MR, magnetic resonance

MRA, magnetic resonance angiography

MRI, Magnetic Resonance Imaging

MSA, Mean Strain Amplitude

msec, millisecond

MSPSC, Mean Strain at Peak Systolic Compression

n, number (as in number of subjects or number in sample population)

NASCET, North American Symptomatic Carotid Endarterectomy Trial

NIHSS, National Institutes of Health Stroke Scale

NIVE, Non-Invasive Vascular Elastography

PDA, pixel distribution analysis

PDGF, Platelet-derived growth factor

PDW, proton density-weighted

PET, positron-emission tomography

PNS, Peripheral nervous system

Post. Comm., posterior communicating artery

PW, pulse wave

r, Pearson correlation coefficient

RBANS, Repeatable Battery for the Assessment of Neuropsychology Status

RF, radiofrequency

ROC curve, Receiver Operating Characteristic curve

ROI, region of interest

RR, relative risk

$r_{s,}$ Spearman correlation coefficient

rSI, relative signal intensity

sBP, systolic blood pressure

SD, standard deviation

SMC, smooth muscle cell

SNR, signal-to-noise ratio

SSWI, supersonic shear wave imaging

T, Tesla

T1W, T1-weighted

T2W, T2-weighted

TGF-β, Transforming growth factor Beta

TIA, transient ischemic attack

TOF, Time-of-Flight

US, Ultrasound

USPIO, ultra small superparamagnetic iron oxide

VCAM-1, ICAM, Vascular and Intercellular adhesion molecules

VP, vulnerable plaque

VWV, vessel wall volume

z, acoustic impedance

Ce n'est pas l'espèce la plus forte qui survit, ni la plus intelligente, mais bien celle qui s'adapte le mieux au changement

Charles Darwin

Advance, and never halt, for advancing is perfection.

Gibran Khalil Gibran

À ma mère, mon père, et mes deux frères

À mon khalou Richou

ACKNOWLEDGEMENTS

Je tiens tout d'abord à remercier Gilles Soulez pour m'avoir offert cette opportunité inégalée de travailler avec son équipe sur ce projet innovateur. Sa disponibilité, son empathie, et ses grandes qualités d'académicien m'ont guidée et permis de terminer ce travail avec succès. Il a été un mentor pour moi, et n'a jamais cessé de m'encourager et de croire en ma persévérance; je lui serai, pour toujours, sincèrement reconnaissante. Je remercie Guy Cloutier pour m'avoir accueillie au LBUM. Par sa rigueur scientifique et sa pédagogie, il a guidé notre équipe d'élastographie quasi-statique et m'a aidée à réaliser le travail présenté dans ce mémoire. Je souhaite également remercier Dr. Soulez et Dr. Cloutier pour m'avoir soutenue avec de nombreuses lettres de références et pour m'avoir accordé le temps nécessaire à mes études et applications aux études médicales post-doctorales. Leur soutien a porté fruit et a contribué à la poursuite de mon rêve de devenir radiologiste.

Merci à Elizabeth Mercure et Zhao Qin, collègues d'une gentillesse infinie, qui ont travaillé méticuleusement à l'obtention d'élastogrammes et qui sont demeurées disponibles pour répondre à mes nombreuses questions. Merci à Hasti « joon », mon amie proche depuis mes débuts au CRCHUM-LBUM, qui m'a encouragée à persévérer et avec qui j'ai passé de nombreux bons moments. Merci à tous les membres du LBUM et du département de recherche en radiologie pour leur support, travail d'équipe, et leur sourire quotidien. Je souhaite associer à ces remerciements Dr. Marie-France Giroux, Dr. François Guilbert, Andrée Cliche, Walid El-Abyad, Louise Allard, Danielle Blain, Claude Kaufman, Sofiane Hadjaj, Emmanuel Montagnon, Jonathan Porée, Julien Tripette, Stephan Muth, Boris Chayer, Marie-Hélène Roy-Cardinal, François Destrempes, Ali Traore, Cédric Schmitt, Anis Hadj Henni, et tous les étudiants et chercheurs que j'ai cotoyés. Ce fut vraiment agréable de travailler avec vous tous. Je tiens particulièrement à témoigner ma gratitude au Dr. Alain Rivard, qui a m'a fait l'honneur de présider le jury d'évaluation de mon

mémoire, et au Dr. Oury Monchi, qui a accepté d'être membre évaluateur du jury.

Je suis reconnaissante au CRCHUM, au programme de Sciences biomédicales de l'Université de Montréal, et à l'Association Canadienne de Radiologistes pour avoir valorisé mon travail en me décernant des bourses d'études de maîtrise et de recherche.

Un remerciement spécial à mes parents d'avoir mis tout le temps et l'énergie nécessaire à mon éducation, depuis mon enfance jusqu'à aujourd'hui, et sans qui je n'aurais pas pu poursuivre mes ambitions avec succès. Chaque jour je réalise combien ils ont donné par amour pour mes frères et moi afin que nous réussissions nos projets avec succès. Particulièrement, je remercie ma mère pour m'avoir écoutée et gâtée avec des repas équilibrés, mon père pour avoir été patient, travaillant et toujours à l'écoute, ainsi que mes frères, dont je me suis rapprochée énormément depuis les trois dernières années.

Enfin, je remercie le Bon Dieu pour chaque événement, heureux et malheureux, ainsi que pour chaque personne que j'ai rencontrée dans ma vie. Toutes ces expériences continuent d'accroître ma sagesse, mon bonheur, et m'enseignent, à mon tour, à soutenir les autres.

Section I

Clinical Perspectives on Ischemic Stroke and Carotid Atherosclerosis

CHAPTER 1

Stroke, a Cerebrovascular Disease

1. Stroke, a Cerebrovascular Disease

1.1. *Background*

Cerebrovascular disease is a term that designates a wide spectrum of disorders of the arterial and venous circulations of the central nervous system, including ischemic stroke, hemorrhagic stroke, and other cerebrovascular anomalies. A stroke, also called cerebrovascular accident (CVA), is a clinical syndrome[1] characterized by the abrupt onset of a focal neurological deficit due to either inadequate blood flow (i.e. ischemia) or hemorrhage in the brain. Stroke is a major cause of mortality and morbidity worldwide, and it is frequently devastating for both the patient and family. Generally, there are two types of stroke: ischemic and hemorrhagic, accounting for 87% and 13% of all strokes, respectively [1].

This chapter will focus on understanding the clinical and pathological aspects of ischemic stroke and will provide a brief overview of hemorrhagic stroke. Current issues associated with ischemic stroke will be described, and the premise and objectives of the present research project will be explained.

1.2. *Anatomy and Physiology*

The human nervous system is divided into three specialized sub-systems. The central nervous system (CNS) consists of the brain and spinal cord; it functions to initiate decisions and coordinate actions. The peripheral nervous system (PNS) consists of neurons coming out from the CNS; it is responsible for

[1] Syndrome: a group of signs and symptoms that occur together and characterize a particular abnormality, such as a disease, psychological disorder, or other abnormal physiological condition. A syndrome is not synonymous with disease but merely describes a constellation of symptoms that may characterize a disease.

executing functions dictated by the brain in muscles and relaying sensory information from the skin back to the brain. Finally, the autonomic nervous system (ANS) consists of nerve cells overlapping in location between the CNS and PNS, and controls subconscious bodily functions such as blood pressure, heart rate and digestion.

The brain alone contains close to 100 billion nerve cells [2]. It is responsible for motor function, sensory perception, autonomic regulation, memory, learning, language, emotions, and thoughts, to name only a few. Hence, the brain is central to all bodily functions of the nervous system. Brain anatomy is complex and beyond the scope of this thesis, but a very basic knowledge of anatomy is provided here to help understand the clinical aspects of ischemic stroke.

The brain is divided into three main parts: cerebrum, cerebellum and brainstem (figure 1.1). The cerebrum consists of two cerebral hemispheres of folded tissue called cortex, each divided into 4 lobes that serve distinct functions. The cerebellum has a similar structure to the cerebrum, but is smaller. The brainstem is covered by the cerebral hemispheres, and extends inferiorly to become the spinal cord.

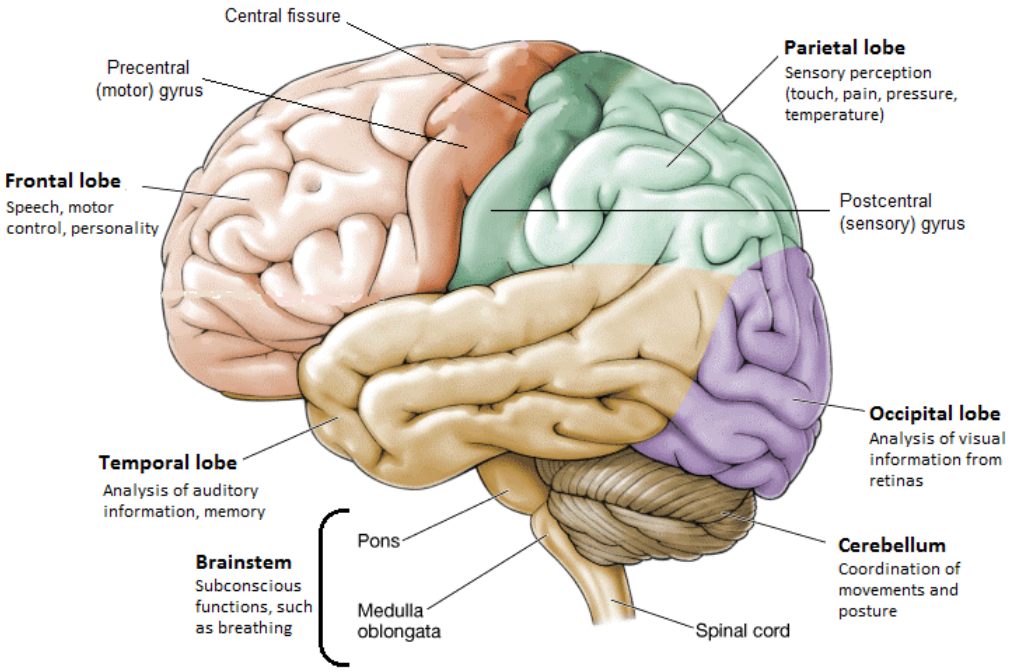

Figure 1.1: Left lateral view of the brain. Each part of the brain identified serves a specific function. Adapted and modified from: Morton DA, Foreman KB, Albertine KH. *The Big Picture: Gross Anatomy*, 1st edition: www.accessmedicine.com

Despite the extraordinary power of the brain, it is extremely fragile. Neuronal cells of the brain do not readily repair or regenerate after an injury or cell death. Therefore, a brain injury is often very serious with permanent sequelae, such as paralysis, cognitive changes, coma, and even death. Protection of the brain from external insults is provided by the skull, meninges[2], and head gear for certain sports activities. On the other hand, function and survival of neuronal cells depends on a good and constant blood supply of oxygen and glucose, provided by 15 to 20% of the total cardiac output[3] at rest and an effective networking of cerebral arteries, namely the Circle of Willis.

[2] Meninges are layers of connective tissue that surround the brain, underneath the skull.

[3] Cardiac Output is the amount of blood coming out of the heart per minute (mL/min). Cardiac Output = Heart Rate X Stroke Volume.

There are two main arterial supplies to the brain: the internal carotid artery and the vertebral artery (Figure 1.2). Two internal carotid arteries supply the anterior circulation of the brain, and two vertebral arteries supply the posterior circulation of the brain. The internal carotid artery (ICA) branches into the anterior cerebral artery (ACA), the middle cerebral artery (MCA), and the ophthalmic artery which supplies the retina. The vertebral arteries join to form the basilar artery, which further divides into two posterior cerebral arteries (PCA). Hence, three major pairs of arteries supply the cerebral hemispheres: ACA, MCA, and PCA. The anterior and posterior circulations are connected through communicating arteries of the Circle of Willis. Anatomy of these vessels is shown on figures 1.2 and 1.7.

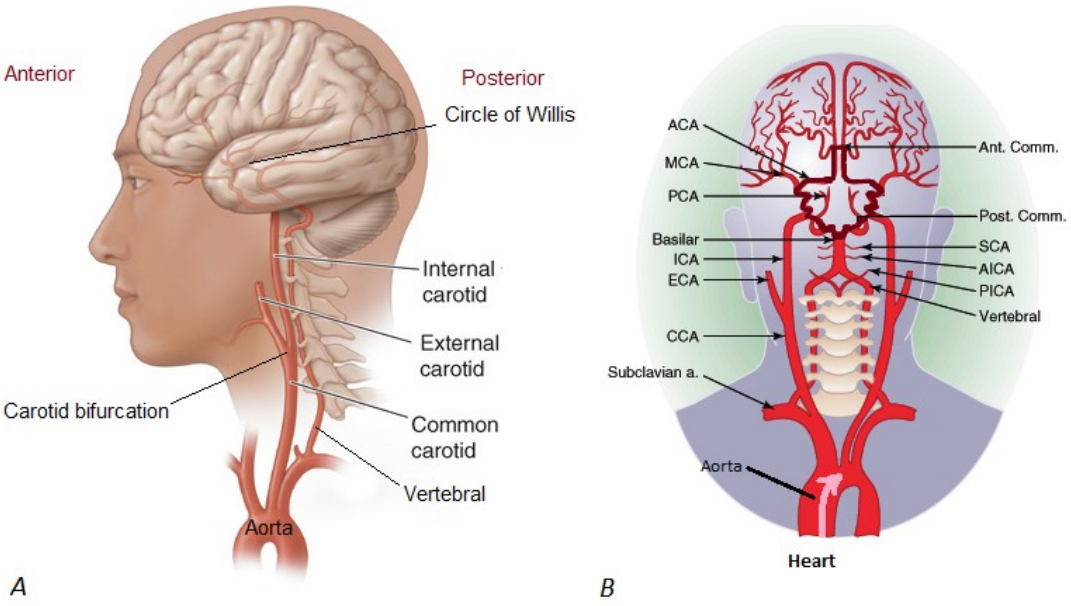

Figure 1.2: A. Lateral and B. coronal views of extracranial and intracranial[4] arteries. A: The common carotid artery bifurcates into the external and internal carotid artery. The external carotid supplies blood to the face. The internal carotid supplies the anterior part of the brain. The vertebral artery arises from the subclavian artery, and supplies the posterior part of the brain. *B*: The anterior and posterior circulations are linked through the posterior communicating artery (Post. Comm.), forming the Circle of Willis

[4] Extracranial: outside of the bony skull; Intracranial = inside the bony skull. The brain is intracranial.

(highlighted in dark red). This architecture provides collateral circulation of blood in case of obstruction in one of the major intracranial arteries. The pink arrow demonstrates the direction of blood flow arising from the heart. ACA = Anterior cerebral artery; Ant. Comm.= Anterior communicating artery; MCA = Middle cerebral artery; PCA = Posterior cerebral artery; ICA = Internal carotid artery; ECA = External carotid artery; CCA = Common carotid artery; SCA = Superior cerebellar artery; AICA = Anterior Inferior cerebellar artery; PICA = Posterior inferior cerebellar artery; a.= artery. Figure 1.2A adapted and modified from Longo DL, Fauci AS, Kasper DL, Hauser SL, Jameson JL, Loscalzo J. *Harrison's Principles of Internal Medicine,* 18th edition: www.accessmedicine.com. Figure 1.2B adapted and modified from: Andreoli TE, Carpenter CCJ, Griggs RC, Loscalzo J. *Cecil Essentials of Internal Medicine,* 6th edition: consulted on CD-ROM.

Each main intracranial artery supplies specific areas of the brain (figures 1.3 and 1.4). In turn, each area of the brain has a different role in the nervous system (figures 1.1 and 1.4). Therefore, from the specific symptoms and signs of stroke that a patient has, a physician can localize the area of the brain that is deprived of oxygen before examining imaging studies.

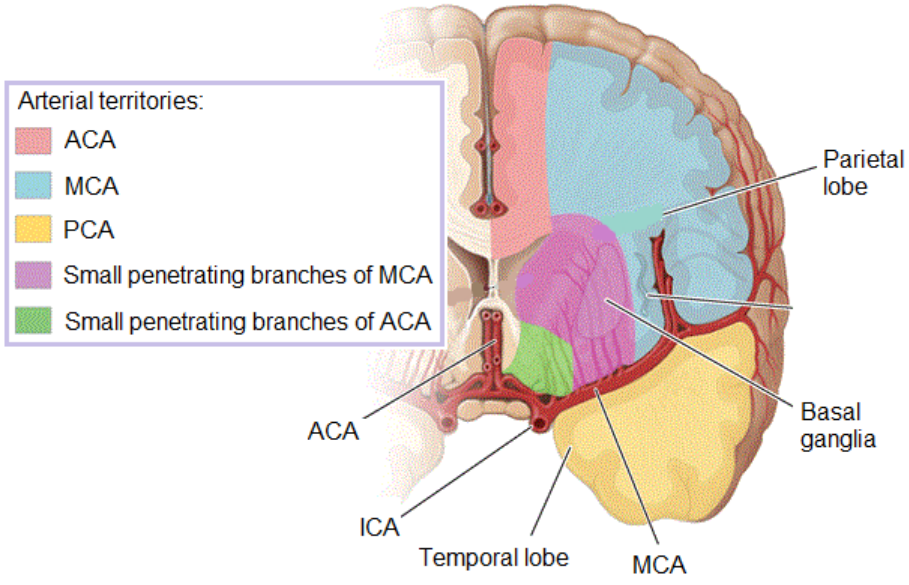

Figure 1.3: Blood supply to the brain by arterial territory. Adapted and modified from Longo DL, Fauci AS, Kasper DL, Hauser SL, Jameson JL, Loscalzo J. *Harrison's Principles of Internal Medicine,* 18th edition: www.accessmedicine.com

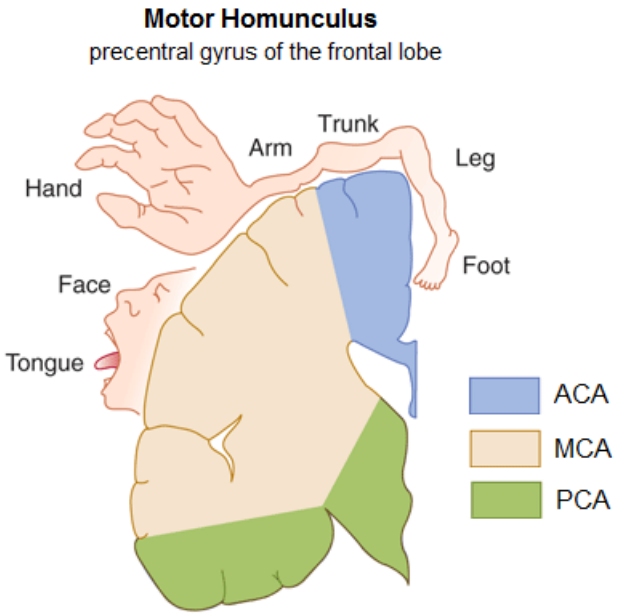

Figure 1.4: Coronal view of the brain showing the motor homunculus[5] and blood supply areas of the precentral gyrus of the frontal lobe. Image modified and adapted from: Waxman SG. *Clinical Neuroanatomy*, 26th edition: www.accessmedicine.com

1.3. *Pathophysiology*

In ischemic stroke, a sudden interruption of blood flow in a blood vessel to the brain occurs, inhibiting neurons downstream from receiving oxygen and glucose (figure 1.5). The inadequate blood flow to the brain is termed *cerebral ischemia*, and results in cellular hypoxia[6], depletion of adenosine triphosphate (ATP) molecules (i.e. loss of energy), and loss of normal cellular functions. Neuronal cells undergo a number of biochemical changes and can no longer maintain ionic gradients. Consequently, water passively shifts into cells, and they swell (cytotoxic edema). If blood flow is not immediately restored within

[5] Motor homunculus: map of brain areas that control muscle movement. On figure 1-4, the map shows which brain part controls muscle movement of the limbs, hand, face, tongue.

[6] Hypoxia: low oxygen levels.

a few minutes, cerebral ischemia evolves into *cerebral infarction*[7]. It only requires 4 to 10 minutes [3] of complete oxygen deprivation to cause cerebral infarction. The popular expression physicians say, "time is brain", reflects how important it is to act very quickly to prevent as much neuronal cell death as possible.

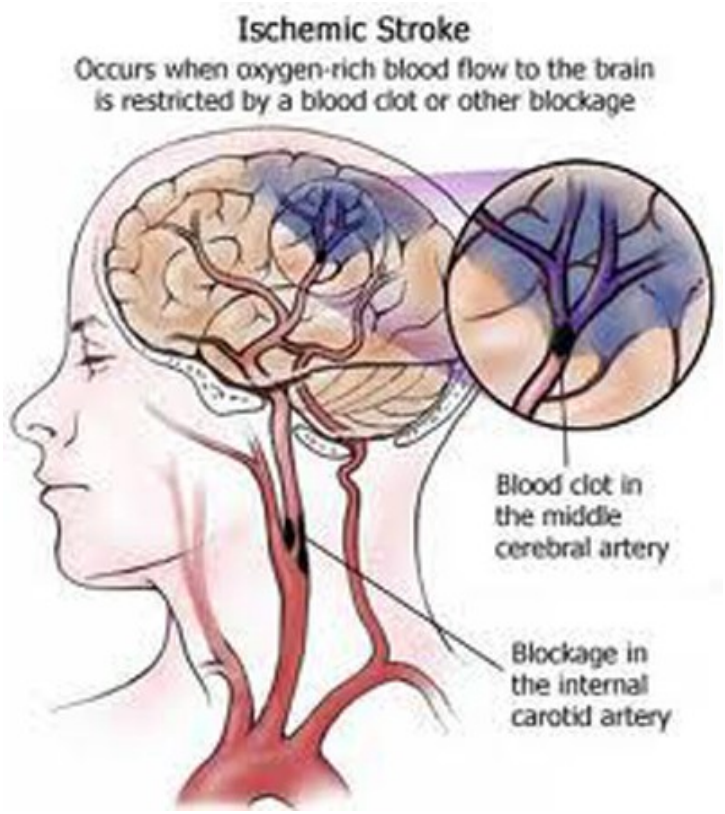

Figure 1.5: Ischemic brain tissue downstream of arterial occlusion. Adapted from: www.neurologiaroma.it

An ischemic stroke implies that *cerebral infarction* has occurred. Patients suffering a stroke have variable recovery afterwards. A *transient ischemic attack* (TIA) is clinically similar to an ischemic stroke, but the neurologic deficit lasts less than 24 hours, and there is full recovery of symptoms with no evidence of cerebral infarction on imaging studies. The mechanisms underlying an ischemic stroke are the same as those for TIA. However, in TIA,

[7] Infarction: cellular death.

the vascular obstruction does not last long enough to cause infarction, probably because the thrombus or embolus is small enough to spontaneously dissolve and allow timely reperfusion. Although harmless, a TIA is an important warning sign: it precedes 15% of all strokes [4], and it considerably increases the risk of developing a stroke within the next 90 days (9 to 20% risk), especially in the first 2 days (3 to 10% risk) [5-7]. Unfortunately, half of all patients who experience a TIA do not report it to their healthcare provider [8].

In hemorrhagic stroke, there is bleeding in the brain tissue. The focal area where bleeding is occurring produces a toxic effect on neuronal cells, vasospasm[8] of blood vessels, and may produce a mass effect[9] compressing surrounding vessels and brain tissue. Moreover, a breakdown of the vascular barrier can cause fluid to leak interstitially in the brain (vasogenic edema), which in turn can also cause a mass effect. These events can compromise blood flow, leading to ischemia and infarction, or cause brain herniation, leading to massive cellular death and loss of vital bodily functions.

1.4. *Etiology*[10]

Cerebral ischemia may occur in a specific vascular territory as a result of a thrombotic or embolic occlusion of a major vessel, or it may occur globally because of decreased systemic blood pressure. Causes of focal and global cerebral ischemia are enumerated in Table I-I.

---

[8] Vasospasm: contraction of muscular layer of blood vessels, causing decrease in lumen diameter. Also called constriction.

[9] Mass effect: compression of surrounding brain tissue due to the presence of a mass, such as a collection of blood, swelling, or a tumour. A mass effect requires imminent treatment because it may cause deadly brain herniation, where the brain tissue is pressed and pushed away from its normal position inside the bony skull.

[10] Etiology: cause underlying the disease.

Focal Cerebral Ischemia	Global Cerebral Ischemia
Disease of the Vascular wall Atherosclerotic plaque with occlusive thrombosis in situ Vasculitis (inflammation of blood vessels) Vasospasm (migraine or hemorrhage) Mass effect (compression of cerebral vessels) Dissection of arterial wall Other vascular disease (moyamoya, fibromuscular dysplasia) *Embolus* Cardiac origin (atrial fibrillation, cardiac tumour) Artery-to-artery (i.e. embolus from an upstream atherosclerotic plaque) Venous origin (paradoxical embolus due to cardiac defect) *Hyperviscosity of blood* Inflammatory disease (Lupus) Sickle cell disease Inherited hypercoagulability Medication-induced (e.g. oral contraceptive)	Hypoperfusion (e.g. massive hemorrhage, dehydration) Cardiac arrest Other cause of hemodynamic compromise (e.g. septic, anaphylactic, or cardiogenic shock states)

Table I-I: Common Causes of Cerebral Ischemia

Thrombosis is the formation of a thrombus (blood clot) in the blood stream. Hypercoagulability, stasis of blood circulation, and vessel wall injury are predisposing factors of thrombosis. Atherosclerotic plaque rupture is an injury of the diseased vessel wall. As a response to this injury, a thrombus forms at the site of rupture and may occlude the artery in situ or travel distally[11] to a smaller vessel, at which point it is called an embolus. These concepts are important for understanding etiology and mechanisms of ischemic stroke (figure 1.6). Four common mechanisms are discussed below.

[11] Distal: located further from the heart. Antonym = proximal.

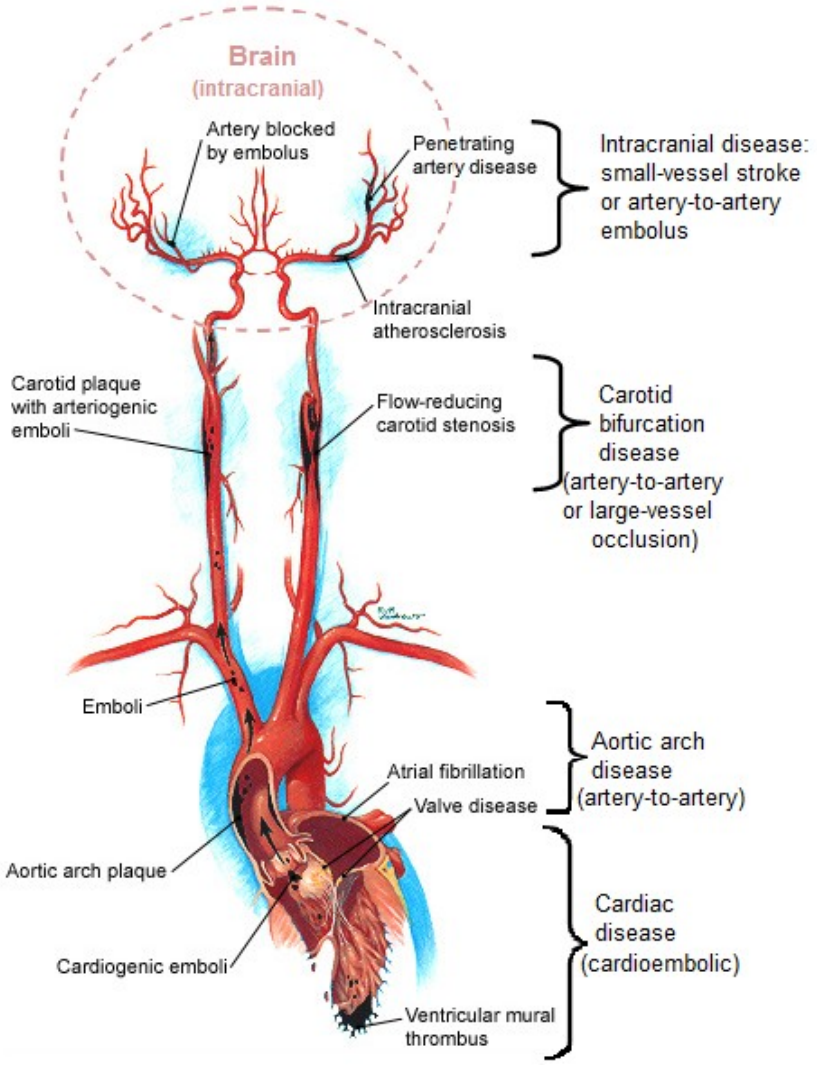

Figure 1.6: Mechanisms of ischemic stroke. Adapted and modified from [9].

1. Cardioembolic stroke causes up to 20% of all ischemic strokes [3]. A thrombus forms in the heart due to cardiac arrhythmia (e.g. atrial fibrillation), a structural cardiac defect, or valvular disease. Fragments of thrombi then detach and embolize to the brain. Emboli frequently lodge in the major arteries (MCA, PCA, ACA). Cardioembolic strokes may affect a single cerebral vascular territory or multiple vascular territories. The latter suggests "embolic showers" (multiple emboli), which are strongly associated with cardiac thromboembolism.

2. Large-vessel occlusion is another possible but less common mechanism of stroke. It involves total occlusion of the internal carotid artery due to an advanced atherosclerotic plaque that ulcerates and forms an obstructive thrombus in situ. A border-zone cerebral infarction ("watershed infarction") ensues; this zone is located most distally and between major cerebral vascular territories. If collateral arterial circulation has sufficiently developed to bypass the severe carotid stenosis, then a total carotid occlusion could be completely asymptomatic and not cause any cerebral infarction.

3. Artery-to-artery embolus results from the formation of a thrombus at the surface of a ruptured atherosclerotic plaque, and distal embolization of it or of a fragment toward the brain. More about atherosclerosis is discussed in chapter 2. Sites with a predilection for developing atherosclerotic plaque include the ICA, carotid bifurcation, and aortic arch (figure 1.7). The proximal ICA and bifurcation are the most common sources of artery-to-artery embolus. An estimated 20% of all ischemic strokes are caused by carotid atherosclerosis alone [10]. Emboli from the ICA may go to any of its major branches. Other less common sources of emboli that go to smaller vessels in the brain include intracranial atherosclerosis (proximal MCA, ACA, or ophthalmic artery), and dissection of the carotid artery (traumatic or spontaneous).

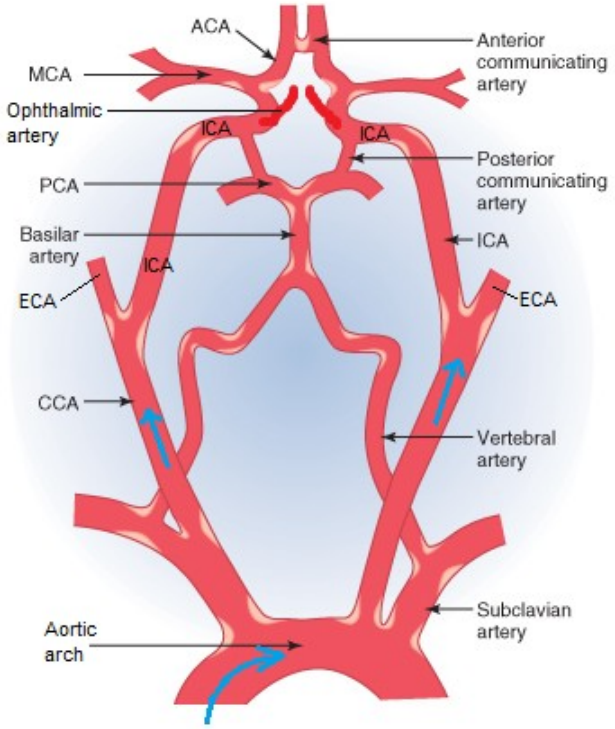

Figure 1.7: Anatomy of cerebral arteries and sites of predilection of atheromatous plaque. Blue arrows show direction of blood flow. Plaque has a tendency to form in areas of flow turbulence, such as bifurcations. Adapted and modified from: Andreoli TE, Carpenter CCJ, Griggs RC, Loscalzo J. *Cecil Essentials of Internal Medicine,* 6th edition: consulted on CD-ROM.

4. Small-vessel strokes are small infarctions in the territory of deep penetrating arteries of the brain, affecting areas of the basal ganglia (figure 1.3) and the brainstem. They are also termed "lacunar strokes". Microvascular obstruction in situ occurs due to microatheroma or lipohyalinotic vessel wall thickening associated with hypertensive disease. Approximately 20% of all strokes are small-vessel strokes [3].

Causes of spontaneous hemorrhagic stroke include vascular diseases (hypertensive, amyloid angiopathy, arteriovenous congenital malformation, drug-induced), intracerebral tumours pressing on vessels, and bleeding disorders (congenital or induced by blood thinners).

1.5. *Epidemiology, Risk Factors, Prognosis, and Cost*

In the western world, stroke is the third leading cause of death after heart disease and cancer [11], and it is a leading cause of long-term disability [12]. Approximately every 40 seconds, a person suffers a stroke [11], and every 4 minutes, someone dies from stroke in the United States [13]. Each year, 795 000 people in the USA suffer from a new or recurrent stroke, of which 610 000 are first attacks, and the remainder are recurrent attacks [11]. In people aged 45 to 84 years, the age-adjusted stroke incidence rate varies from 2.3 to 6.6 per 1000 person-years [1]. Stroke incidence increases with age, is higher in blacks than in whites, and higher in men than in women.

Risk factors for ischemic stroke are presented in Table I-II. Modifiable implies that risk factors can be controlled with lifestyle changes and medications.

Non-modifiable risk factors	Modifiable risk factors	Other risk factors
Age	Hypertension	Atrial fibrillation
Race	Diabetes mellitus	Carotid stenosis
Sex	Smoking	Transient Ischemic Attack (TIA)
History of migraines	Physical inactivity	
Sickle cell disease	Hyperlipidemia	Previous ischemic stroke
Fibromuscular dysplasia	Alcohol or illicit drug abuse	
Family history of stroke	Oral contraceptive use	
Hyperhomocysteinemia		

Table I-II. Risk Factors for ischemic stroke

Stroke can be deadly or result in a significant loss of autonomy due to permanent paralysis, speech or cognitive impairment. Prognosis after an acute ischemic stroke is highly variable, because it depends on stroke severity, development of complications, and presence of other comorbid diseases. Life-threatening complications that may occur after an ischemic stroke include brain herniation (mass effect), aspiration pneumonia (stroke can cause impaired swallowing and choking), acute myocardial infarction, and an expanding collection of blood (hematoma) due to hemorrhagic transformation of the infarct. The 30-day case fatality rate of ischemic stroke is 8-12%, and

that of hemorrhagic stroke is around 40% [14,15]. Among stroke survivors, 15 to 30% remain permanently disabled [16]. In addition to the burden on the patient and family, elevated health care and economical costs ensue. In 2007, the direct and indirect cost of stroke was $40.9 billion in the USA [11].

1.6. *Clinical Presentation*

1.6.1. History

Patients suffering a stroke or TIA present with an abrupt onset neurologic deficit or altered consciousness. The time of symptom onset is very important. If the onset is within 6 hours of consultation in the emergency room and ischemic stroke is confirmed with computed tomography (CT) scan of the head, treatment with immediate thrombolysis[12] is possible. Neurologic deficits elicited on medical history include:

- facial or limb weakness (hemiparesis) or paralysis (hemiplegia), usually on one side
- sensory loss in extremities
- Visual deficit: blindness in one or both eyes, visual field defect, double vision
- Speech disorder: slurred (dysarthria) or incoherent ("word salad")
- Language disorder: lack of output (expressive aphasia) or understanding (receptive aphasia)
- Dizziness, loss of balance, loss of coordination
- Headache, nausea, vomiting
- Decreased level of consciousness

[12] Thrombolysis: dissolution or breaking apart of a thrombus.

Depending on the location of the brain that is ischemic, patients will present a specific symptom or a combination of symptoms termed stroke syndromes. Symptoms that worsen over time may indicate progressive intracranial edema, hemorrhagic transformation, or a stroke-in-evolution (area of ischemia and infarction that is increasing in size because of worsening occlusion). Some symptoms are suggestive of hemorrhagic stroke, like severe headache, nausea, vomiting, neck stiffness, and loss of consciousness, but they are not of diagnostic value since they also occur in ischemic stroke.

Risk factors for ischemic stroke and other co-morbidities must be elicited with medical history. Hypertension, diabetes mellitus, smoking, elevated cholesterol levels, and family history of stroke or heart disease may be present. Also, the patient may have recently suffered a similar but transient attack in the past few weeks, suggesting TIA as a warning sign for current ischemic stroke. Other clues must also be elicited, such as cardiac arrhythmia (palpitations, shortness of breath), carotid stenosis, trauma, medication use, and causes of hypercoagulability (hormonal therapy).

Many people suffer from “silent” ischemic strokes, in other words, small strokes with no apparent symptoms. They are usually discovered incidentally on brain imaging, and the patient and family report no history of previous stroke or TIA. Etiology of silent ischemic strokes is the same as cerebral ischemia discussed above (cardioembolic, artery-to-artery, small vessel obstruction). The prevalence of silent ischemic strokes varies from 11% in people aged 55-64 years, to 43% in those aged over 85 years [17,18]. Although no obvious deficits are observed, minor cognitive and memory deficits resulting from silent strokes can be detected with more sensitive neurocognitive and psychological testing (for example, the Repeatable Battery for the Assessment of Neuropsychology Status [RBANS]). Such minor deficits can evolve into dementia and significantly alter quality of life; hence, treatment is aimed at preventing both silent and non-silent ischemic strokes.

1.6.2. Physical Examination

A thorough physical exam is required to determine if indeed the patient suffered a stroke, identify the stroke syndrome, localize and predict the extent of the ischemic lesion, establish a baseline neurological status for follow-up of clinical evolution, and uncover possible etiologies.

If a patient presents with a significant decrease in level of consciousness like stupor or coma, there is a very high risk of severe deterioration and death, and urgent intervention is required (e.g. mechanical respiratory assistance, blood pressure maintenance).

Vital signs frequently show an elevation of systemic blood pressure; it is a normal response to cerebral injury to maintain cerebral perfusion. If there is a brainstem or a very large ischemic or hemorrhagic stroke, the patient's vital signs may be unstable and there may be loss of spontaneous breathing requiring assisted ventilation. A rapid irregular heart rate is indicative of cardiac arrhythmia like atrial fibrillation; in this case, the heart rate must be slowed down to maintain adequate perfusion of the body. A fever can be a clue of aspiration pneumonia or another infection (e.g. meningitis).

Examination of the head and neck can show signs of trauma like a contusion, swelling, and laceration, which can be associated with intracranial hemorrhage or arterial dissection. An ocular examination of retinas with fundoscopy is required to check for evidence of increased intracranial pressure (ICP) (papilledema) or retinal ischemia ("cherry-red spot" appearance of fovea). A stiff neck is suspicious for meningitis or hemorrhagic stroke. Auscultation of the carotid arteries with a stethoscope may reveal a bruit indicative of significant carotid stenosis.

On cardiac auscultation, an irregular rhythm may point to arrhythmia, a murmur may be a sign of valvular disease, and a gallop[13] may be heard when there is cardiac hypertrophy. Pulmonary edema and swelling of the legs are signs of heart failure. All these conditions are associated with the development of an intracardiac thrombosis.

Peripheral pulse intensity asymmetry or systolic blood pressure difference between two arms may indicate aortic dissection. Weak or absent pedal pulses may be indicative of atherosclerotic occlusive peripheral arterial disease, which itself is strongly associated with atherosclerosis in other arteries (e.g. carotid and coronal arteries).

The neurological examination is essential to diagnose stroke and plan management. It is divided into many components: mental status, level of consciousness, cranial nerves, motor function, deep tendon reflexes, sensory function, cerebellar function, and gait. The neurological examination is intricate, but for the purpose of this chapter, a brief description of what physicians on a stroke team[14] use to rapidly assess the patient's neurological status is provided in the Appendix 1, the National Institutes of Health Stroke Scale (NIHSS) [19]. The score of the NIHSS helps localize the lesion, determine stroke severity, outcome, and appropriate patient management. Finally, after the patient's stroke, a Modified Rankin Scale (Appendix 2) score is attributed for purposes of follow-up examinations.

Different stroke syndromes are encountered in ischemic stroke, depending on the vascular territory involved.

[13] Gallop: an additional heart sound other than the first and second normal heart sounds

[14] Stroke team: team of physicians responsible for the care of patients presenting with a stroke in the emergency room. They are responsible for deciding and administering thrombolytic therapy.

- **Middle cerebral artery** occlusion produces contralateral hemiparesis and hemisensory loss of the face and upper limb, aphasia, and partial visual field loss (figure 1.8).

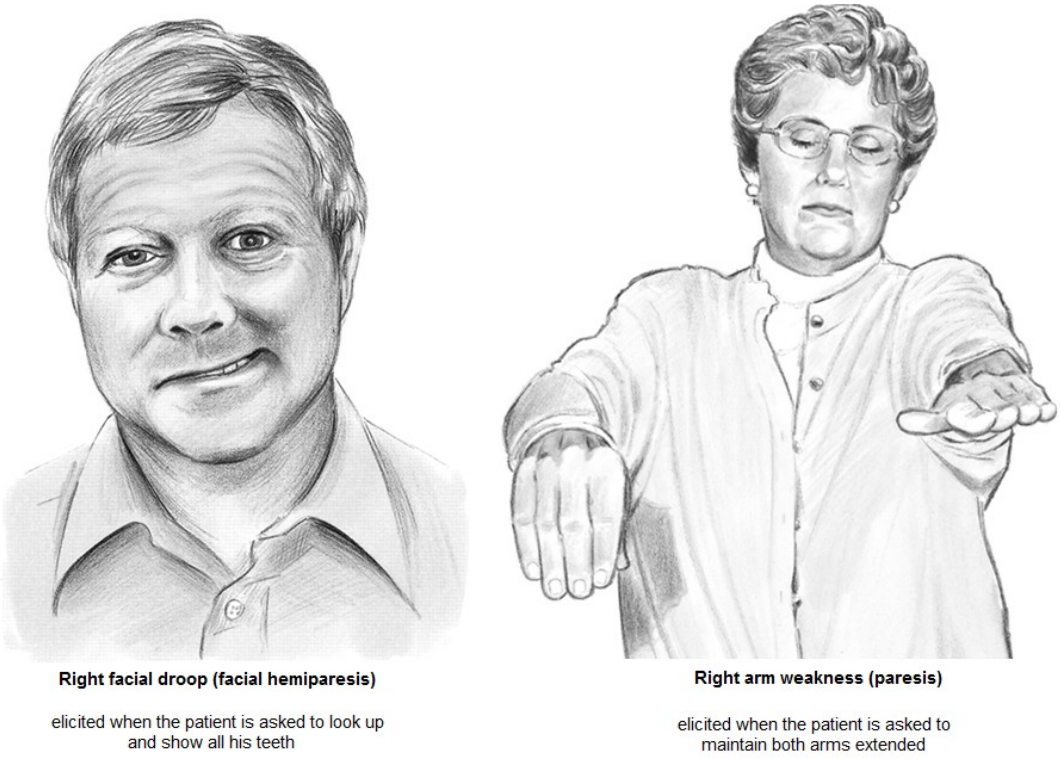

Figure 1.8: Signs of left middle cerebral artery (MCA) stroke. Right facial and upper limb weakness. Adapted and modified from [20].

- **Anterior cerebral artery** occlusion produces contralateral hemiparesis and hemisensory loss of the lower limb, mutism, incontinence, cognitive and personality changes.
- **Ophthalmic or central retinal artery** occlusion produces acute monocular blindness due to retinal ischemia. Patients may report seeing a black curtain moving in the visual field of one eye. If the symptom is transient, it is termed *amaurosis fugax* ("transient monocular blindness"), which is equivalent to a TIA. If the symptom is permanent, retinal infarction has occurred, much like an ischemic stroke. Amaurosis fugax is often an indicator of artery-to-artery embolization, originating either in the carotid or ophthalmic artery, as evidenced by the presence of a cholesterol embolus in the retinal artery.

- **Posterior cerebral artery** occlusion produces visual field deficits (blindness may be partial in one or both eyes), loss of visual recognition (persons, objects, shapes), and amnesia.
- **Vertebrobasilar artery** occlusion produces dizziness, double vision, visual field losses, difficulty swallowing, slurred speech, and uncoordinated gait (ataxia).
- **Lacunar strokes** typically produce pure motor loss, pure sensory loss, or ataxic gait.

1.7. *Differential diagnoses*

A physician elaborates a differential diagnosis based on all available clinical information. A differential diagnosis is a list of all possible disorders that can present in a similar fashion. Before making the final diagnosis, each possible disorder should be explored through focused investigations like blood tests and imaging; in other words, a *workup*. This helps narrow down the differential to a single diagnosis, after which appropriate treatment can begin. Disorders that present similarly to acute ischemic stroke are presented in Table I-III.

Differential diagnosis of acute ischemic stroke	
Neurological disorders	*Cardiovascular disorders*
Hemorrhagic stroke	Syncope
Transient ischemic attack (TIA)	Myocardial infarction
Seizure (especially post-ictal state)	Arrhythmia
Brain tumour (abscess, malignant tumour)	
Meningitis	*Metabolic disorders*
Benign vertigo	Severe infection
Neuropathies (Bell's palsy, spinal cord trauma)	Drugs (illicit or prescription)
Multiple sclerosis	Low serum sodium
	Hypoglycemia

Table I-III. Differential diagnosis of acute ischemic stroke

1.8. *Workup*

Once an acute stroke is suspected, the next step is determining if it is ischemic or hemorrhagic. Emergent treatment (thrombolysis, surgery) depends on this distinction. An immediate computed tomography (CT) of the head without contrast injection is required; it is a rapid and very accurate imaging examination to differentiate ischemic stroke from hemorrhage. A serum glucose level and electrocardiogram (ECG) should also be checked promptly.

On CT scan, hemorrhage appears bright (white), and infarction appears as darker (more lucent) than healthy brain parenchyma. Also, subtle early signs of infarction include loss of gray-white matter differentiation and effacement of cortical sulci (the normal folds in the cortex). If there is no hemorrhage but a suspected infarction, a CT scan with contrast injection or CT angiography (CTA) of the head and neck vessels is performed to search for occlusion of a major artery, localize the area of decreased perfusion, the infarct core and ischemic penumbra. CT scan images of the brain are shown in figures 1.9 through 1.11.

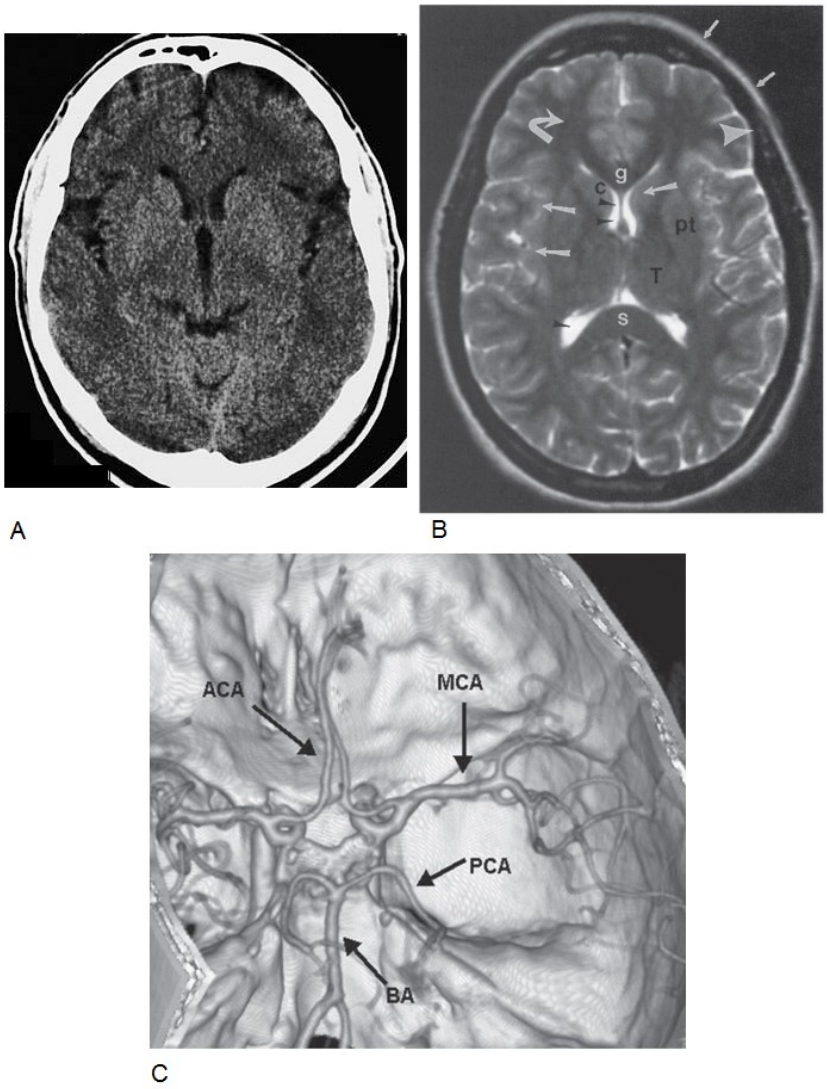

Figure 1.9: Normal brain images. A. Axial CT scan of the brain. Adapted from: Moeller TB, Reif E. *Normal Findings in CT and MRI,* 1st edition, page 7. B. Axial T2-weighted MRI of the brain. MRI provides a good assessment of brain structures with differences in signal intensity. C. CT angiogram of intracerebral arteries with 3-dimensional volume rendering (axial and slightly oblique view). Gray matter (large white arrows), white matter (curved white arrow), lateral ventricles (black arrowheads), fat (small white arrows), and cortical bone (large arrowheads) on different pulse sequences. Structures identified are the genu (g) and splenium (s), caudate head (c), putamen (pt), and thalamus (T). For B and C, images adapted from: Chen, Pope and Ott. *Basic Radiology,* 2nd edition, Chapter 12.

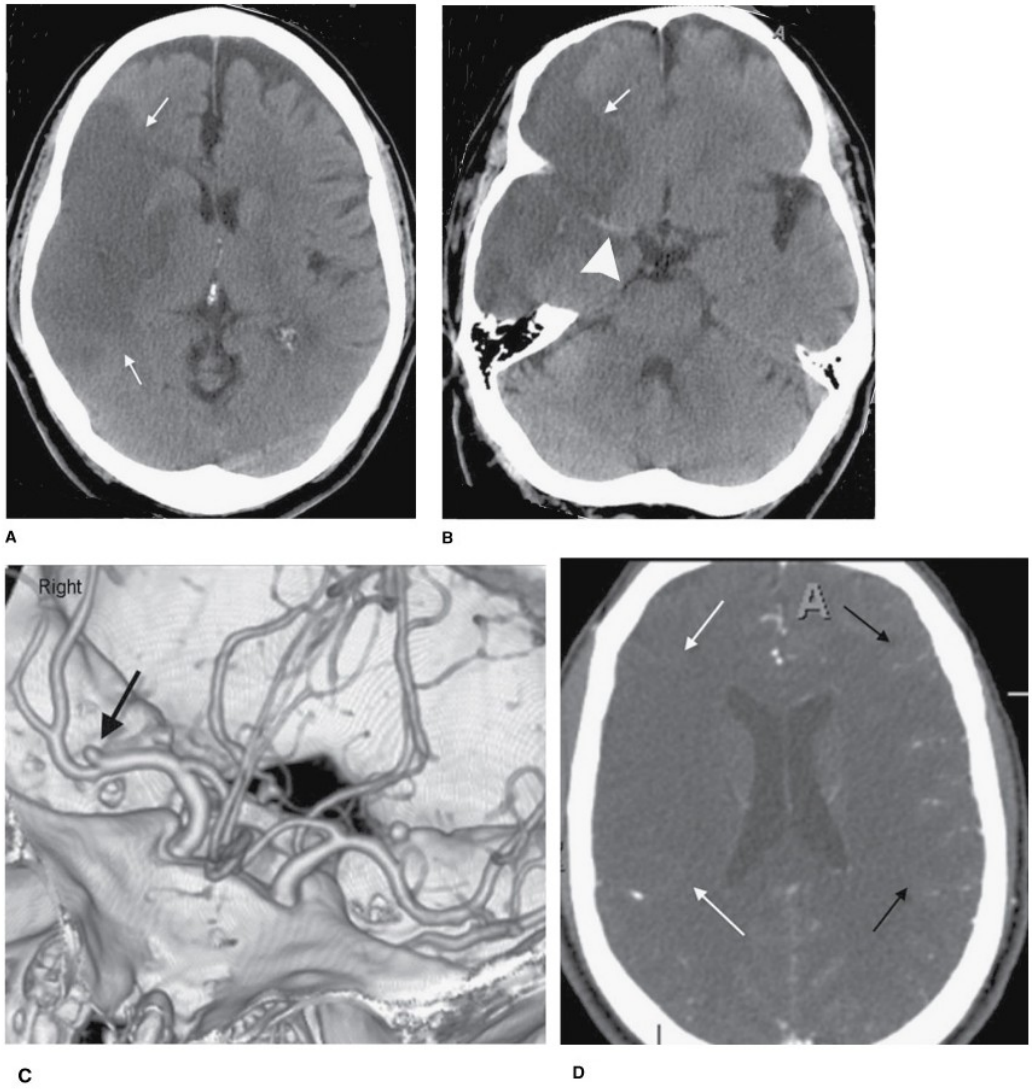

Figure 1.10: CT scan of a cerebral infarction in a 56 year old hypertensive and diabetic male who presented with left hemiparesis in the emergency department. A and B. Axial CT at 2 different levels without contrast injection showing a well-defined hypodense area in the right MCA territory (between white arrows) and a mass effect on the surrounding brain tissue (compression of right ventricle). The right MCA is brighter than the left (large white arrow head on B) and corresponds to an occluding thrombus. C. A 3-D volume rendering CT angiogram shows the occlusion in the superior branch of the right MCA. D. Axial CT with contrast injection shows decreased filling of blood vessels in the right MCA territory (between white arrows) compared to the left (black arrows). Images adapted from: Chen, Pope and Ott. *Basic Radiology,* 2nd edition, Chapter 12.

Figure 1.11: Axial CT scan without contrast of a 68 year old hypertensive female who was found unresponsive. There is a large bright (hyperdense) area consistent with hemorrhage in the right basal ganglia (black arrow), mass effect (small white arrows), bleeding into the ventricles (arrowheads), and entrapment of the left ventricle (large white arrow). This bleed is probably due to a vascular defect induced by chronic hypertension. Thrombolysis is contra-indicated, and immediate neurosurgical consultation is required for surgical decompression. Image adapted from: Chen, Pope and Ott. Basic Radiology, 2nd edition, Chapter 12.

Magnetic Resonance Imaging (MRI) with Diffusion-Weighted Imaging (DWI) has a greater sensitivity to detect acute cerebral infarction in the first 6 hours of stroke compared to CT scan without contrast. It is also the best modality to see the area and extent of infarction. However, MRI is often not the first imaging modality used to diagnose acute ischemic stroke. This is because the priority in patient management is to rapidly determine if there is hemorrhage and prevent delay in therapy. CT scanning acquires images more rapidly than MRI and is very sensitive to detect acute hemorrhage. Otherwise, when CT is unremarkable but there remains high suspicion of ischemic stroke, MRI with DWI is typically indicated. Figures 1.9B and 1.12 show normal and abnormal MRI examinations, respectively.

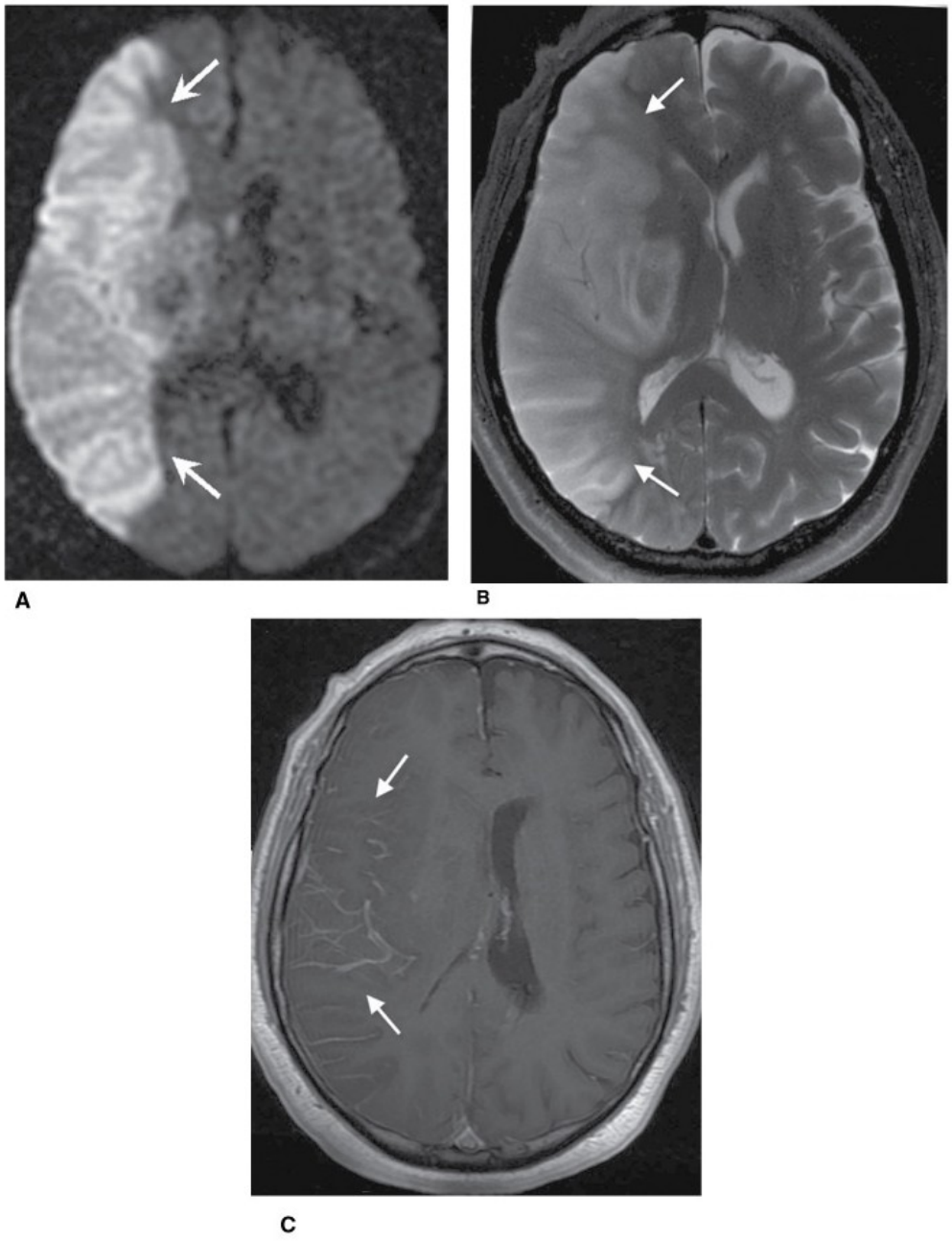

Figure 1.12: Axial MR images of the patient with right MCA territory infarction shown in Figure 1.10. Images are at the same anatomic level. A. DWI demonstrating restricted movement of water in the infarcted area (increased signal intensity between white arrows). B. T2-weighted image demonstrating area of hyperintensity and mass effect on surrounding structures. C. T1-weighted image with contrast injection showing enhancement of vasculature in the territory of infarction, corresponding to slow flow of intravascular contrast. Images adapted from: Chen, Pope and Ott. *Basic Radiology,* 2nd edition, Chapter 12.

To rule out or rule in other suspected diagnoses and comorbidities, the following investigations are ordered as needed: complete blood count (CBC), serum electrolytes, urea, creatinine, coagulation studies, troponins and creatinine kinase (cardiac enzymes), toxicology screen, and lumbar puncture[15].

Finally, once acute ischemic stroke is confirmed, a search for the underlying etiology is begun with specific investigations. For a suspected cardioembolic mechanism, a trans-thoracic or trans-esophageal echocardiography can efficiently image the cardiac structure and reveal an intracardiac thrombus. For suspected arrhythmia not detected on ECGs, a Holter monitor (24-hour continuous monitoring of ECG) is prescribed. For a suspected large artery occlusion or artery-to-artery embolus, angiography (CT or MR) from the aortic arch to the intracranial vessels or carotid Doppler ultrasound can be used to confirm presence of large atherosclerotic plaques and measure carotid stenosis. Transcranial Doppler ultrasound through the infratemporal fossa[16] can be used to evaluate the MCA, vertebral artery, intracranial ICA, and presence of embolic signals. When still in doubt about the vascular pathology despite other imaging methods, conventional angiography is indicated. It is the gold standard imaging technique for evaluating vascular disease, degree of stenosis, and is performed as part of endovascular interventions.

1.9. ***Treatment: Primary and Secondary Prevention***

Primary prevention of ischemic stroke is recommended for patients who have never suffered a stroke. The goal is to decrease the risk of developing an ischemic stroke by acting on modifiable risk factors (Table I-II). This involves maintaining blood pressure at normal levels, treating atrial fibrillation with anticoagulants and antiarrhythmics, appropriate glucose control in diabetics,

[15] Lumbar puncture: sampling of the cerebrospinal fluid to test for hemorrhage or meningitis.

[16] Infratemporal fossa = bony cavity just medial to the mandible.

lowering serum cholesterol levels, and lifestyle modifications like smoking cessation, weight loss, healthy diet, and regular exercise.

On the other hand, *secondary prevention* involves treatment of patients who have already suffered a stroke (or TIA), with the goal of decreasing the risk of stroke recurrence. Once determination of the underlying cause is found, treatment can be targeted to prevent recurrence. For example, patients with atrial fibrillation will require anticoagulation with warfarin (Coumadin) or dabigatran, and patients with severe carotid stenosis will require recanalization with surgery or an endovascular stent. Furthermore, all modifiable risk factors for cerebral ischemia must be treated concomitantly. Finally, physical rehabilitation is necessary to optimize patient autonomy, improve quality of life, and prevent death from stroke-related medical complications (aspiration pneumonia, cardiac disease).

Pharmacological therapies that are commonly used in both primary and secondary prevention include cholesterol-lowering agents (HMG-CoA[17] reductase inhibitors, known as statins), antihypertensive medications (thiazides, angiotensin-converting-enzyme (ACE) inhibitors, angiotensin II receptor blockers (ARBs), Beta-blockers, Calcium-channel blockers), and antiplatelet agents like aspirin, clopidogrel (Plavix) or dipyridamole with aspirin (Aggrenox).

1.10. *Carotid atherosclerosis*

Carotid atherosclerosis is the development of an atherosclerotic plaque in the carotid artery, most commonly at the CCA bifurcation and proximal ICA regions, and most importantly on the posterior aspect of the vessel wall (figure 1.13). Risk factors for atherosclerosis are essentially the same as those for

[17] HMG-CoA reductase inhibitor: 3-hydroxy-3-methylglutaryl-coenzyme A reductase inhibitor.

stroke, including male gender, older age, smoking, hypertension, diabetes mellitus, and hyperlipidemia.

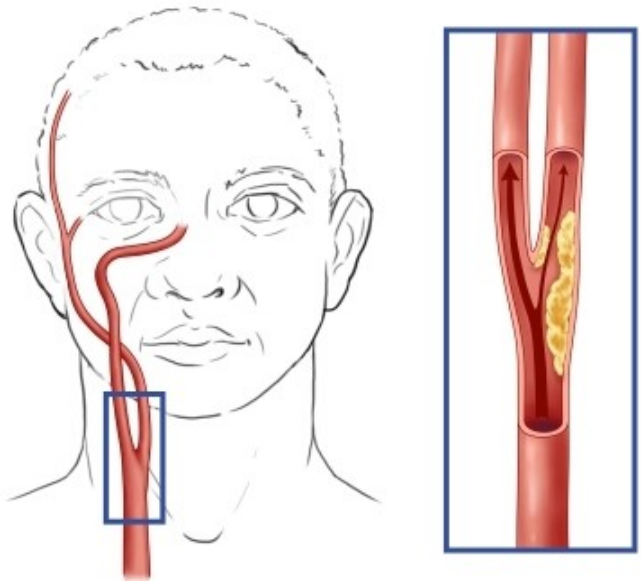

Figure 1.13: Site of carotid plaque formation. It can cause significant obstruction of blood flow or rupture and embolize to a smaller vessel in the brain. Adapted from: *http://chicago.medicine.uic.edu/departments___programs/departments/neurosurgery/clinical_services/neurovascular_surgery/carotid_disease/*

Carotid atherosclerotic disease is characterized by the severity of stenosis and the presence or absence of associated neurological symptoms (stroke or TIA). The degree of stenosis assessed on angiography (CT, MR, or conventional) is measured according to the North American Symptomatic Carotid Endarterectomy Trial (NASCET) criteria [21], using the diameters of the lumen at the point of greatest stenosis and at the normal distal ICA (figure 1.14). Stenosis is qualified as mild (<30%), low-moderate (30-49%), moderate (50-69%), severe (70-99%), near-occlusion (99%), and total occlusion (100%). Carotid stenosis can be symptomatic or asymptomatic; symptomatic stenosis has a greater risk of future ischemic stroke.

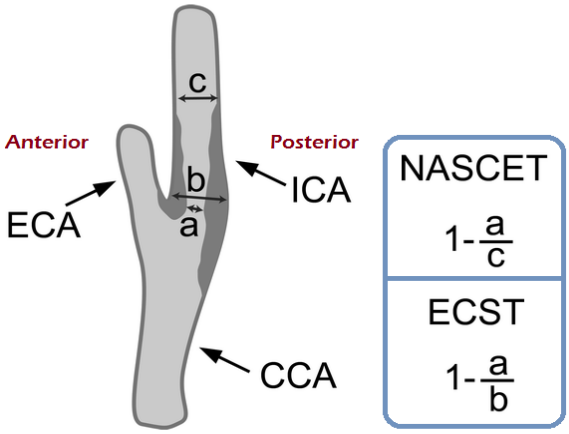

Figure 1.14: Two different criteria can be used to measure degree of carotid stenosis on angiography: NASCET and European Carotid Surgery Trial (ECST) criteria. Adapted and modified from [22].

Treatment of carotid atherosclerosis includes medical prophylaxis (statins, antihypertensives, aspirin), and carotid endarterectomy (CEA) surgery or endovascular stent angioplasty (Figure 1.15). Stent angioplasty is usually reserved for patients with important comorbidities and elevated risks of surgical complications.

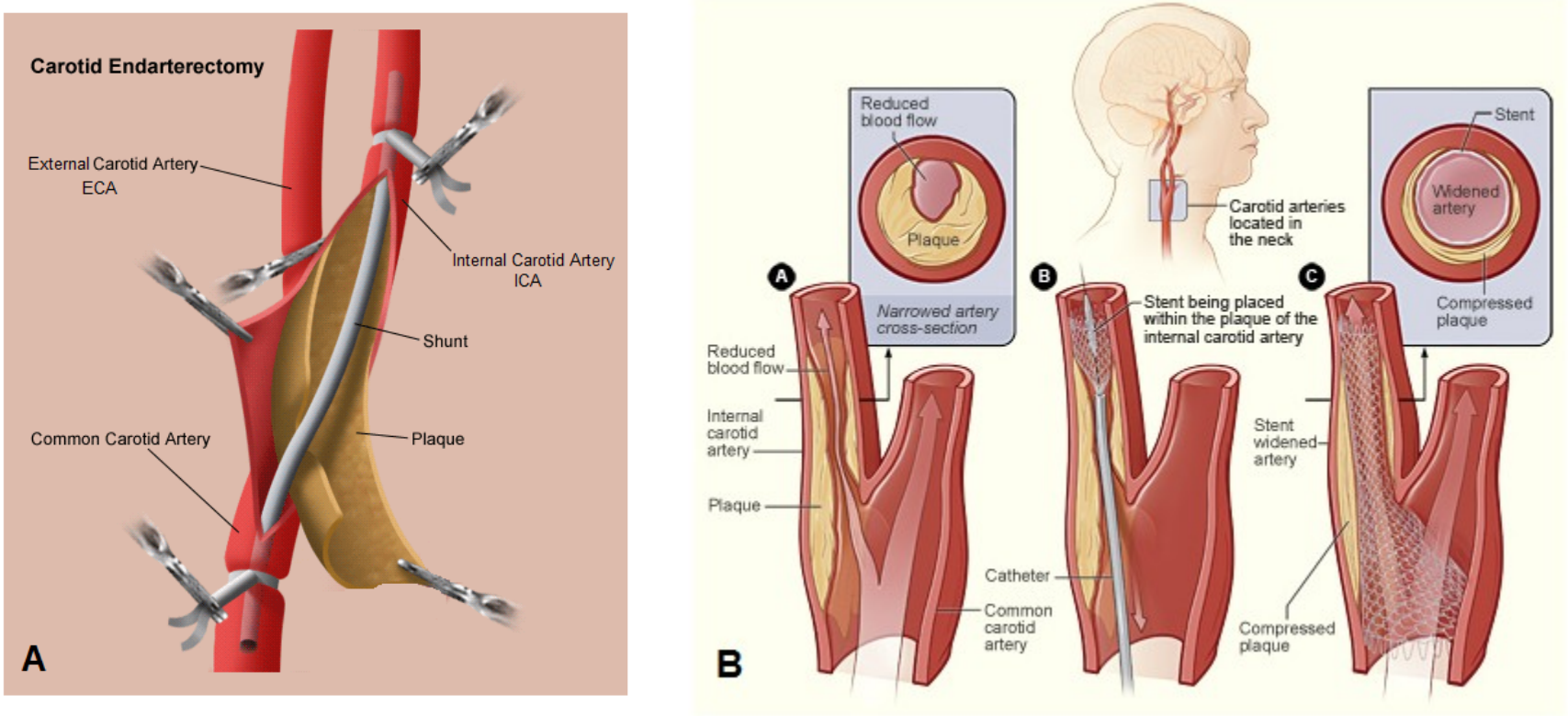

Figure 1.15: A. Carotid Endarterectomy (CEA) procedure. Adapted and modified from:

http://stanfordhospital.org/clinicsmedServices/COE/surgicalServices/vascularSurgery/patientEducation/carotid.html

B. Endovascular carotid angioplasty (stenting) procedure. Adapted and modified from:

http://www.sfveincenter.com/images/stories/med_images/carotid_stent.jpg

1.10.1. Treatment Limitations and Current Issues: a need for diagnostic tools in asymptomatic patients

Symptomatic extracranial carotid artery occlusive disease is currently managed by endarterectomy (or angioplasty). The severity of internal carotid artery (ICA) luminal stenosis is used as an indication for carotid endarterectomy (CEA), based essentially on the results of the North American Symptomatic Carotid Endarterectomy Trial (NASCET) [23,24] and European Carotid Surgery Trial [25]. According to NASCET, symptomatic patients with a carotid stenosis of less than 50% had an 18% risk of stroke at 5 years under medical treatment. This risk climbed to 22% for patients with a carotid stenosis of 50 to 69%, and was even higher for patients with a carotid stenosis greater than 70%, with a stroke risk of 26% at 2 years.

In asymptomatic patients, however, indications for CEA are still debated. In asymptomatic patients with a stenosis of at least 60%, the 5-year risk of stroke or death when receiving optimal medical therapy is 11 to 12% [26,27], compared to about 6% for those receiving early CEA, which includes a 3% perioperative hazard [27]. Recently, results of the ACST-1 trial reported a 10-year risk of stroke of 17.9% in the medical treatment group, compared to a significant lower risk in the CEA group (net risk reduction of 4%) [28]. Within the medical treatment group, patients receiving lipid-lowering therapy at study onset had a lower risk of stroke at 10 years (14.5% versus 24.9%); however, their risk was still significantly higher than for the CEA group [28]. These trials demonstrated a small but significant benefit in CEA compared to medical treatment alone in asymptomatic patients with significant stenosis, both at 5 and 10 years. Nevertheless, the setting of these trials is different than that of non-trial routine clinical settings, where perioperative risk of CEA is likely to be higher than 3%. With the annual rate of stroke varying from 0.6 to 3.8% [26-32], the true benefit of CEA in the general population of asymptomatic

patients with severe stenosis may be lower than in reported studies. Furthermore, degree of carotid stenosis in asymptomatic patients was not associated with long-term incidence of stroke [26,28]. Severity of carotid stenosis and presence of clinical risk factors are useful but insufficient to evaluate the risk of stroke in such patients. Consequently, treatment of asymptomatic patients with >60% carotid stenosis still poses a significant challenge for clinicians.

Further risk stratification is necessary to better determine the risk of stroke in asymptomatic patients with carotid stenosis, and identify a high-risk subgroup that would benefit most from CEA. Current research seeks to develop imaging modalities capable of differentiating "vulnerable" from stable carotid atherosclerotic plaques in asymptomatic patients. Vulnerable atherosclerotic plaque, as defined by histopathological criteria [33], is a thrombosis and rupture-prone plaque associated with clinical ischemic events. Some features of vulnerable plaque have been identified with experimental imaging techniques. It is hypothesized that patients presenting imaging criteria of plaque vulnerability would benefit from early surgical intervention, whereas patients with stable plaque on imaging could be managed medically. In order to verify this hypothesis, a validated non-invasive imaging technique for plaque characterization is required in order to prospectively study carotid plaque progression.

To date, there is no single imaging technique that can reliably identify the vulnerable plaque. This is because (1) there is uncertainty as to which plaque characteristic is the most predictive of vulnerability, (2) a single imaging technique cannot characterize all atherosclerotic plaque features (morphological, molecular, and biomechanical), and (3) few imaging techniques are currently validated with both histopathology correlation and clinical events. In order to recognize the issues at hand with non-invasive imaging techniques of carotid plaque, a thorough understanding of

atherosclerosis pathology is required. Hence, Chapter 2 discusses atherosclerosis, followed by Chapter 3, which describes non-invasive imaging modalities of atherosclerosis in carotid plaques.

This page is left intentionally blank

CHAPTER 2

Atherosclerosis and the Vulnerable Plaque

2. Atherosclerosis and the Vulnerable Plaque

2.1. *Overview*

Atherosclerosis is a chronic systemic inflammatory disease of large and medium-sized arteries. It is characterized by thickening of the arterial wall due to an accumulation of lipids and fibrous elements [34], forming lesions called *atheromas* or *atherosclerotic plaques.* Atherosclerotic plaque formation is complex, and the consequences of this disease are dismal, including heart disease, aortic disease, cerebrovascular disease, and renal disease. With heart and cerebrovascular diseases being the first and third causes of death in the Western countries, an estimated 30% of all deaths could be attributed to atherosclerosis [13]. To understand this complex disease, knowledge of anatomy and physiology is provided, followed by a more in-depth discussion of atherosclerosis pathogenesis.

2.2. *Epidemiology*

The Framingham Heart Study and the Atherosclerosis Risk in Communities Study (ARIC) are prospective studies that identified traditional risk factors for coronary heart disease (CHD) caused by atherosclerosis [35,36]. Non-modifiable risk factors include: increasing age, male gender, and family history. Modifiable risk factors include: hyperlipidemia, hypertension, cigarette smoking, diabetes mellitus, and an elevated serum C-reactive protein (CRP, a marker of systemic inflammation).

2.3. *Normal Structure and Function of Arteries*

The general architecture of blood vessels is shown on figure 2.1. Oxygenated blood pumped out by the heart is transported by the arterial system. Arteries sustain elevated blood pressures; hence they have a thicker wall in comparison to veins, which in turn transport deoxygenated blood back to the heart.

Blood vessels consist of three concentric layers: intima, media, and adventitia (figure 2.1B). The intima contains a single layer of endothelial cells and the internal elastic lamina; the media consists of multiple layers of smooth muscle cells (SMCs) and an external elastic lamina; and the adventitia consists of connective tissue, nerve fibers, and *vasa vasorum* (small arterioles that feed the outer layers of the media in large and medium-sized arteries). Large-sized arteries (e.g. aorta, common carotid artery, iliac artery) have a media rich in elastic fibers, allowing propulsion of blood flow by expansion during systole and recoil during diastole. Medium-sized muscular arteries (e.g. coronary, renal, and internal carotid arteries) have a media rich in SMCs; these arteries can alter the lumen diameter by vasoconstricting and vasodilating (i.e. SMCs contract and relax) in physiological responses. Lumen diameter is known to greatly affect resistance to flow by Poiseuille's law[18], thus medium-sized arteries (sometimes called "resistance arteries") are responsible for regulating systemic arterial resistance.

[18] Poiseuille's law: Resistance = (difference in pressure) / flow = (8*viscosity*length)/ π*radius^4 = $8\eta l / \pi r^4$

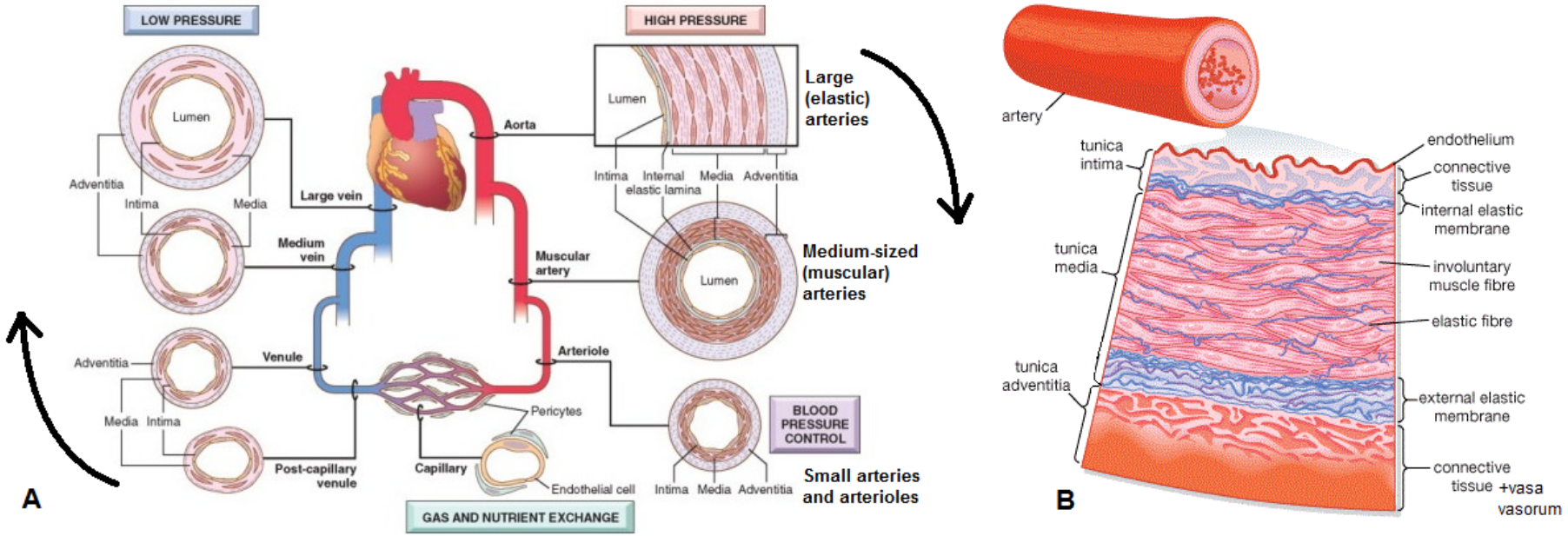

Figure 2.1: Normal vascular architecture (A) and anatomy (B).

A. General organization of vascular system. Arrows show the direction of flow. Modified and adapted from Kumar: *Robbins&Cotran Pathologic Basis of Disease, Professional Edition*, 8th ed. (2009). B. Structure of the arterial wall. *Modified and adapted from: artery: transverse section of an artery. [Art]. Encyclopædia Britannica Online. Retrieved 17 April 2012, from* http://www.britannica.com/EBchecked/media/121565/Transverse-section-of-an-artery

Endothelial cell function

Endothelial cells have multiple functions and properties:

- Maintain a barrier permeable only to selected small molecules;
- synthesize anticoagulant and prothrombotic molecules (e.g. plasminogen activator, tissue factor, von Willebrand's factor);
- synthesize collagen and proteoglycans;
- synthesize vasoconstrictor (endothelin, angiotensin-converting enzyme [ACE]) and vasodilator (nitric oxide [NO]) molecules;
- secrete cytokines (e.g. interleukins) and adhesion molecules (VCAM-1, ICAM and selectins);
- regulate cell growth by secreting growth factors (Platelet-derived growth factor [PDGF], Fibroblast growth factor [FGF], macrophage colony-stimulating factors [M-CSF]) and growth inhibitors (Transforming growth factor Beta [TGF-β]);
- oxidize low-density lipoprotein (LDL).

The intact endothelium can maintain a non-thrombogenic surface with blood, regulate vascular resistance, inflammation, growth of SMCs and other cells. Endothelial cells are also tightly connected with intercellular junctions that are impermeable to larger molecules. In areas of low shear stress and turbulent flow (in vessel curvatures and bifurcations), these junctions can loosen and allow passage of macromolecules like LDL.

The endothelium does not constantly perform all of its functions simultaneously; a balance of activities is maintained. Some functions are "turned on" or induced by pathological stimuli: this is termed *endothelial activation* [37], and is believed to be involved in the first step of atheroma formation. The most common pathological stimuli of endothelial activation are

hemodynamic stresses and elevated serum LDL. Once endothelial cells are activated, they start expressing adhesion molecules, produce cytokines that attract and recruit macrophages, growth factors that stimulate SMC hyperplasia, and they synthesize less NO. Endothelial activation can lead to *endothelial dysfunction*, an imbalance of normal regulatory functions.

Smooth muscle cell function

SMCs are responsible for vessel constriction and dilation. They also function to repair blood vessels by proliferating, synthesizing extracellular matrix collagen, and secreting growth factors. SMCs migrate and proliferate in response growth factors and cytokines secreted by the endothelium.

Physiological response to vascular injury

When there is a vascular injury that causes either endothelial dysfunction or denudation, SMCs are stimulated and intimal thickening of the arterial wall occurs, much like healing and formation of a scar in other tissues. A permanent slight thickening called *neointima* results, which itself is not a herald of disease. However, if vascular insults are repetitive or persistent, excess vessel wall thickening will occur and evolve into a stenotic atherosclerotic lesion.

2.4. *Pathogenesis of Atherosclerosis*

The term *arteriosclerosis* defines arteries that are hardened due to thickening and loss of elasticity. Two types of arteriosclerosis exist: *arteriolosclerosis*, which is a lipohyalinotic thickening of small arteries and arterioles associated with hypertension and diabetes; and *atherosclerosis*, which affects large and medium-sized arteries and is discussed in this section.

2.4.1. **Cellular interactions in atherosclerosis plaque progression**

Atherosclerosis is a chronic inflammatory and healing response of the arterial wall to endothelial injury. This definition is based on the *response-to-injury hypothesis* [38], which proposes the following sequence of events portrayed in figures 2.2:

1. Endothelial injury and dysfunction
2. Accumulation of lipoproteins (LDL), followed by oxidation of LDL
3. Monocyte recruitment, adhesion to endothelium, migration into intima, and transformation into macrophages. Activated macrophages engulf oxidized LDL, becoming lipid-laden *foam cells*
4. Platelet adhesion and release of inflammatory and growth mediators (e.g. PDGF)
5. SMC recruitment, migration to the intima, proliferation, and production of extracellular matrix (collagen and proteoglycans)
6. Extracellular and intracellular (foam cells) lipid accumulation

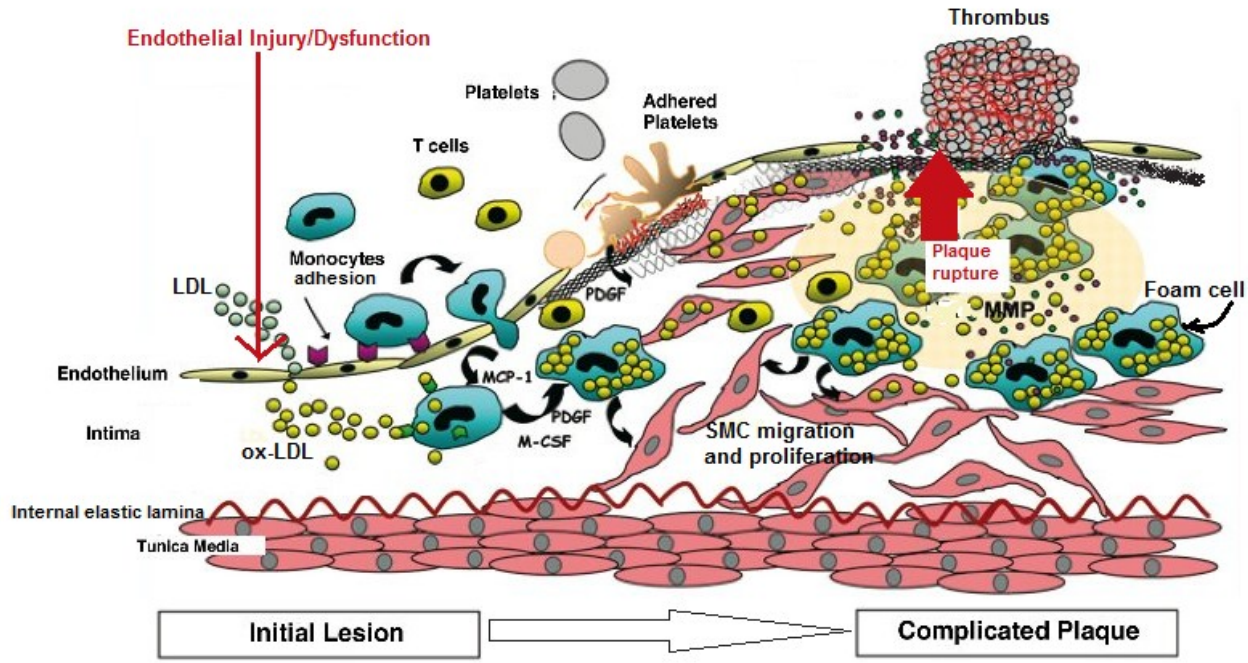

Figure 2.2: Cellular interactions in atherosclerosis plaque progression. SMC, smooth muscle cell; MCP-1, monocyte chemoattractant protein 1; LDL, low-density lipoprotein; ox-, oxidized; PDGF, platelet-derived growth factor; M-CSF, macrophage colony-stimulating factor; MMP, matrix metalloproteinase. Adapted and modified from [39].

Possible causes of endothelial injury include hemodynamic stresses (turbulent flow, high blood pressure, low shear stress), elevated serum LDL from a high-fat diet, inflammatory cytokines in the circulation (for example, from a bacterial/viral infection), excess glycosylation of proteins from diabetes, toxins from tobacco smoking, and hypoxia. Most plaques form in areas of blood flow turbulence, such as bifurcations and curved areas [40]. The turbulence in these areas is believed to be associated with differently-shaped endothelial cells that have increased permeability to macromolecules like LDL [41].

LDL diffuses passively through the endothelium into the intima, and is removed from the intima with high-density lipoprotein (HDL), a protective cholesterol molecule. Accumulation of LDL in the intima will occur if there is an imbalance (excess LDL and/or insufficient HDL). Once LDL accumulates, LDL oxidation occurs; once enough LDL is oxidized, the endothelium activates and expresses adhesion receptors that attract circulation-derived monocytes to enter into the intima. Once in the intima, monocytes differentiate into macrophages with scavenger receptors and engulf oxidized LDL. Eventually, macrophages become lipid-laden and transform into *foam cells*. Endothelial cells, macrophages and platelets produce cytokines and growth factors that attract SMCs to the intima and stimulate their proliferation and production of extracellular matrix (ECM).

Extracellular lipid consists of cholesterol and cholesterol esters. It originates from circulatory LDL and degenerating cells, accumulates in the plaque and eventually forms a lipid-rich necrotic core. Concomitantly, a fibrous cap composed of dense collagen forms superficially to the lipid core.

2.4.2. **Macroscopic changes in atherosclerosis plaque progression**

The modified AHA classification of atherosclerotic plaques reflects the sequence of events in the development of atherosclerotic plaque at a more

macroscopic level (Table II-I) [42-44]. An atherosclerotic plaque is usually eccentric[19] and its size varies from 0.3 to 1.5 cm in diameter in coronary arteries. Although atherosclerosis is a multifocal disease that affects many blood vessels, individual atherosclerotic plaques will often be at different stages of development.

Lesion	Description
Type I	Intimal xanthoma (or fatty streak)
Type II	Fatty streak with multiple foam cell layers
Type III	Pre-atheroma with extracellular lipid pools
Type IV	Atheroma with a confluent extracellular lipid core
Type V	Fibroatheroma
Type VI	Complex plaque with possible surface defect and/or haemorrhage and/or thrombus
Type VII	Calcified plaque
Type VIII	Fibrotic plaque without lipid core

Table II-I. Modified AHA classification of atherosclerotic plaques*
***Adapted from data published in references [42-44]**

Early Type I and II lesions consist of an accumulation of foam cells ("fatty streak"); they are not raised, do not impinge on the lumen diameter, and have been observed in newborns' aorta and in children. Although this is the first step in atherosclerosis, early lesions are not necessarily destined to become advanced plaques.

Type III lesions contain extracellular *lipid pools*. An extracellular lipid pool is a collection of lipid within the ECM. This is distinct from a lipid-rich *necrotic core*, which in addition to lipid, contains debris from dead cells (necrosis), free cholesterol crystals, and sometimes thrombus.

[19] When examining the cross-sectional view of an artery and plaque, if the plaque is not concentric with the vessel wall and has a disease-free arc, it is eccentric.

Type IV and V lesions contain a well-defined lipid-rich necrotic core covered by a fibrous cap. By definition they are atheromas. Type V fibroatheroma is a more advanced lesion than atheroma because it has additional layers of fibrous tissue covering the necrotic core (SMC proliferation and ECM deposition). The plaque periphery often shows small proliferating blood vessels (*neovascularisation*) which attempt to supply oxygen to the plaque core. Type IV and V plaques are prone to becoming complicated Type VI plaques.

Type VI atherosclerotic lesions result from repeated injury to atheromas, inducing an excessive remodeling response and a further increase in plaque size. Type VI lesions have one or a combination of the following: a surface defect (fibrous cap rupture or erosion), intraplaque hemorrhage, or thrombosis at the plaque surface. These complicated Type VI plaques are associated with rapid lesion progression, total occlusion, and acute ischemic events; hence they are types of vulnerable plaque.

Atheromas or complicated Type VI lesions can become “old” lesions over time, either calcified (Type VII), or less frequently, fibrous with minimal lipid (Type VIII). Calcification results from cellular death and can be present at all stages of atherosclerosis. In early stages, when there is minimal cellular death, calcium is sparse or present as microcalcifications. In later stages of atherosclerosis, with an enlarging plaque and increased cellular death in the necrotic core, there are larger quantities of calcification, often arranged in “sheets”[45].

2.5. *The Vulnerable Plaque*

The term vulnerable plaque (VP) emerged over 20 years ago to describe an atherosclerotic plaque that is susceptible to rupture, thrombose, and subsequently cause a cardiac ischemic event [46]. Later, a consensus on the definition of VP was reached. The term "vulnerable plaque" is applicable to prospective studies and describes any thrombosis-prone plaque with high probability of undergoing rapid progression, thus becoming a culprit plaque [33,47]. Culprit coronary plaque features associated with acute coronary syndromes were retrospectively identified in pathology studies: plaque rupture was the most frequent feature (65-70%), followed by erosion (25-30%) and superficial calcium nodule (2-5%) [44]. Based on these findings, major and minor criteria defining VP and different possible types of VP were proposed (table II-II and figure 2.3) [33]. The concept of VP is also applied to carotid atherosclerotic lesions associated with cerebral ischemic events; these lesions were found to have a similar histopathology to that of culprit coronary plaques [48], with 90% of culprit carotid plaques being ruptured [49].

Major criteria	Active inflammation
	Thin cap with large lipid core
	Endothelial denudation with superficial platelet aggregation
	Fissured plaque
	Stenosis >90%
Minor criteria	Superficial calcified nodule
	Glistening yellow (seen on angioscopy)
	Intraplaque haemorrhage
	Endothelial dysfunction (measurement of flow-dependent coronary artery dilatation and other emerging techniques)
	Outward (positive) remodelling

Table II-II. Criteria Defining Vulnerable Atherosclerotic Plaque. Presence of at least one major criterion qualifies a plaque as vulnerable. Adapted from data published in reference [33].

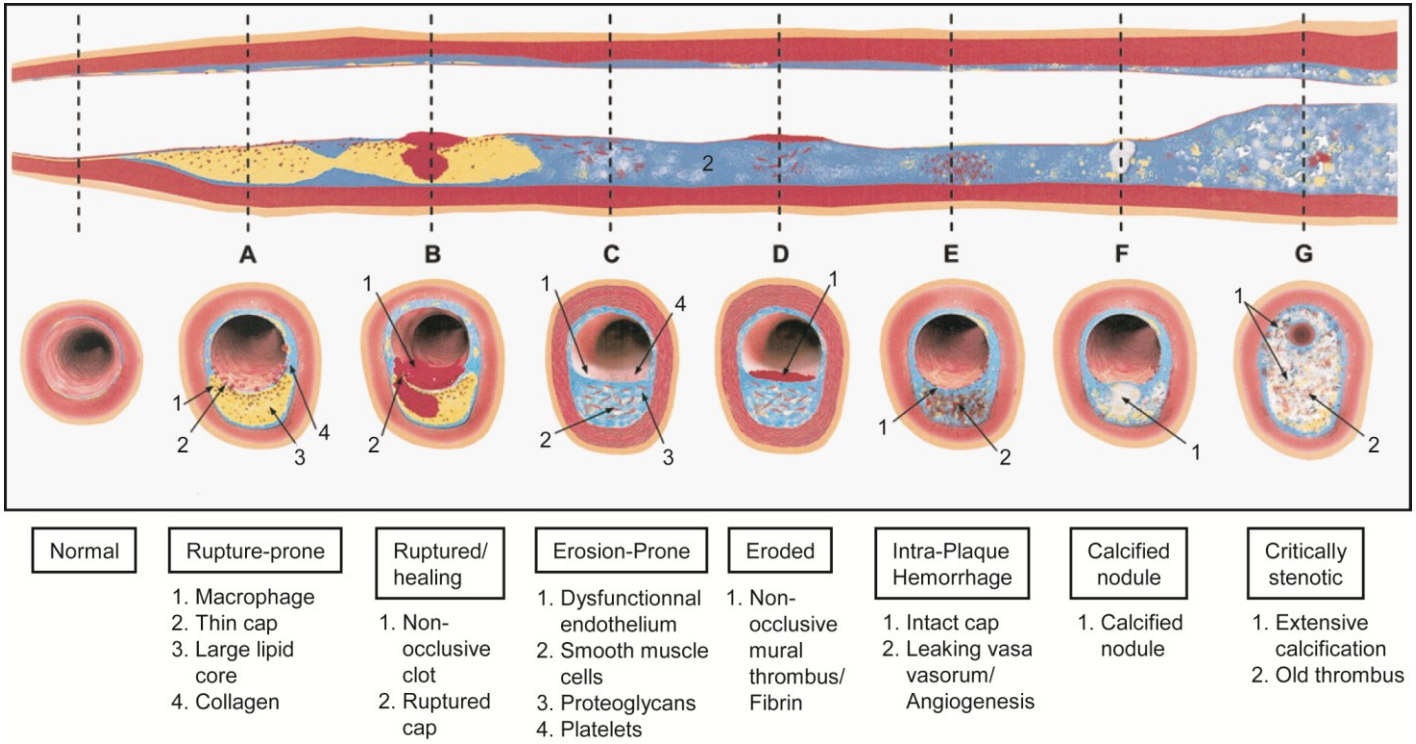

Figure 2.3: Different Types of Vulnerable Plaque. Adapted from [33].

A ruptured plaque is defined as "a plaque with a real defect or gap in the fibrous cap that had separated its lipid-rich atheromatous core from the flowing blood, thereby exposing the thrombogenic core of the plaque" [47]. Therefore, a ruptured plaque requires the presence of both a fibrous cap and a lipid core; in other words, an atheroma. The mechanism underlying plaque rupture begins with formation of a large lipid core that erodes the fibrous cap from below, followed by fibrous cap thinning, weakening, and rupture [50]. Other mechanisms believed to contribute to plaque rupture are inflammation, neovascularisation, intraplaque hemorrhage, and expansive remodelling.

In carotid plaques, a large lipid core is defined as at least 25% cross-sectional total plaque area [48], with an average 40% plaque area [51]. Intraplaque hemorrhage from fragile neovessels was suggested as a contributor to rapid growth of the lipid-rich necrotic core [52].

In coronary arteries, a thin fibrous cap is defined as <65 μm thick [44]. In carotid arteries, pathology from post-CEA symptomatic patients revealed the thinnest fibrous cap portion to be at least 80 μm thick [53] and less than 200 μm, with a representative cap thickness less than 500 μm [54]. Fibrous cap thinning is associated with inflammatory changes and ECM degradation within the cap: there is a localized increase in macrophages that secrete proteolytic enzymes that lead to ECM breakdown (matrix-metalloproteinases [MMPs]) [55,56], and a low number of SMCs, possibly due to apoptosis [57], that are insufficient to compensate for the loss of ECM support. Fibrous cap thinning with a large lipid core leads to a "rupture-prone plaque" (figures 2.3 and 2.4). A stable atheroma with a large fibrous cap is shown in figure 2.5 for comparison.

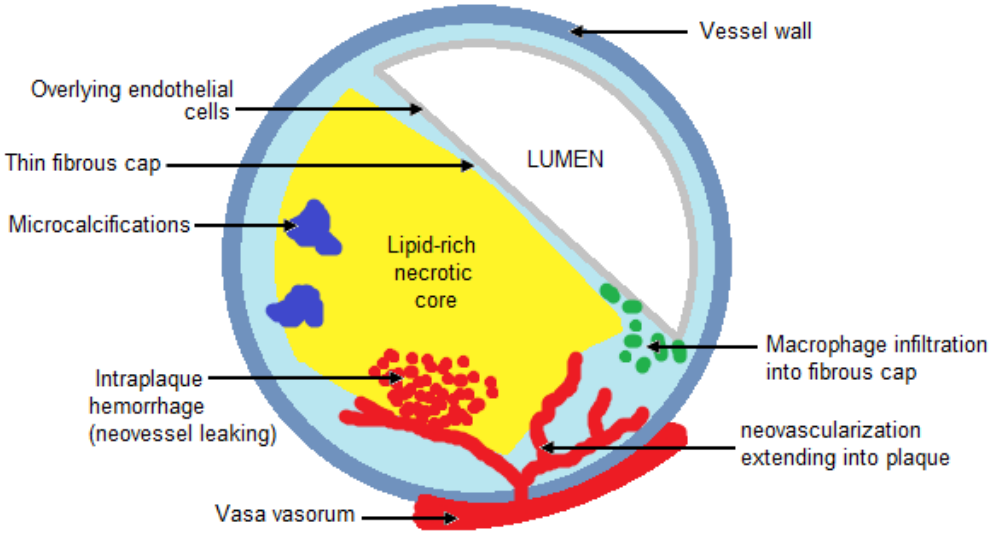

Figure 2.4: Typical thin fibrous cap atheroma with a large lipid core, neovascularisation, intraplaque hemorrhage, and inflammatory macrophages in the shoulder of the cap. This plaque is considered a "rupture-prone" vulnerable plaque.

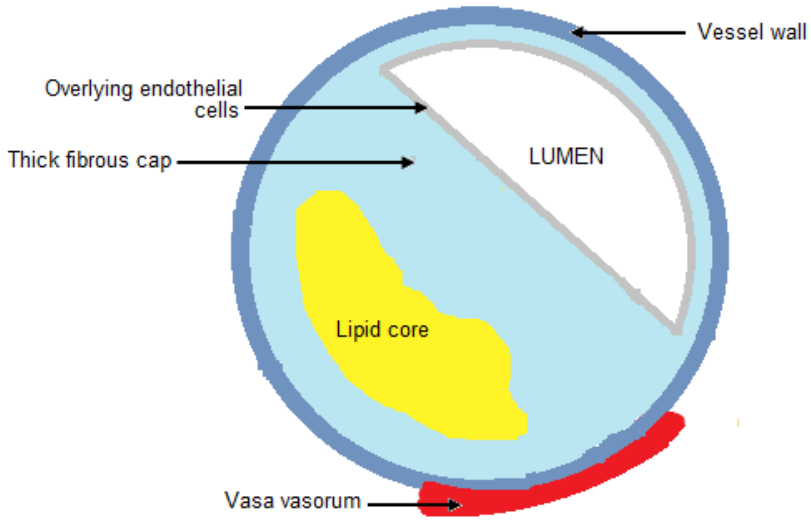

Figure 2.5: A stable plaque with a thick fibrous cap. This plaque is unlikely to rupture.

Neovascularization occurs mostly in larger plaques as a response to plaque growth. It grows at the periphery and shoulders of the plaque. These neovessels are fragile and leaky; they are responsible for intraplaque hemorrhage (figure 2.4). When there is intraplaque hemorrhage, macrophages are recruited, further inflammation ensues, and the plaque enlarges (55). Plaque hemorrhage is distinct from intraplaque hemorrhage because it is defined as luminal blood seeping into a ruptured plaque.

Expansive remodeling (or positive or outward remodeling) is the growth of the atherosclerotic plaque toward the outer vessel wall. This type of growth minimally changes the size of the lumen area because plaque grows toward the outer vessel wall (figure 2.6). Although seemingly harmless on arteriography, expansive remodeling is associated with high-risk plaques and ruptured plaques observed in acute coronary syndromes [44,58,59]. With excessive expansive remodeling, there could be a paradoxical increase in lumen area that will exacerbate the low shear stress environment, which in turn will lead to a perpetuating cycle of increased LDL accumulation, inflammation, outward remodeling, and fibrous cap thinning [60].

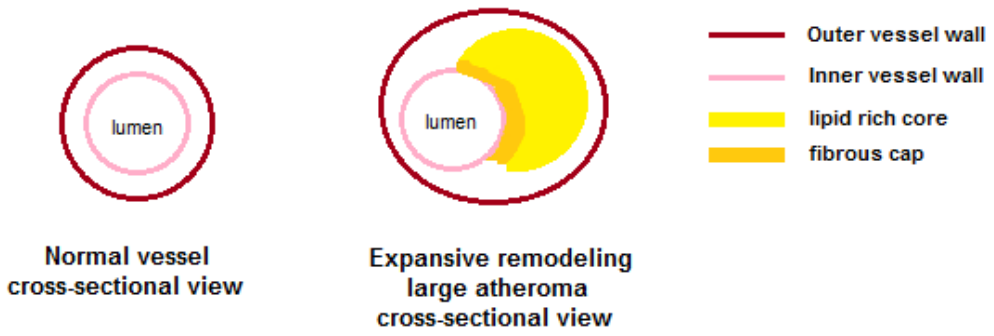

Figure 2.6: Expansive (outward) vessel remodeling with minimal change in lumen diameter.

2.6. *Clinical Consequences*

The mechanism of an acute clinical event partially depends on the type of vessels involved and plaque stability. In general, small arteries occlude (microatheroma), medium-sized arteries form VPs that thrombose or embolize, and large elastic arteries like the aorta often have plaques with outer vessel wall degeneration, leading to aneurysmal dilation, thrombosis, ulceration and/or vessel rupture[20]. Acute clinical consequences of atherosclerotic disease include myocardial infarction (heart attack), cerebral infarction (stroke), aortic aneurysm rupture, acute limb ischemia (peripheral vascular disease), and renal failure. Chronic obstruction of blood flow due to a significant stenosis leads to chronic oxygen insufficiency of the tissues downstream; this mechanism underlies chronic ischemic heart disease (angina and heart failure), ischemic encephalopathy (dementia), bowel ischemia, claudication and gangrene of the lower limbs.

It is important to note that not all vulnerable plaque thromboses lead to ischemic events [61]. This is because there could be formation of collateral circulation, or the thrombus formed at the plaque surface could be small, non-occlusive, and become an organized thrombus that heals with plaque progression. Hence, for clinical prospective studies, the frequency of VPs detected is expected to be higher than the incidence of ischemic events.

[20] Aortic artery aneurysm rupture is a serious condition because it leads to massive internal bleeding and high mortality. Immediate surgical operation is required.

2.7. *Prevention*

The natural history of atherosclerosis begins in childhood, and development of atherosclerotic plaques requires decades. Not all people suffer symptoms or consequences from atherosclerosis; some may have small stable plaques that never cause disorders. Traditional risk factors for coronary atherosclerotic disease are helpful in determining and treating those at high risk, but remain poor predictors of first-time stroke or cardiac event [62-65]. Epidemiologically, atherosclerosis has a prolonged subclinical (incubation) phase; this provides the opportunity to screen for presence of asymptomatic (subclinical) disease. The Screening for Heart Attack Prevention and Education (SHAPE) Program recommends non-invasive screening of asymptomatic patients 45 years of age and older to detect subclinical VP [66]. This is also valuable for stroke prevention associated with carotid atherosclerosis. If subclinical VP could be reliably identified before the advent of stroke, then asymptomatic patients at high risk could benefit from an effective prevention treatment strategy, progression of VP could be halted, and the incidence of acute ischemic events could decrease (figure 2.7).

To screen for VP, a low-risk, cost-effective validated technique is required. Numerous types of experimental non-invasive imaging techniques are currently being developed for this purpose, but none has yet been validated for widespread clinical use. Discussion of each of these non-invasive imaging techniques is presented in the following chapter.

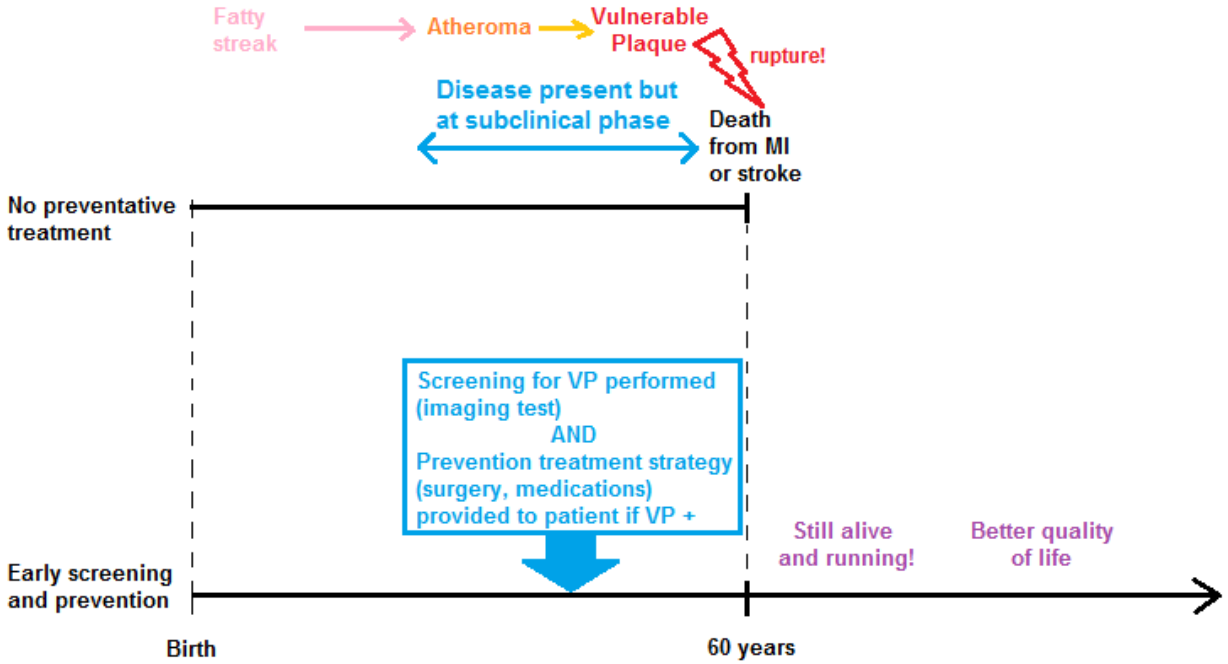

Figure 2.7: How primary prevention could be effective in high-risk patients with no warning symptoms. If atherosclerosis is not detected at the subclinical phase, and a sudden rupture of a VP develops, for example at 60 years of age, a potentially fatal clinical ischemic event will occur. On the other hand, if screening for VP and effective preventative therapy are offered early (during the "blue" subclinical phase), the atheroma will be less likely to evolve into a thrombotic plaque, the risk of having a clinical ischemic event at the same age will be lower, and the patient will have a prolonged and better quality of life.

CHAPTER 3

Imaging Carotid Atherosclerotic Plaque

3. Imaging Carotid Atherosclerotic Plaque

3.1. *Introduction to the manuscript*

The manuscript presented in section 3.2 is a slightly longer version of the final article that will be submitted to the Canadian Association of Radiologists Journal (CARJ). In addition, appropriate formatting of images will be performed for submission. The images of section 3.2 are the same as those that will be submitted with the final article to the CARJ. Finally, please note that the introductory paragraphs of the article, including those describing vulnerable plaque and pathophysiology, contain information already detailed in Chapters 1 and 2 of the current thesis. These paragraphs have been kept in order to maintain the entirety of the article to be submitted.

3.1.1. A brief overview of basic principles of ultrasound, CT, and MR imaging

Ultrasound

The principles of diagnostic ultrasound imaging lie within a sequence of events, beginning with the production of a high-frequency sound wave (typically 5-15 MHz) by transducer elements, transmission and propagation of this wave in tissues, reflection of sound wave signals back to the transducer, transmission of electrical signals to the scanner for processing, and ending with formation of an image. Image formation is based on time to echo arrival (depth of reflecting interface), and signal amplitude (brightness). Acoustic impedance (z) is responsible for the amplitude of reflected sound waves; it is proportional to both tissue density and tissue speed of sound. A tissue such as bone (dense

and high speed of sound) has high acoustic impedance compared to muscle or water (less dense and slower speed of sound). Consequently, the incident ultrasound beam is poorly transmitted through bone and predominantly reflected back to the transducer, resulting in a bright, white signal. Tissues deep to bone will be shadowed by it (acoustic shadowing) and therefore appear black. Water has lower acoustic impedance and reflects minimal signal back to the transducer. Hence, when examining carotid plaques, the blood flow in the lumen will appear black, muscle and other tissues will appear gray, and calcified areas of plaque will appear white. B-mode ("brightness mode") ultrasound scanning provides a two-dimensional image mapping brightness and location of reflecting interfaces, allowing assessment of tissue morphology. Pulsed wave (PW) Doppler imaging, a technique that evaluates blood flow velocity with the Doppler principle, is often combined with B-mode US; together the technique is called Duplex ultrasound. Color and Power Doppler imaging detect direction of blood flow and amplitude of Doppler signal, respectively, with colour-coding superimposed on B-mode images. These latter two techniques are sensitive to detect blood flow in carotid near-occlusions and anatomically tortuous vessels.

Contrast agents in US imaging consist of acoustically-active microbubble particles. These microbubbles are 2 to 5 μm in diameter, and consist of inert non-toxic gas (e.g. sulfur hexafluoride, perfluorocarbon) encapsulated within a lipid shell of phospholipids. When under an ultrasound field, microbubbles expand and compress rhythmically, producing increased amplitude of the reflected signal detected by the transducer, thereby improving image resolution [67,68].

Elastography

Palpation is a common physical exam maneuver to determine tissue rigidity and presence of disease; it has been practiced by physicians for millennia.

Elastography uses the same principle: it is a measure of the elastic deformation of biological tissues and gives us an idea of their rigidity. The physical principle is mathematically described by the tensile (elasticity) modulus, Young's modulus, *E* (Pascal units), which is a measure of tissue rigidity. It is equivalent to the stress applied to the tissue (σ, sigma) divided by the deformation of tissue (ε, epsilon) (Figure 3.1). In a soft tissue, a defined stress σ will produce a deformation ε. In a more rigid tissue, the same stress σ applied will produce a smaller ε deformation. Hence each tissue has its signature stress-strain curve and rigidity.

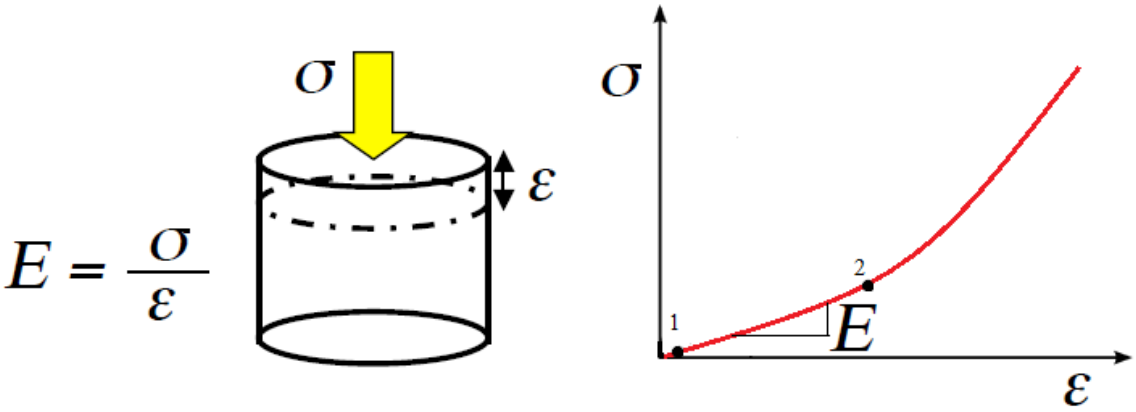

Figure 3.1. Scheme explaining relation between stress, strain and elastic modulus in an isotropic elastic material. A corresponding stress-strain curve is plotted. Beyond a certain compression force (dot "2" on the graph), the material loses its elastic behaviour, i.e. it does not return to its original length. 1 = true elastic limit; 2 = elastic limit.

Computed Tomography

The word "tomography" signifies "to graph a slice". Computed tomography (CT), also termed computed axial tomography (CAT), refers to an imaging technique that uses X-ray images of transverse slices. Images are acquired with a spinning X-ray tube and detector positioned opposite to each other in a gantry; this provides a series of image slices processed in real time by a computer, from which 3D images can be generated (Figure 3.2).

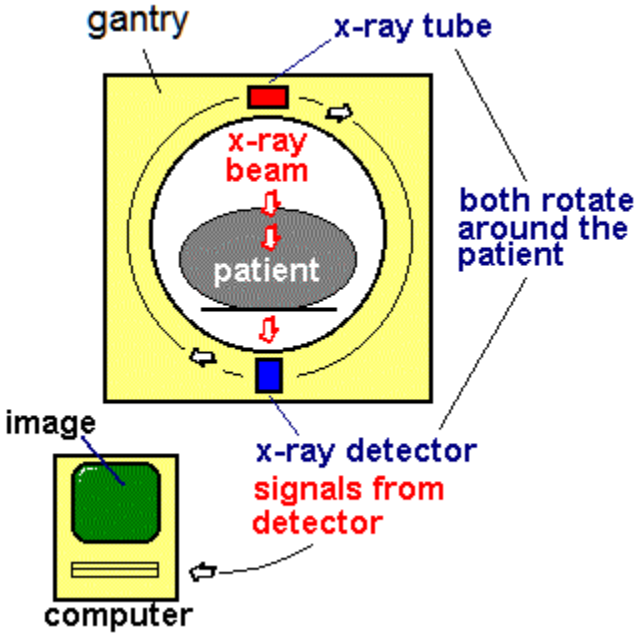

Figure 3.2. How a CT machine works. Adapted and modified from: http://www.bchsys.org/bchserv/Imaging/CT

Modern CT scanners, called spiral or helical CT, perform continuous image acquisition of one cross-sectional image at a time simultaneously with table movement through the gantry (the table is where the patient lies). Later, in the late 1990's, CT scanners were improved by adding multiple spinning detectors that could produce a greater number of image slices simultaneously, decrease image acquisition time, improve spatial resolution, and allow a larger anatomic coverage for arterial imaging by CT angiography (CTA) without intervening venous contrast enhancement. Such CT scanners are termed multi-detector helical CT (MDCT). For both CT and simple X-ray imaging, image interpretation is based on examining tissue densities. Dense tissues such as bone and calcifications appear bright in images because they absorb more X-rays; in other words, they are more attenuating. Conversely, less dense materials, such as air, will appear black. CT can provide an actual measure of tissue density (X-ray absorption or attenuation) per image pixel with Hounsefield units (HU). Bone is at least 400 HU, water is 0 HU, and air is

approximately -1000 HU. Intravenous injection of iodine-based contrast media, which appears bright, helps better depict pathologies by optimizing image contrast and visualization of blood vessel lumina.

Magnetic Resonance Imaging (MRI)

MRI is based on nuclear magnetic resonance. A few definitions will help understand this concept. A magnetic field, *B*, is a force that is created by a rotating electrical charge. For example, the nuclei of atoms rotate around their own axes and produce a magnetic field. In the human body, the most prevalent atom and the one with the highest rotation frequency per magnetic force (gyro magnetic ratio, 42.6 MHz per Tesla) is hydrogen. The hydrogen nucleus consists of a single proton that spins (rotates); accordingly, the hydrogen atom is often termed "spin". All spins in the body are randomly aligned in a manner that maintains magnetic forces in equilibrium. MR images are produced from these spins. MRI uses a large magnet in which the patient is placed. A homogeneous magnetic field, B_0, is applied inside the magnet. In response, spins align in parallel with this magnetic force: a little over half align in the same direction as B_0 (low-energy state), and the remainder align in the opposite direction (high-energy state). This results in a net magnetization in the same direction as B_0. This *net magnetization* can be manipulated to obtain images, following four main steps:

1. **Excitation**

   This consists in sending a radiofrequency (RF) pulse by a gradient coil at a specific frequency that spins will respond to; in other words, *resonance* of nuclei occurs. Spins absorb energy from the RF pulse; as a result, part of the net magnetization is flipped in another direction.

2. **Relaxation**

Spins attempt to return to their initial low-energy state by releasing the energy they absorbed. This released energy is in the form of RF waves. Depending on which vectorial direction of emitted energy is examined, different types of relaxation occurring simultaneously can be recorded (T1 or T2 relaxation).

3. **Acquisition**

   RF waves emitted during relaxation are picked up by a radiofrequency receive coil. An RF coil can be designed for imaging of specific parts of the body, such as a head coil or a dedicated neck coil to examine carotid arteries. It can also function as both an emitting and receiving RF coil.

4. **Computing and Display**

   The RF waves are analyzed and multiple algorithms are applied to translate these RF signals into an image displayed on the monitor, ready for interpretation.

MRI parameters can be manipulated to optimize visualization of certain pathologies based on their respective physico-chemical properties. Multiple sequence parameters can be modified, such as flip angle, repetition time, echo time, inversion time, field of view, matrix size, resolution, gradient switches and signal collecting. Hence, different types of *pulse sequences* can be created, each of which can be tailored to a specific contrast weighting, for example (Turbo) Spin Echo sequences (Proton density-, T1- and T2-weighted contrast images) and Inversion Recovery sequences (T1-weighted, fluid attenuated, and short inversion recovery contrast images). New pulse sequences are continuously being developed in research to optimize contrast resolution of targeted pathologies.

Interpretation of MRI is based on molecular structure and strength of chemical bonds of hydrogen atoms, which affect spin relaxation rapidity and therefore

signal intensity. Furthermore, image interpretation also depends on the pulse sequence and contrast weighting. For example, on T1-weighted images, water appears dark and fat appears bright, whereas on T2-weighted images, water appears bright and fat appears dark. Structural anatomy is well-depicted on T1 images, whereas pathologies producing surrounding edema are well-depicted on T2 images (edema consist of water and water is hydrogen-rich). In MRI, there are no absolute values of tissue brightness like in CT where brightness is representative of density. Rather, MRI interpretation uses relative signal intensities of regions of interest (ROIs) that are compared to a reference tissue intensity in the same image. The chosen reference tissue often is skeletal muscle, such as sternocleidomastoid muscle in neck imaging. Hence, ROIs are described as hyperintense, iso-intense, or hypointense to the reference muscle. Injection of gadolinium-based contrast agents helps optimize contrast resolution and visualize the lumen of blood vessels in a similar manner as CT. The main advantages of MRI over CT imaging include its excellent contrast resolution in soft tissues, lack of ionizing radiation, better-tolerated contrast agents, and possibility to choose any plane of imaging. However, MRI requires longer acquisition times and has a lower spatial resolution than CT. Thus, MRI is better at imaging soft tissues and CT is better at imaging bony structures.

3.1.2. Role of authors

Maxime Douziech, MD, PhD: original author of this review article. He performed literature review and wrote the manuscript. This manuscript was submitted for publication in 2008 to *Radiographics* (refused), and later to *American Journal of Roentgenology* (refused).

Cyrille Naim, MD: performed update of literature review and provided major corrections and changes to the manuscript. I will correct and format figures and submit this manuscript to the *Canadian Association of Radiologists Journal* as a review article.

Gilles Soulez, MD, MSc: senior supervising author. He performed literature review and corrections for the manuscript.

3.2. *Review article manuscript submitted to CARJ*

Manuscript title:

Vulnerable Atherosclerotic Carotid Plaque Evaluation by US, MDCTA and MRI: An Overview

Abstract

Ischemic syndromes associated with carotid atherosclerotic disease are often related to plaque rupture. The benefit of endarterectomy for high-grade carotid stenosis in symptomatic patients has been established. However, in asymptomatic patients, the benefit of endarterectomy remains equivocal. Current research seeks to risk stratify asymptomatic patients by characterizing vulnerable, rupture-prone atherosclerotic plaque. Plaque composition, physiology and biomechanics are studied by non-invasive imaging techniques such as magnetic resonance imaging (MRI), computed tomography (CT), ultrasound (US), and ultrasound elastography. These techniques are at a developmental stage and have yet to be used in clinical practice. This review will describe non-invasive techniques in US, MRI, and CT imaging modalities used to characterize atherosclerotic plaque, and will discuss their potential clinical applications, benefits and drawbacks.

Introduction

Stroke ranks third among all causes of death after cardiac disorders and cancer in western countries [11]. Of all strokes, 87% are ischemic [1], and an estimated 20% are caused by carotid atherosclerotic disease [10]. Symptomatic extracranial internal carotid artery (ICA) occlusive disease is currently managed by carotid endarterectomy (CEA), using severity of ICA luminal stenosis as an indication, based essentially on the results of the North American Symptomatic Carotid Endarterectomy Trial (NASCET) [21] and European Carotid Surgery Trial (ECST) [69,70]. According to NASCET, symptomatic patients with carotid stenosis of less than 50% had an 18% risk of stroke at 5 years under medical treatment. This risk climbed to 22% for 50 to 69% stenosis, and 26% for 70 to 99% stenosis at 2 years [21].

In asymptomatic patients, however, indications for carotid endarterectomy (CEA) remain controversial. The annual risk of stroke or stroke-related death in asymptomatic patients with >60% stenosis is approximately 2% (11-12% at 5 years and 17.9% at 10 years) [26-28]. In addition, stenosis severity is a poor predictor of fatal or non-fatal stroke in asymptomatic patients [26,28]. Medical treatment for atherosclerotic disease has improved over the past 20 years, especially with lipid-lowering therapy. In Halliday et al.'s study, a subgroup analysis of the medical therapy patient group revealed that patients who were already on lipid-lowering therapy at study onset had a lower risk of stroke at 10 years in comparison to those who did not receive such therapy before study onset (14.5% versus 24.9%) [28]. However, when comparing each medical therapy group with the surgical therapy group, CEA still offered significant benefits at 5 and 10 years [28]. Hence, choosing the most appropriate treatment to prevent stroke in asymptomatic patients continues to pose a significant challenge for physicians. Given that a large proportion of asymptomatic carotid stenoses do not have warning signs before the advent of a stroke [31], and that

stenosis severity and clinical risk factors are still insufficient to decide on optimal management, further risk stratification of asymptomatic patients is required. Coronary artery literature [33] and more recently carotid atherosclerosis studies [48,54] suggest examining pathology of atherosclerosis non-invasively to help determine which patients would benefit from early intervention. For instance, an imaging screening test could be performed to characterize carotid plaque when evaluating an asymptomatic patient with a carotid stenosis. Consequently, patients with a vulnerable plaque prone to causing an ischemic stroke could be managed with early CEA, and those with stable-appearing plaques could be managed medically.

Plaque imaging is becoming increasingly used in clinical studies and trials; therefore, radiologists involved in the management of cerebrovascular diseases need to be aware of the pathophysiology of atherosclerotic carotid disease and the development of non-invasive imaging techniques that can characterize atherosclerotic plaques. This review will provide a basic understanding of atherosclerosis pathology, the concept of vulnerable plaque, and will describe non-invasive imaging techniques in US, MRI, and CT imaging modalities used to characterize atherosclerotic plaque. The potential clinical applications, benefits and drawbacks of each technique will be discussed; this will offer readers a better outlook on technical developments to come.

The Vulnerable Atherosclerotic Plaque

The term vulnerable plaque (VP) emerged over 20 years ago to describe an atherosclerotic plaque that is susceptible to rupture, thrombose, and subsequently cause a cardiac ischemic event [46]. Culprit coronary plaques that cause acute coronary syndromes were retrospectively identified in pathology studies [44]. The features of these culprit lesions were plaque rupture (65-70%), plaque erosion (25-30%), and superficial calcium nodule (2-

5%) [44]. Based on these findings, different possible VPs and major and minor criteria defining VP were proposed (Table III-I and Figure 3.2.1) [33]. Briefly, a VP either has a ruptured fibrous cap, a large lipid core with a thin fibrous cap, or intraplaque hemorrhage. The concept of VP is also applied to carotid atherosclerotic lesions associated with cerebral ischemic events; these lesions were found to have a similar histopathology to culprit coronary plaques [48].

Table III-I. Criteria Defining Vulnerable Atherosclerotic Plaque*

Major criteria
Active inflammation
Thin cap with large lipid core
Endothelial denudation with superficial platelet aggregation
Fissured plaque
Stenosis >90%
Minor criteria
Superficial calcified nodule
Glistening yellow (seen on angioscopy)
Intraplaque haemorrhage
Endothelial dysfunction (measurement of flow-dependent coronary artery dilatation and other emerging techniques)
Outward (positive) remodelling

*Presence of at least one major criterion qualifies a plaque as vulnerable
Adapted from data published in reference [33]

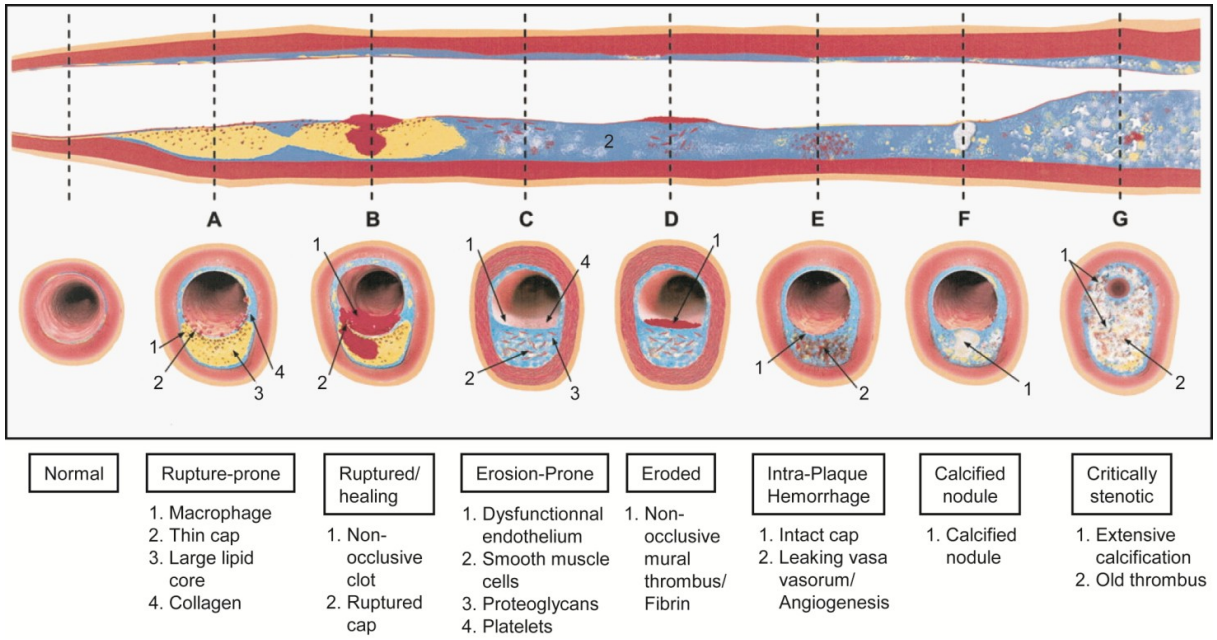

Figure 3.2.1. Different Types of Vulnerable Plaque

(A) Rupture-prone plaque with a large lipid core, a thin fibrous cap and macrophages. (B) Ruptured plaque with a sub-occlusive thrombus and ruptured cap. (C) Erosion-prone smooth muscle cell-rich plaque with a proteoglycan matrix. (D) Eroded plaque with a sub-occlusive thrombus. (E) Intra-plaque haemorrhage from the vasa vasorum. (F) Calcified nodule protruding into the vessel lumen. (G) Chronic critically stenotic plaque with extensive calcification and an old thrombus. ***Adapted from Naghavi et al with permission [33].***

Pathophysiology of atherosclerosis

Endothelial activation and leukocyte recruitment

Atherosclerosis is a chronic systemic inflammatory disease of large and medium-sized arteries. It is characterized by thickening of the arterial wall due to an accumulation of lipids and fibrous elements [34]. The formation of atherosclerosis lesions is complex, involving processes such as shear stress, endothelial dysfunction, inflammation, neovascularisation, and thrombosis. The modified AHA classification of atherosclerotic lesions summarizes the natural history of atherosclerosis (Table III-II) [42-44].

Table III-II. Modified AHA classification

Lesion	Description
Type I	Initial lesion with foam cells (intimal xanthoma or fatty streak)
Type II	Fatty streak with multiple foam cell layers
Type III	Pre-atheroma with extracellular lipid pools
Type IV	Atheroma with a confluent extracellular lipid core
Type V	Fibroatheroma
Type VI	Complex plaque with possible surface defect and/or haemorrhage and/or thrombus
Type VII	Calcified plaque
Type VIII	Fibrotic plaque without lipid core

Adapted from data published in references [42-44]

Under physiological conditions, the endothelium functions as a selective barrier between blood and tissues, inhibits adhesion of leukocytes to the endothelium [55], and is involved in thrombosis and inflammation. In areas of low shear stress and flow turbulence (curved and bifurcating arteries), the endothelium is more permeable to large molecules like low-density lipoprotein

(LDL). Atheromas preferably form in those areas, and their growth is enhanced with elevated serum LDL levels [41].

Endothelial dysfunction triggers oxidation of LDL in the intima and stimulates the overlying endothelium to produce chemotactic factors (interleukins), express adhesion molecules at its surface (vascular cell and intercellular adhesion molecule-1 [VCAM-1 and ICAM-1], selectins) and secrete growth factors (macrophage colony-stimulating factor [M-CSF]). Monocytes and T-lymphocytes from the circulation bind to VCAM-1 surface adhesion molecules [55] and enter the arterial wall by diapedesis. Monocyte-derived macrophages phagocytose oxidized LDL and become foam cells [34]. Foam cells accumulate in layers to form a clinically-silent intimal xanthoma ("fatty streak"). Macrophages also release cytokines and growth factors that induce smooth muscle cell (SMC) migration, proliferation, and production of extracellular matrix (ECM).

Atheroma formation

Confluence of extracellular lipid pools, degenerating foam cells and necrosis of other cells result in formation of a lipid-rich necrotic core. SMCs attempt to "heal" the atherosclerotic lesion by proliferating and producing ECM (collagen and proteoglycans), which covers the lipid core and forms the fibrous cap. With plaque progression, angiogenesis originating from the vasa vasorum takes place to supply oxygen to the growing plaque.

Vulnerable Plaque: From Asymptomatic Atheroma to Culprit Plaque

Plaque vulnerability is associated with unstable plaque morphology, mechanical instability, and inflammation. As endothelial dysfunction continues, the atheroma grows: the lipid core increases in size, neovessels leak

(leading to intraplaque hemorrhage), and macrophages within the fibrous cap secrete matrix-degrading enzymes (matrix metalloproteinases [MMP]). Eventually, the plaque becomes structurally fragile: the fibrous cap thins and ruptures, the thrombogenic lipid core is exposed, and thrombosis at the plaque surface occurs. A thin fibrous cap is defined as less than 65 μm in coronary arteries [44] and less than 200 μm in carotid arteries [54]. In carotid plaques, a large lipid core is defined as an average and minimal plaque area of 40% and 25%, respectively [48,51].

The definition of VP is based on the assumption of plaque features that precede those of culprit plaques. There is no single imaging modality that can characterize all relevant plaque features (morphological, molecular and biomechanical); hence, the best imaging technique to identify the VP is yet to be established.

US, MDCTA and MRI features of plaque vulnerability

Currently, carotid atherosclerosis burden is assessed by measuring luminal stenosis with duplex ultrasound, CTA, MRA, or X-ray angiography, but this measure remains insufficient to risk-stratify asymptomatic patients. Multiple imaging techniques have been developed to characterize plaque composition and identify the key features of vulnerable atherosclerotic plaque. Some techniques (B-mode US, MRI, MDCTA) have been studied to greater extent, whereas others, like targeted contrast agents and non-invasive US elastography, are under investigation.

Ultrasound

Ultrasound (US) is a well-known method of atherosclerotic carotid disease evaluation; it is clinically used to assess the presence of plaque, the degree of

carotid stenosis with blood flow velocity profiles, and the carotid intima-media thickness. Ultrasound is reliable, reproducible, and often the only diagnostic imaging modality used for the assessment of carotid arteries before CEA [71]. It is also a low-cost, low-risk, and an accessible imaging modality that is well-tolerated by patients. The following section will focus on the US evaluation of carotid plaque vulnerability using morphology, echo texture and surface details.

Two-Dimensional B-mode US imaging

Carotid plaque echogenicity has been correlated with plaque composition [72,73]**.** Hyperechoic plaques are considered to contain fibrous or calcified tissue, whereas echolucent plaques are considered to contain soft plaque materials such as lipid or hemorrhage. Stable asymptomatic carotid plaques tend to be homogeneous and echogenic because of their calcium and/or fibrous content. They have a uniform internal architecture and smooth surface contour (Figure 3.2.2a). Unstable symptomatic plaques are associated with an irregular surface and tend to be heterogeneous and echo-lucent [72,74,75] (Figures 3.2.2b, 3.2.3 and 3.2.4).

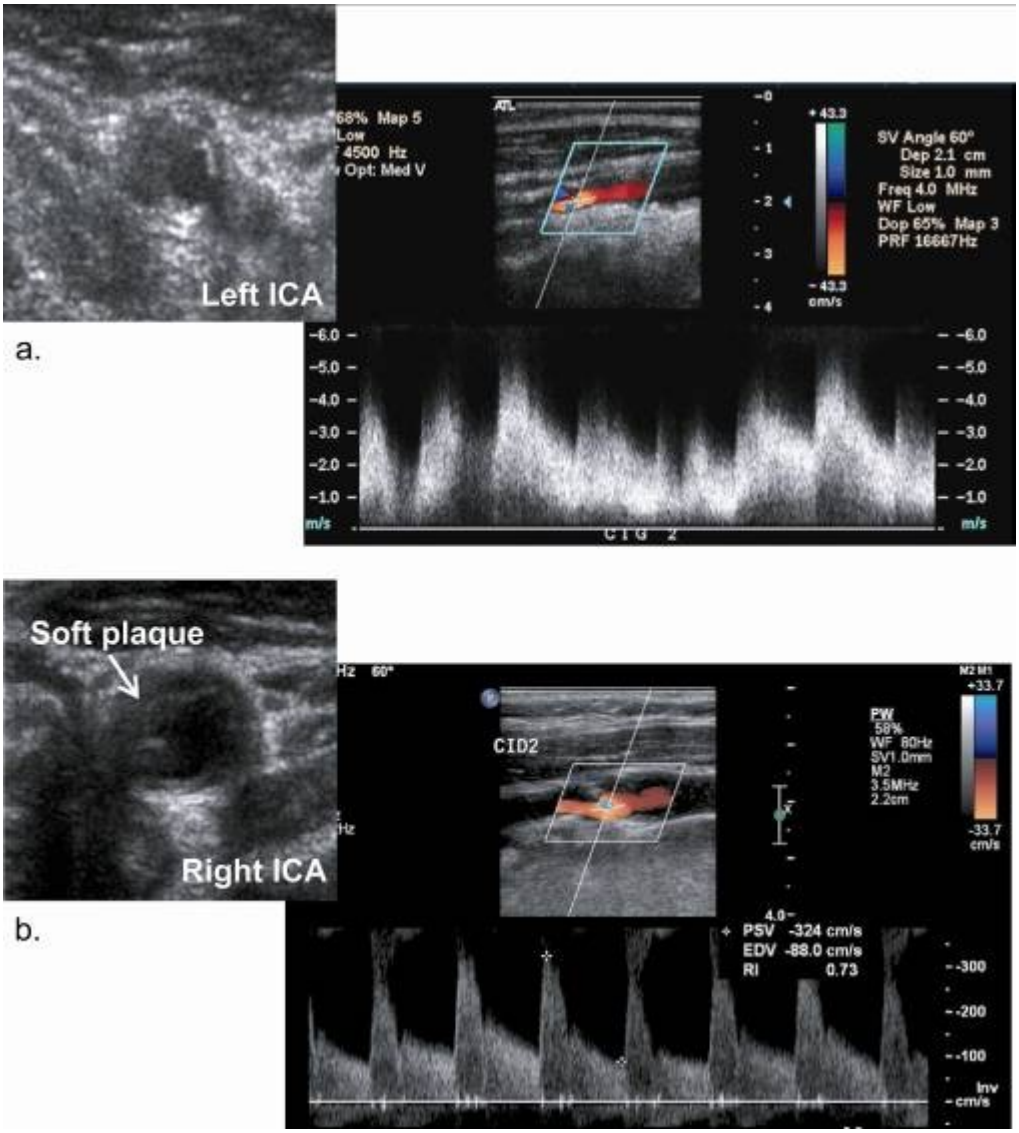

Figure 3.2.2. Doppler ultrasound of carotid arteries of a 46-year-old woman with hypercholesterolemia and transient cerebral ischemia of the right middle cerebral territory. (a) Significant stenosis of the left internal carotid artery from an echogenic homogeneous plaque that narrows the vessel lumen. (b) 80% right internal carotid artery stenosis (in diameter reduction, according to criteria from [76]). The stenotic plaque is echolucent (soft plaque) likely because of its high lipid content, haemorrhage and low calcium content.

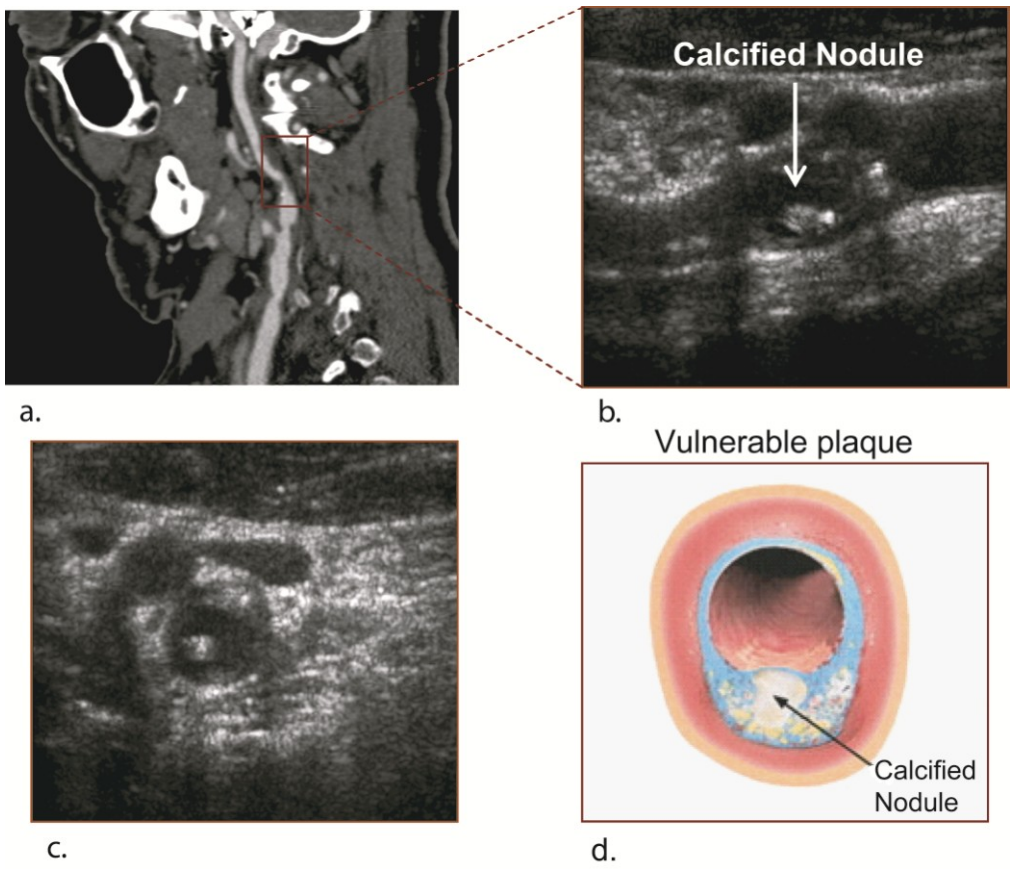

Figure 3.2.3. Doppler ultrasound of the left carotid artery of a 75-year-old asymptomatic man. (a) Sagittal reconstruction of the carotid artery lumen on MDCTA of the left ICA with a small calcified nodule (an inset of this image zoomed in on the lesion will be provided for article submission). (b) Doppler ultrasound longitudinal image of the region of interest (red rectangle in a) showing 70% stenosis. The plaque meets criteria of vulnerability with plaque heterogeneity and a calcified nodule protruding into the vessel lumen. (c) Axial image centered on the calcified nodule. (d) A schematic representation of this plaque showing a calcified nodule protruding into the vessel lumen. Image (d) adapted and modified from [33] with permission.

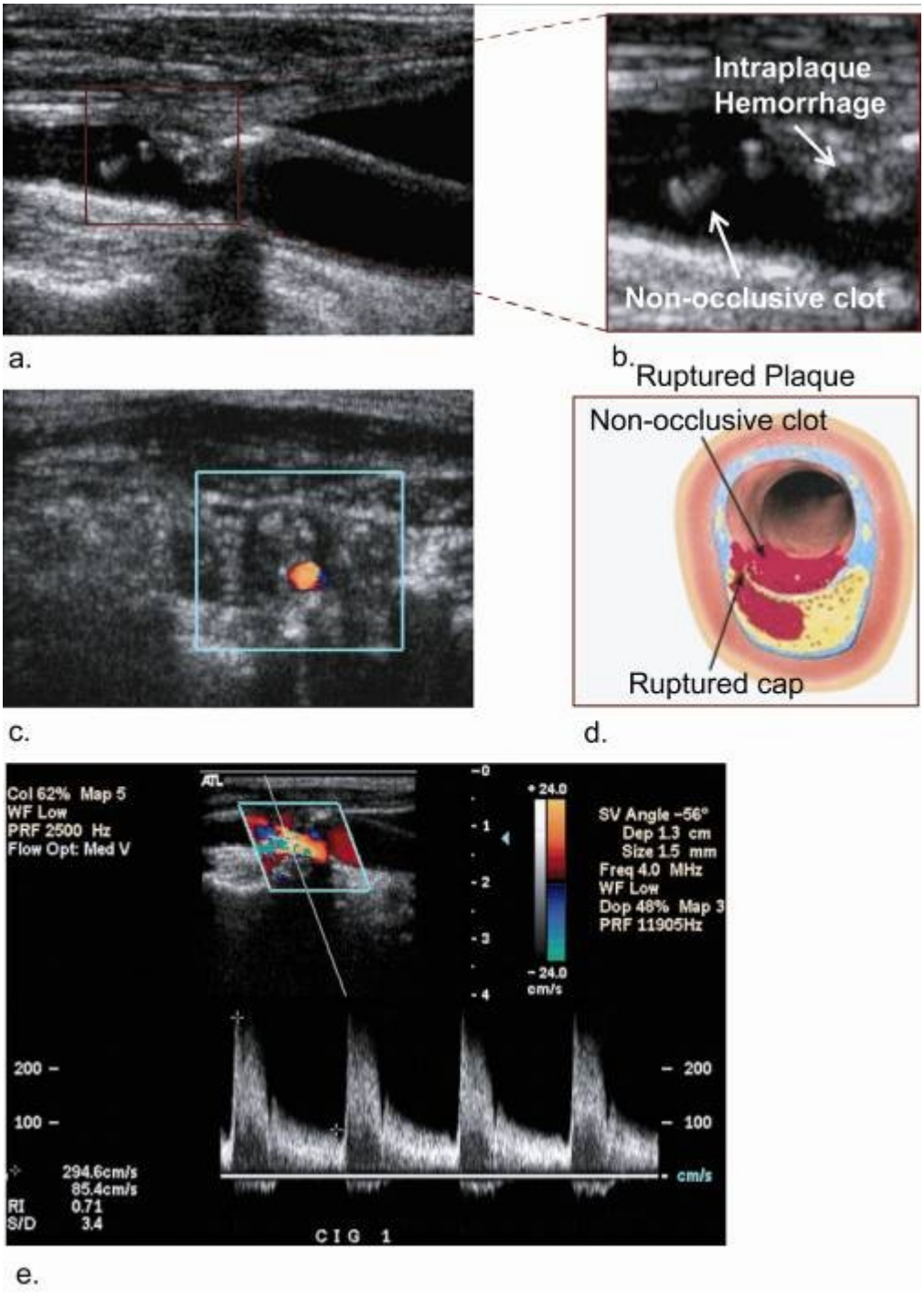

Figure 3.2.4. Doppler ultrasound of the carotid artery of an 82-year-old male with amaurosis fugax and transient left MCA territory ischemia. (a) Ultrasound image showing 75% left internal carotid artery stenosis with ruptured plaque and a non-occlusive clot. (b) Enlargement of the region of interest (red rectangle in a) where heterogeneous plaque can be seen. The echo-lucent zone may reflect hemorrhage or a lipid core. (c) Axial Doppler image centered on the plaque where stenosis is maximal,

showing plaque heterogeneity. (d) Schematic representation of plaque with a non-occlusive clot and ruptured cap may reflect the plaque features seen on ultrasound in this case. This patient has undergone CEA demonstrating a ruptured and thrombotic atheroma intraoperatively. (e) Doppler spectral analysis. Maximal systolic velocity is 295 cm/s. Image (d) adapted and modified from [33] with permission.

Irregular plaque surface or ulcerations could be detected on US with utilisation of color Doppler or gray-scale flow imaging demonstrating eddy flow within the plaque [77]. Gronholdt *et al.* reported that echolucent plaques were associated with increased risk of stroke in symptomatic patients with significant stenosis (relative risk (RR) of 4.2 at 4 years) [78]. Other studies reached similar conclusions [79-81], but the Asymptomatic Carotid Stenosis Trial (ACST) revealed no association between ipsilateral stroke and echogenicity [27]. These conflicting results could be explained by limited reproducibility of B-mode ultrasound [82] associated with operator-dependent technique and subjective characterization of plaque echogenicity. A more reproducible way of objectively measuring echogenicity is gray-scale median scores. Gray-scale median (GSM) scores measure plaque echogenicity by assessing overall plaque brightness from the frequency distribution (histogram) of gray-level pixels within the plaque. The technique for comparing plaque echogenicity involves standardization of B-mode images and adjustment with the signals from blood (GSM = 0) and adventitia (GSM = 190) [74,78]. Correlations between subjectively echolucent plaques and low GSM score have been found, with an association between them and symptomatic plaques [74,83,84]. Moreover, a significant inverse relationship between GSM scores and the percentage of necrotic core areas was found [83]. There are many limitations B-mode ultrasound. First, GSM measures can be affected by settings like time-gain compensation and log compression. Ideally, tissue echogenicity should be analysed by an appropriate processing of the raw radio-frequency (RF) data, such as Integrated Backscatter (IBS) [85] or Pixel

Distribution Analysis (PDA). Second, GSM does not take into account plaque heterogeneity. Echo-texture analysis, a computer-aided system that can characterize both echogenicity and heterogeneity, can detect focal hypoechoic areas [86,87]. However, calcifications impair echo-texture analysis. Finally, 2D imaging limits visualization of areas of interest.

Three-Dimensional B-mode US Imaging

Three-dimensional ultrasound of carotid arteries has been developed and validated to measure plaque volume and vessel wall volume (VWV) changes over time [88-90]. This technique uses a conventional transducer that produces two-dimensional images in the composite imaging (SonoCT) mode [89,91]. Composite imaging (SonoCT) is an ultrasound mode that acquires several images based on transmitted ultrasound waves, resulting in a single composite image. This mode helps reduce speckle artefact and sharpens tissue boundaries. The probe, attached to a mechanical motorized mover, is displaced along the neck at a constant speed of 3 mm/s while two-dimensional image frames are acquired at regularly-spaced intervals. Image reconstruction and multiplanar reformatting provide 3D images that can be segmented manually or automatically, one cross-sectional slice at a time. To determine plaque volume, each slice area is computed, summed with all other slice areas, and multiplied by inter-slice distance [89,91]. A semi-automated segmentation algorithm was developed and validated to measure VWV, and considerably reduced operator time [92]. The effect of pharmacological agents on plaque volume assessed by three-dimensional ultrasound (3D US) was demonstrated over short periods of time (3 to 6 months) with cilostazol (antiplatelet agent) [93] and atorvastatin [89,94]. Even with small sample sizes of less than 40 patients, these medications showed a significant decrease in plaque volume in comparison to placebo groups, making 3D US plaque volume assessment more effective than intima-media thickness in detecting size differences over time. Finally, 3D US was more effective than 2D US in detecting plaque ulcers [95], and can quantify and follow-up 1 mm ulcerations [91]. More studies with 3D

US are warranted to validate its ability to assess plaque composition, surface morphology, and vulnerable plaque before use in large clinical studies.

Contrast-enhanced US

Microbubble contrast agents are strictly intravascular: they help better outline lumen contours and can penetrate microvasculature. Kono et al. found that contrast-enhanced US (CEUS) imaging depicted unsuspected wall irregularities and ulceration [96], but this is not yet validated with histology. Visualization of neovascularisation within plaque has also been achieved (Figure 3.2.5). Significant correlations were found between the degree of intra-plaque contrast-enhancement on US and amount of angiogenesis on histopathology [97-99]. Increased US contrast-enhancement in the plaque also correlated significantly with symptomatic carotid plaques [100,101], cardiovascular disease, events and risk factors [102], and echolucent plaques [103].

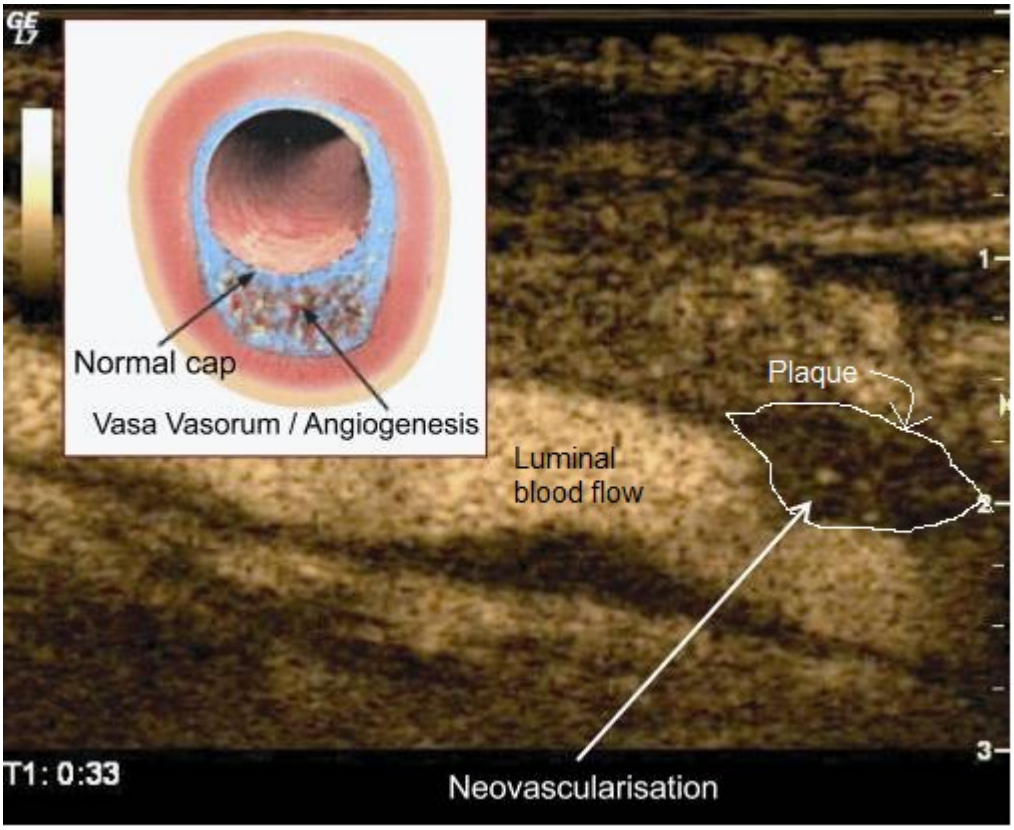

Figure 3.2.5. Carotid artery contrast-enhanced ultrasound. Hyperechoic foci within the plaque represent neovessels. Sonovue® is an aqueous suspension of stabilized sulfur hexafluoride (SF6) microbubbles (precontrast image currently unavailable for pre and post-contrast comparison). Courtesy of Christian Greis, Bracco Diagnostics. The color image is a schematic representation of vulnerable plaque with a normal cap and neovessels. Schematic inset adapted and modified from [33] with permission.

Molecular imaging can also be achieved with CEUS by designing microbubbles with monoclonal antibodies in their lipid shell. Antibodies targeted to VCAM-1, ICAM-1, selectins, and CD81 expressed by endothelial cells provided an in vivo assessment of endothelial dysfunction in animals and humans [104-106] and plaque proteolysis [107]. Shalhoub and al. demonstrated the use of late-phase CEUS and microbubbles targeted to CD31 (angiogenesis marker) and CD68 (macrophage inflammation marker) and significant correlations with immunohistological staining [108]. More studies on CEUS molecular imaging are required to determine if the detected

endothelial dysfunction or neovascularisation can predict cerebral ischemic events.

Drawbacks of CEUS include rare and minor side effects such as headache and injection site bruising and pain [109]. There is also a theoretical risk of potentiating plaque instability, since a small number of microbubbles destroyed during US scanning can potentially damage neovessels and lead to intraplaque hemorrhage [110].

Non-Invasive Vascular Elastography by Ultrasound

Elastography is a map of local deformations of a biological tissue in response to a mechanical stress. Elastography techniques function in three steps: application of a stress (force) on the tissue; measure of tissue displacement (strain) in response to the applied stress; and estimation of tissue elasticity (rigidity). For the same applied stress, rigid tissues will have smaller displacements than supple tissues. The applied force could either be external (compression or dynamic vibration) or internal (natural arterial pulsation or shear wave propagation resulting from an acoustic radiation force). There are two types of elastography: static (or quasi-static) and dynamic. Static elastography consists in measuring the strain gradient between two different levels of stress application [111]. It cannot provide an estimation of the tissue elasticity because the absolute stress force is unknown; instead it displays a map of tissue strain called “elastogram”. In contrast, dynamic elastography estimates tissue elasticity (Young’s tensile modulus) by measuring both strain and the absolute force applied to the tissue.

Ultrasound non-invasive vascular elastography (NIVE) is a quasi-static elastography technique that measures the elastic deformation of the arterial wall. When compressed and relaxed by the natural pulsation of the artery, the displacement between pairs of pre- and post-compression radiofrequency (RF)

lines is estimated and a strain profile can be determined by computing the gradient of the displacement field. The time-varying images obtained are called elastograms [112]. Currently, researchers studying plaque deformations hypothesize that deformations can potentially distinguish symptomatic from asymptomatic plaques and lipid-rich from calcium-rich plaques. A feasibility study showed that maximal strain concentration was located close to the vessel lumen and at the interface between hard and soft materials [113] (Figure 3.2.6).

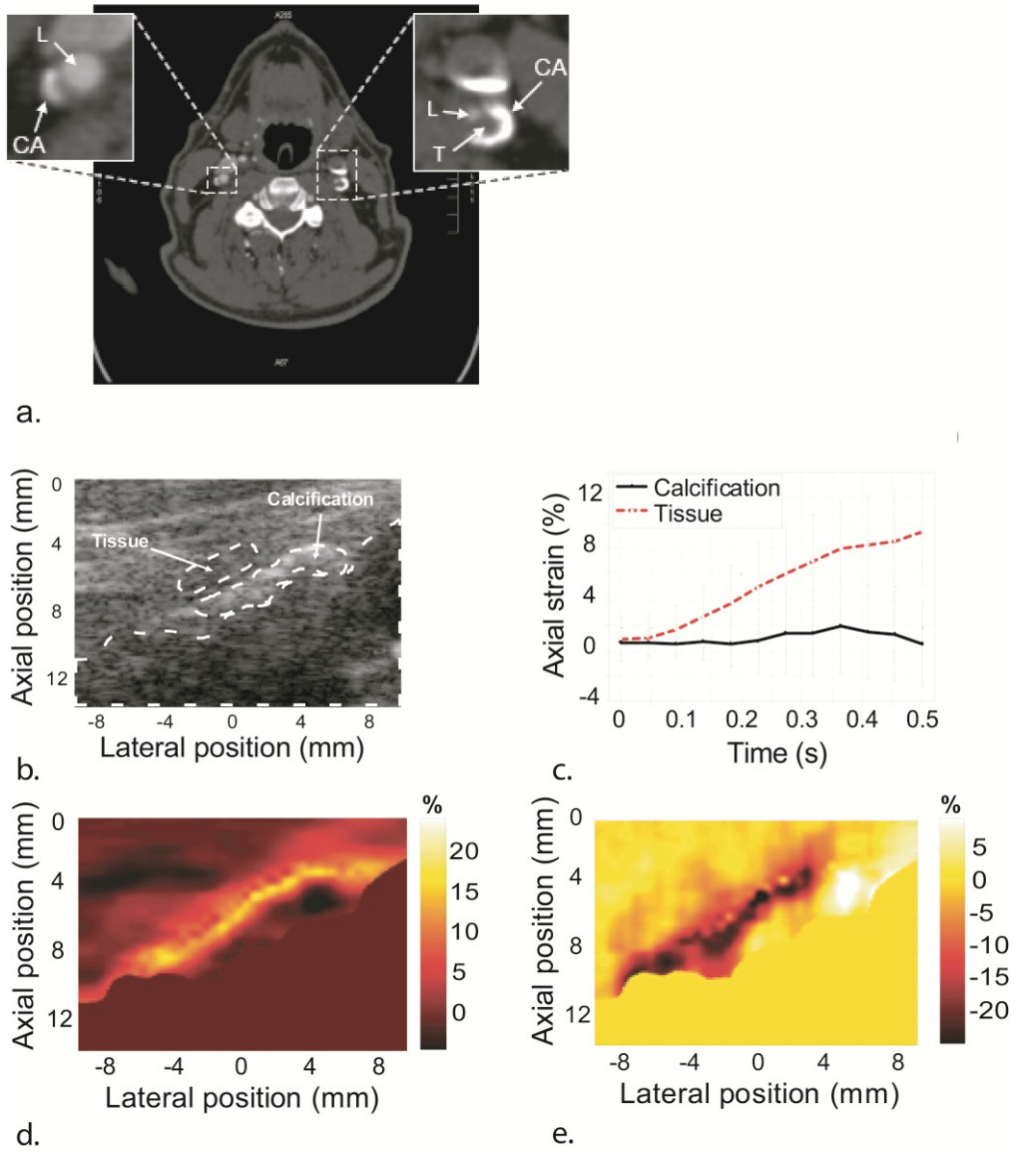

Figure 3.2.6. (a) CT scanner of carotid bifurcation showing a stenosis on the left side surrounded by calcifications. (b) B-mode image of the same plaque from reconstructed raw radiofrequency (RF) signals, used for vascular elastography. (c) Strain profile of

segmented areas in (b). Rigid structures, such as calcifications, have stable cumulative strain values whereas soft plaque areas have increasing cumulative strain values. (d) For the same B-mode image, strain values can be displayed by colour code (elastogram). Dark zones represent calcifications with low strain values. (e) In a similar manner, shear stress (mechanical behaviour at the interface of 2 different structures) can be displayed by color code and help locate areas of high mechanical stress (white and dark areas). T=fibrous tissue; CA=calcification; L=lumen. Adapted from [113] with permission.

The presence of inhomogeneous strain distribution of deformation may hypothetically lead to biomechanical instability and VP. A study by Maurice et al. used US NIVE in vivo to determine arterial wall strain in healthy carotid arteries; higher strains were observed in women and a good inter-observer reproducibility was achieved for common carotid artery strains [114]. Another study on 16 patients compared 2 strain parameters, relative lateral shift and accumulated axial strain, with US-identified calcified and non-calcified plaque areas; there was a greater variability and higher strain values in non-calcified echolucent areas [115]. Vascular cognitive decline was significantly associated with a greater maximum accumulated strain, but with a sample size of 10 patients and analysis of a single cardiac cycle per patient [116]. Currently, methodology of US NIVE differs among authors, such as the choice of ROI and strain parameter, leading to difficulty in comparing results among studies. Recent work on US NIVE technical optimisation has been done, including an improved implementation of the Lagrangian Speckle Model Estimator (LSME) algorithm [117], a semi-automatic plaque segmentation algorithm [118], and the elimination of signal artefacts associated with respiratory motion and noise using power spectrum sampling [119]. More studies are needed to validate US NIVE, notably appropriate visualization and choice of ROIs, as well as elucidating associations between axial strain, plaque composition, and clinical symptoms.

Few dynamic elastography techniques are used for carotid plaque analysis, partly because of their relatively recent technical developments. Acoustic

radiation force imaging (ARFI) consists in generation of an acoustic radiation force of very short duration (less than 300 μsec) to small volumes of tissue, followed by mapping of tissue displacements (< 10 μm) resulting from shear-wave propagation. Limitations of ARFI include the inability to estimate absolute values of displacement and elasticity for comparison among patients [120], and low temporal resolution (low frame rate on commercially available scanners) which may lead to non-representative strain values in arteries since strain varies with the cardiac cycle. Supersonic shear-wave imaging (SSWI) is another dynamic elastography technique also using a radiation force, but with a much higher temporal resolution than ARFI (5000 image frames per second). Instead of measuring tissue displacements, shear wave propagation speed is measured; this provides a more accurate estimation of tissue stiffness. There are no studies of SSWI in patients with carotid atherosclerotic plaques yet, but an in vivo study of the common carotid artery of a healthy subject showed an elevation of the shear modulus (stiffness) at the onset of systole in every cardiac cycle [121].

Multidetector computed tomography angiography (MDCTA)

MDCTA provides an excellent assessment of degree of carotid stenosis, and has the potential to characterize carotid plaque morphology in asymptomatic patients with significant stenosis. The first studies with single slice helical CT showed elevated standard deviations (SD) of plaque component density and low sensitivity for detection of ulcers, likely due to excessive volume averaging [122]. With the advent of multi-slice helical CT, improved resolution resulted in better accuracy of plaque composition assessment (Figure 3.2.7).

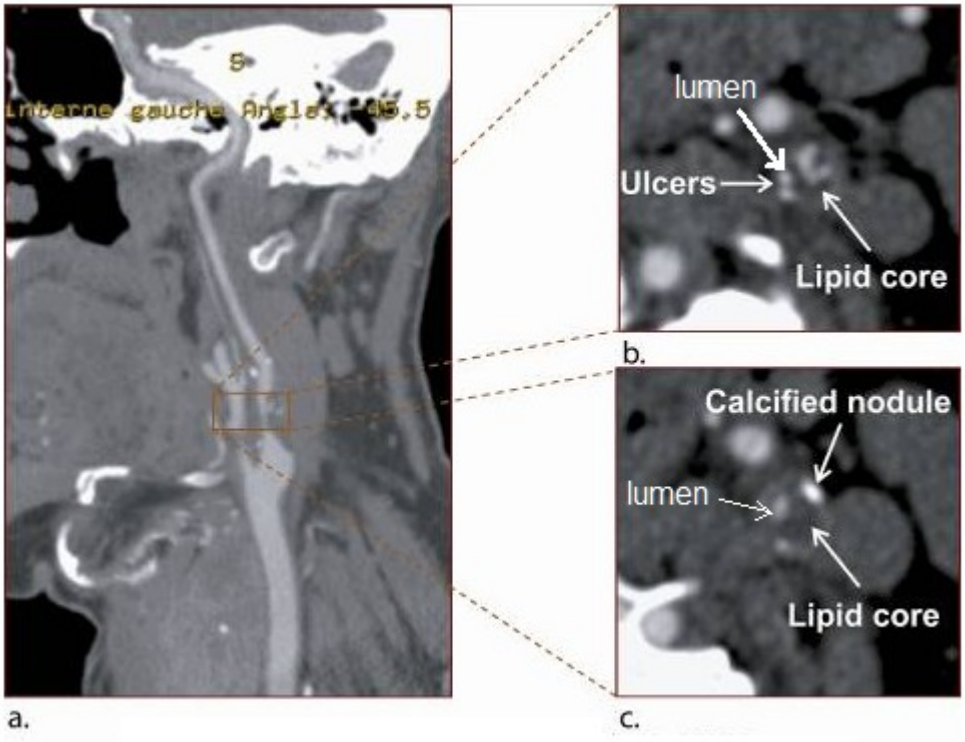

Figure 3.2.7. Patient with left-sided amaurosis fugax. (a) Sagittal reconstruction of the carotid artery lumen on MDCTA. Severe left internal carotid artery stenosis and a small ulceration. (b) and (c) Cross-sectional images from the regions of interest (red rectangle in a). (b) The plaque likely contains a lipid core with an ulcer because the contrast agent in the lumen has an irregular contour. (c) A large lipid core and a calcified nodule are found inferiorly to the image in (b).

The minimal fibrous cap thickness of plaque can be measured on MDCTA (R^2 = 0.77, $p < 0.001$) [123]. It can also detect ulcerations more accurately than US echo color Doppler (93% sensitive and 98% specific; $\kappa = 0.855$) [123,124]. DeWeert et al. demonstrated that MDCTA could quantify calcifications and fibrous tissue with good histological correlation ($R^2 > 0.73$, $p < 0.001$), but could not quantify lipid core except in mildly calcified plaques [125]. Later, the same authors used cut-off attenuation values to identify calcium (>130 HU), fibrous tissue (60-130 HU), and lipid or hemorrhage (<60 HU), and found a good inter-observer variability in plaque and component volume measurements (interclass correlation coefficient (ICC), 0.76 to 0.99;

coefficients of variation <50%) [126]. A classification of plaque into 3 categories (i.e. fatty (<50 HU), mixed (50-119 HU), and calcified (>120 HU)) showed good interobserver agreements [127] and sensitivities of 85%, 89%, and 100% respectively [128]. An automated classification computer algorithm based on a calculated Hounsfield attenuation threshold for each carotid plaque histological component has been reported (Table III-III) [123]. This classification was useful to characterize carotid plaque according to the AHA classification system adapted for CT images (Table III-IV). The authors concluded that MDCTA can accurately evaluate plaque composition compared to histopathology, but could not differentiate lipid cores from hemorrhage except for large plaques that are mainly fatty or hemorrhagic [123]. A study of 31 patients demonstrated that MDCTA with plaque density analysis could detect hemorrhage with 100% sensitivity and 64.7% specificity, but only in plaques that have a median density below 31 HU [129,130].

Table III-III. Hounsfield values (HU) for each plaque component as determined by in-vivo MDCTA studies (mean ± SD)

Study	Lipid core	Fibrous tissue	Intra-plaque hemorrhage (IPH)	Calcium	Chosen cut-offs (HU)
deWeert et al. [125,126]	25±19	88±18	n/d	657±416	>130: calcium 60-130: fibrous <60: lipid or IPH
Wintermark et al. [123]	32.6±20 95%CI (-7, 72)	46±19 95%CI (6, 86)	97±22 95%CI (53, 141)	256±30 95%CI (216, 297)	<39.5: lipid 39.5-72: fibrous 72-177: IPH >177: calcium
Ajduk et al. [129]	median: 59 (range, 6-150)		median: 22 (range, 17-31)	n/d	>31: no IPH <31: IPH

n/d = not determined; CI = confidence interval

Table III-IV. Modified AHA classification for MDCTA [123] and MRI [131]	
Lesion	**MDCTA description**
Type I-II	Thin plaque with no calcification
Type III	Plaque with small lipid cores and no calcification
Type IV-V	Plaque with a large lipid core, covered by a fibrous cap, possible small calcifications
Type VI	Ulcerations and/or wide haemorrhage and/or thrombosis
Type VII	Plaque with a lipid core or fibrotic tissue, with large calcifications
Type VIII	Plaque with fibrous tissue, no lipid core, possible calcifications
Lesion	**High-resolution MRI description**
Type I-II	Near-normal wall thickness, no calcification
Type III	Diffuse intimal thickening or small eccentric plaque with no calcification
Type IV-V	Plaque with a lipid or necrotic core, surrounded by fibrous tissue with possible calcification
Type VI	Complex plaque with possible surface defect, haemorrhage or thrombus
Type VII	Calcified plaque
Type VIII	Fibrotic plaque without lipid core and with possible small calcifications

The major advantages of MDCTA lie in its availability, rapidity, relatively low-cost, ability to measure absolute tissue density, and identify and quantify calcifications with great accuracy. The role of MDCTA in plaque component characterization shows promise, but still lacks specificity in identifying lipid core and intraplaque hemorrhage, especially in calcified plaques. Beam-hardening artefacts associated with calcification alter Hounsfield values and contribute to inaccurate plaque characterization. Although calcified carotid plaques detected by MDCTA are significantly associated with asymptomatic

patients [132], calcification is not an absolute marker of plaque stability. MDCTA is yet to be sufficiently accurate for risk stratification of asymptomatic patients with calcified plaques. Other drawbacks of MDCTA include exposure to ionizing radiation and nephrotoxic iodine-based contrast agents.

Following contrast injection in MDCTA, the lumen of blood vessels and neovessels arising from the vasa vasorum are enhanced. Thus, carotid plaque enhancement has been explored in multiple studies. The association between circumferential plaque enhancement and neovascularisation density on histopathology was recently validated [133]. A retrospective study found that carotid wall circumference enhancement on MDCTA was more frequent in symptomatic or fatty plaques compared to calcified carotid plaques (OR 3.625, p=0.01) [134,135]. However, due to differences in methodology, results from other studies are discrepant. For instance, asymptomatic and fibrous plaques had greater plaque enhancement on delayed-phase images [136], and plaque characterization was significantly different in post-contrast compared to pre-contrast MDCTA, leading to fatty plaques being misclassified as mixed plaques [137].

Macrophage-Designed Nanoparticle Contrast Agents

Plaque evaluation with conventional contrast relies on multiple factors, such as blood flow and time delay of CT image acquisition. They affect intensity of luminal enhancement, which in turn, influences measures of carotid plaque size [138] and density [139], resulting in a large variability of density measures. To overcome this important limitation, researchers have developed N1177, an iodinated nanoparticle contrast agent selectively phagocytosed by macrophages [140]. In rabbits, 2 hours after intravenous N1177 administration, the contrast agent made it possible to visualize macrophage-rich atherosclerotic plaque by increasing plaque density. The same authors later found that the intensity of enhancement of N1177 correlated significantly with increased

glucose uptake on positron-emission tomography (PET)[21] and macrophage density on histology [141]. Another team found that N1177 nanoparticles were only present in macrophage-rich areas of ruptured plaques, but not in those of non-ruptured plaques, suggesting specificity for identifying ruptured atherosclerotic plaques [142]. This technique has not yet been experimented in humans because optimal dosage of N1177 has not been determined; also the required pre- and post-injection image acquisition protocol doubles the radiation dose compared to MDCTA with conventional contrast agents.

High-Resolution Magnetic Resonance Imaging (MRI)

Since the first characterization of atherosclerosis with MRI in 1995 [143], high-resolution MRI of carotid plaques has evolved considerably. Studies with histological validation determined that multi-contrast high-resolution MRI can characterize carotid plaque morphology [144,145], identify and measure plaque components like lipid-rich necrotic core, fibrous cap thickness and calcifications [146-148], and measure plaque progression and regression with a very good accuracy.

MRI can distinguish intermediate from advanced atherosclerotic lesions as defined by the modified version of the AHA criteria for MRI (Table III-IV) [131,149] and vulnerable plaque definition by Naghavi et al. [33]. Important possible predictive features of plaque vulnerability by MRI include thin or ruptured fibrous cap, and intraplaque hemorrhage. The fibrous cap appearance on 3D TOF bright-blood images highly agrees with histological findings [145]. Multi-contrast MRI (T1, T2, PD and 3D TOF) had 81% sensitivity and 90%

[21] FDG-PET is an imaging technique that detects areas with high metabolism of glucose; those areas are associated with high metabolic activity and/or inflammation. This technique only studies molecular process of hypermetabolism (nonspecific), not plaque morphology. FDG-PET was not discussed as it was deemed beyond the scope of this thesis and review article.

specificity for identifying a thin or ruptured cap [150]. Fibrous cap thickness on T1W imaging both pre- and post-gadolinium injection also has a good correlation with histology [148]. A retrospective study showed that ruptured fibrous cap by MRI was associated with recent history of stroke or TIA [151], and a prospective study found an increased risk of development of symptoms in patients with a previously detected ruptured fibrous cap by MR [152].

Intraplaque hemorrhage (IPH) is accurately identified by MRI as a hyperintense signal on T1W turbo field echo images with 93% sensitivity and 96% specificity [153], and on T1W 3D gradient echo images (MR direct thrombus imaging) with 84% sensitivity and specificity [154]. Different stages of IPH could be identified with a high sensitivity but moderate specificity (Table III-V) [155]. Retrospective [156,157] and prospective [158,159] studies demonstrated a strong association between IPH and recent or recurrent cerebral ischemic symptoms. IPH detected in asymptomatic patients was associated with significant plaque progression over 18 months [160]. Moreover, a retrospective study found that Type VI plaque was significantly more frequent in patients with ipsilateral TIA or ischemic stroke [161] and a cross-sectional study found that preoperative vulnerable plaque morphology was more frequent in symptomatic than asymptomatic patients [162]. The MRI signal intensity criteria for identifying plaque components are listed in Table III-V. High-resolution MRI of carotid plaques is presented in Figures 3.2.8 and 3.2.9.

Table III-V. Relative Signal Intensity of Plaque Components on MRI*

	MRI weighting				
Plaque components	**3D TOF**	**T1W**	**T1W post-contrast**	**T2W**	**Proton density**
Lipid-rich necrotic core	+/-	+/- to +	+/-	-	+/- to +
Fibrous tissue:					
Dense matrix	+/-	+/-	+/- to +	+/-	+/-
Loose matrix	+/-	+/-	+/- to +	+	+
Fibrous cap:					
Intact thick	hypointense dark band	+/- smooth	+/- to +	+	+/-
Intact thin	absent dark band	not visible	not visible	not visible	not visible
Ruptured	hyperintense signal at plaque-lumen interface	irregular plaque surface	irregular plaque surface	irregular plaque surface	irregular plaque surface
Intraplaque hemorrhage:					
Fresh (<1 week)	+	+	+	+/- to -	+/- to -
Recent (1-6 weeks)	+	+	+	+	+
Old (>6 weeks)	-	-	-	-	-
Calcification	-	-	-	-	-

+, hyperintense; +/-, isointense; -, hypointense; 3D TOF, 3-dimensional time-of-flight.
*Based on data from [131,144,147,151,155,163]

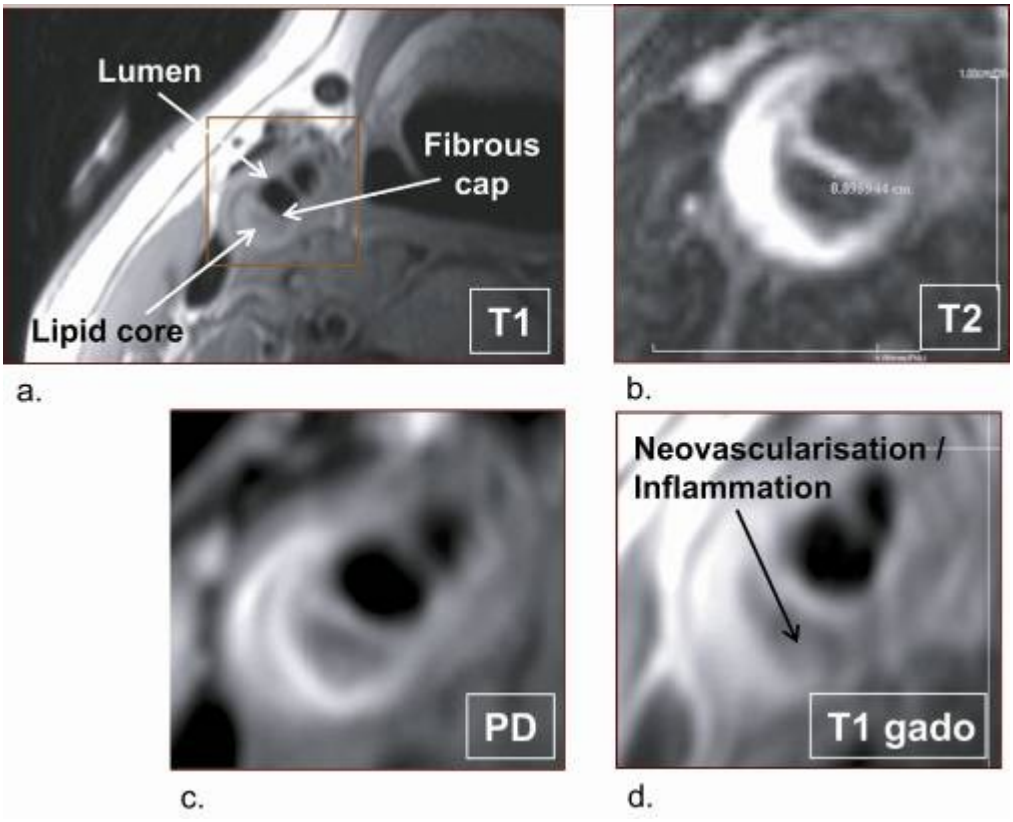

Figure 3.2.8. Cross-sectional high-resolution MRI of an asymptomatic patient's right internal carotid artery plaque. This patient has a 50% stenosis. (a) T1-weighted image showing a thick fibrous cap and large lipid core, easier to depict on the corresponding post-gadolinium injection T1-weighted image in (d). (b) A drop in relative signal intensity on this T2-weighted image (compared to other sequences) characterizes the presence of a lipid-rich necrotic core. (c) Proton density image shows an isointense core. (d) After gadolinium injection, plaque enhancement is observed in the postero-medial aspect of the plaque, suggesting neovascularisation or inflammation.

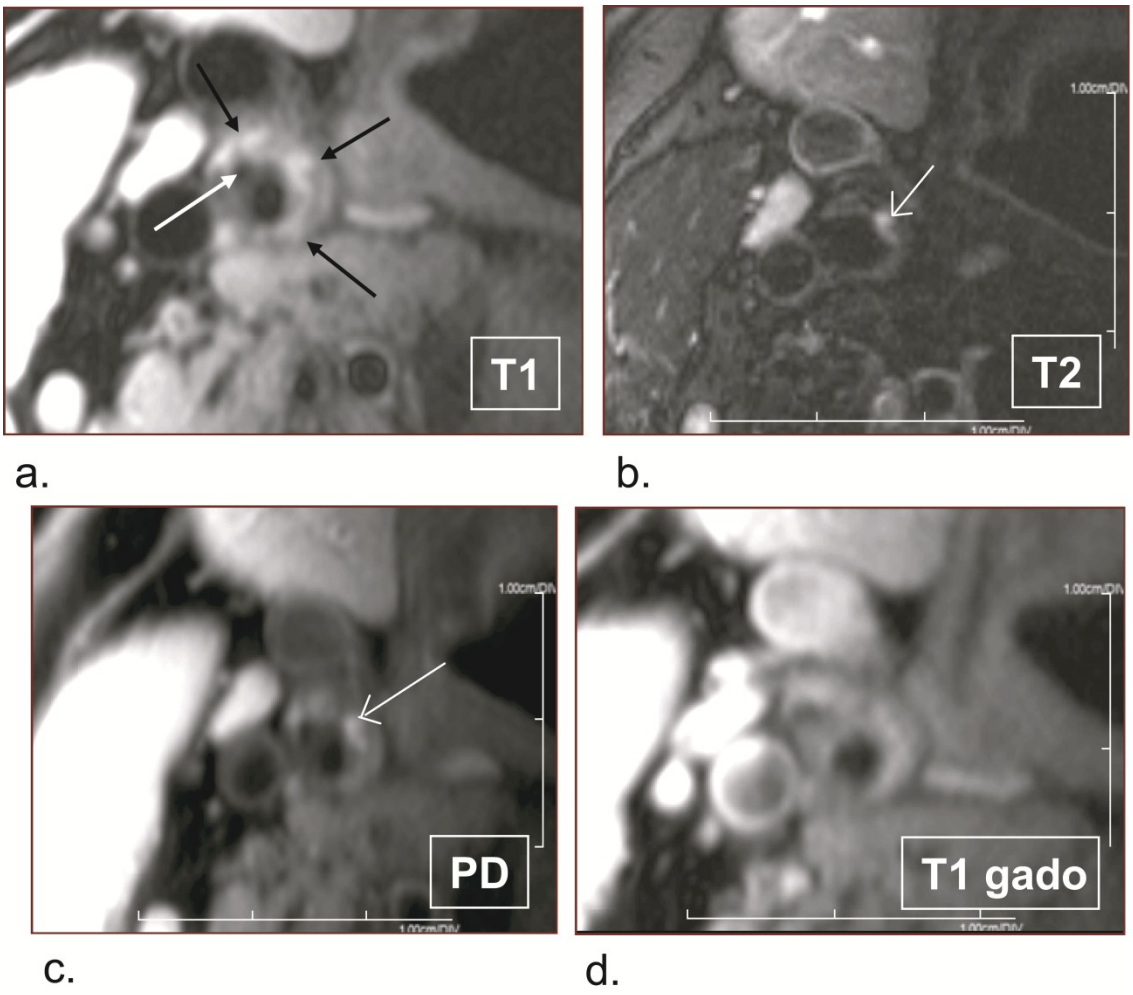

Figure 3.2.9. High-resolution cross-sectional MRI of the right carotid bifurcation of an asymptomatic patient. (a) On T1-weighted acquisition of right internal carotid artery stenosis, the plaque appears to be heterogeneous. The external carotid artery lumen is observed (white arrow), and both vessel walls consist of heterogeneous signals reflecting fibro-calcific tissue. (b) and (c) T2-weighted and Proton Density images show a hyperintense area not clearly apparent on T1 pre and post contrast images. This hyperintense area likely represents loose matrix fibrous tissue. (d) There is no significant plaque enhancement after gadolinium injection, suggesting that there is no neovascularisation or inflammation.

MRI Technique and Reproducibility

Pulse sequences for carotid plaque include black-blood and bright-blood imaging. Black-blood is a technique that suppresses the signal from flowing blood, using double or quadruple inversion recovery sequences (e.g. T1, T2, and proton density). Therefore, the lumen appears black, and the vessel wall and plaque components can be more accurately delineated. Bright-blood is a technique used for MR angiography (the lumen appears hyperintense); it uses gradient-recalled echo sequences (e.g. 3D Time-of-Flight (TOF)). This type of sequence is useful to improve visualization of superficial plaque calcifications, the fibrous cap, and surface hemorrhages. Thus, the current standard for carotid plaque imaging and interpretation requires multiple contrast image sequences: T1, T2, proton density, 3D TOF, and post-contrast (gadolinium) T1-weighted sequences. Post-gadolinium T1-weighted acquisition is an additional sequence that shortens T1 and improves contrast resolution and signal-to-noise ratio. It results in better delineation of the fibrous cap and lipid core, and increased intensity of fibrous tissue and neovascularisation [163,164] All MR sequences are fat-suppressed and cardiac-triggered to minimize motion artefacts. Total scanning time can be up to 40 minutes.

To visualize atherosclerotic plaque components and identify vulnerable plaques, high spatial resolution (voxel size 0.5 X 0.5 mm in-plane and 2 to 3 mm thick) with excellent contrast between plaque components is essential. Hence, a dedicated phased-array surface coil with at least 2 elements on each side of the neck is required to optimize signal-to-noise ratio (SNR). A greater number of elements within the coil improved SNR and contrast-to-noise ratio (CNR)[22] in a study comparing 8-channel to 4-channel phased array coils at 3T [165]. Recent studies on carotid plaque imaging using 3T showed a significant improvement over 1.5T in SNR and CNR [166], stronger inter- and intra-

[22]SNR and CNR are ways of measuring MR image quality.
SNR = signal intensity of ROI / standard deviation of noise
CNR = (signal intensity of ROI #1 – signal intensity of ROI #2) / standard deviation of noise

observer reproducibility for measuring vessel wall contours (Pearson correlation coefficient > 0.9) [167,168], and better repeat scan reliability to quantify plaque components and vessel wall thickness (ICC > 0.87 vs. > 0.38) [169,170]. The measurement of fibrous cap thickness, however, is suboptimal, as the resolution of MRI is usually above 300 μm while the size of thin fibrous caps is less than 200 μm.

Studies on inter-reader reproducibility for plaque morphology are lacking; one study found moderate inter-reader reproducibility for plaque component discrimination at 1.5T [171], and another found good inter-reader reproducibility for fibrous cap measurement of 60 patients at 1.5T (ICC = 0.71) [172].

Inflammation, Neovascularisation and Contrast-enhanced MRI

It has been shown that the degree of plaque enhancement post-gadolinium injection correlates with neovascularisation and the degree of macrophage infiltration (i.e., inflammation) [163,164,173]. Also, a retrospective study found that carotid plaque inflammation detected by contrast-enhanced MRI was a sign of multisite plaque activation and increased coronary ischemic events [174].

Molecular MRI

Contrast agents can be used with MRI to target specific molecules such as cell surface receptors [175,176]. Nanoparticles, such as ultra-small superparamagnetic iron oxide (USPIO), have been shown to be phagocytosed by macrophages in carotid plaques of recently symptomatic TIA patients [177] and to identify plaque inflammation [178]. Howarth et al. found that symptomatic patients had greater areas of signal drop from phagocytosed USPIO [179], and the same author group also demonstrated a significant

decrease in USPIO-identified inflammation with aggressive lipid-lowering therapy over 3 months [180]. Other contrast agents were targeted to lipid core of plaques in a rabbit model by an unknown mechanism [181]. Recently, the contrast agent P947 was found to detect matrix metalloproteinases, angiotensin-converting enzyme, and aminopeptidase N activity in vulnerable plaques ex-vivo and in a rabbit model in vivo [182]. More developments on plaque molecular imaging with these contrast agents are expected for the future.

Clinical and future perspectives

Multicontrast high-resolution MRI of carotid plaque has shown significant promise to detect vulnerable plaque, which is why it is currently used in numerous clinical studies. Compared to other imaging techniques, it has good sensitivity and specificity to identify plaque components and excellent contrast within the small atherosclerotic plaque. However, there are significant drawbacks that prevent high-resolution MRI from being easily introduced into clinical practice. It is an expensive examination with frequent contra-indications, limited availability and lengthy examination duration, thus not suitable for screening purposes. It is also susceptible to poor image quality, reaching at times over 30% of patient examinations, mainly due to motion artefacts [183].

The current area of research focuses on clinical and technical aspects of MRI: prospective studies to measure plaque progression [183-185]; detection of the vulnerable plaque and assessment of its predictive value [186,187]; determining which clinical factors are associated with vulnerable plaque features [188-190]; increasing the use of 3T magnetic field and document its reproducibility; and technical optimization to improve image quality and shorten total examination time. So far, technical improvements have resulted in shorter scanning times: 3T magnetic field with a single excitation instead of

two for black-blood sequences [166]; parallel imaging techniques [191]; and local excitation black-blood imaging [192]. Better blood flow suppression was proposed to improve image quality [193], and a newly developed T1W sequence, rapid acquisition gradient echo (RAGE), had a better diagnostic capability than fast-spin echo sequence to detect IPH [194]. With ongoing development of these technical improvements and clinical studies, multicontrast high-resolution MRI may become the imaging technique of choice to characterize vulnerable carotid plaque morphology.

Conclusion

To date, the best non-invasive imaging modality to study the natural history of atherosclerosis for stroke prevention is yet to come. By describing how ultrasound (US), multidetector computed tomographic angiography (MDCTA) and magnetic resonance imaging (MRI) are used to characterize atherosclerotic carotid disease, this review has helped determine the best avenues to explore for non-invasive carotid plaque imaging. . Newer developments such as ultrasound elastography, targeted contrast agents in ultrasound, CT and MRI, and optimization of MRI techniques are emerging; study of plaque evolution is the next step.

This page is left intentionally blank

Section II

Characterization of Carotid Plaques with Ultrasound Non-Invasive Vascular Elastography: Feasibility and Correlation with High-Resolution Magnetic Resonance Imaging

This page is left intentionally blank

CHAPTER 4

Characterization of Carotid Plaques with Ultrasound Non-Invasive Vascular Elastography (NIVE): Feasibility and Correlation with High-Resolution MRI

4. Characterization of Carotid Plaques with Ultrasound NIVE: Feasibility and Correlation with High-Resolution MRI

4.1. *Introduction to manuscript*

This preamble introduces study rationale. The goal of this master's thesis research project was to develop and validate the ultrasound non-invasive vascular elastography (US NIVE) technique for vulnerable plaque (VP) detection in patients with significant carotid stenosis. In order to do so, a correlation study between plaque strain values and plaque volume composition was undertaken. Plaque composition was determined by a reference standard, multicontrast high-resolution MRI of carotid plaque. Furthermore, an association between plaque strain and clinical symptoms was sought. Hence, patients were grouped as symptomatic or asymptomatic and their strain profiles were compared.

Validation of US NIVE could provide valuable information on the biomechanical aspects of atherosclerotic plaque progression and vulnerable plaques. Ultimately, asymptomatic patients with carotid stenosis could be risk-stratified into low-risk and high-risk groups, and targeted therapy could be efficiently instituted.

The choice of MRI to validate US NIVE was judicious. When validating a new technique such as US NIVE, a gold standard or reference standard technique is required. US NIVE is a technique that measures plaque axial strain non-invasively. The gold standard for measuring plaque axial strain is intravascular ultrasound elastography (IVUS); it consists of a catheter inserted directly into the arterial system (e.g. through the femoral artery) with a transducer element

at its tip and algorithms to calculate tissue axial displacements and produce an elastogram. IVUS of carotid arteries is invasive and carries an elevated risk of stroke for patients who have carotid atherosclerotic plaque. This technique was only validated in coronary arteries. Otherwise, there is no non-invasive gold standard technique that can accurately measure axial strain in vivo in carotid arteries.

An alternative reference standard was sought to help validate US NIVE. Atherosclerotic plaque can be described by its biomechanical properties, morphology, composition, and molecular processes. Since our working hypothesis is the presence of an association between plaque stiffness and plaque composition ("soft" vs. "hard" plaque components), the gold standard technique must characterize plaque composition. This can be achieved by histopathology after surgical excision (CEA) of the plaque "en bloc", followed by laboratory preparation techniques (i.e. slicing, staining) and analysis under the microscope by a pathologist. This implies a standardization of surgical and pathological techniques, along with a thorough cooperation between the clinician, the surgeon, the pathologist, the hospital's laboratory, and all research personnel. It demands significant costs, time constraints, and resources. In addition, validation with histopathology requires that all included patients have a CEA, which is not the case in this study. Thus the patient population would have been limited to symptomatic patients with severe stenosis who already benefit from endarterectomy. It is more relevant to evaluate this technology in a broader population including asymptomatic patients who actually will be the future target population of vulnerable plaque detection. Thus, high-resolution multicontrast MRI was found to be the most appropriate reference standard since it was extensively validated with histology in the past.

4.1.1. Role of authors

The following is the order of authors for this submitted article and corresponding affiliations:

Cyrille Naim, MD[1,2,3,4]; Guy Cloutier, PhD[2,3,4]; Elizabeth Mercure, MSc[3,4]; François Destrempes, PhD[3,4]; Zhao Qin, MSc[3,4]; Walid El-Abyad, MD, MSc[1,3]; Sylvain Lanthier, MD, MSc[1,3,5]; Marie-France Giroux, MD[1,2]; Gilles Soulez, MD, MSc[1,2,3].

Institutions:

1. Department of Radiology, University of Montreal Hospital Center (CHUM), Montréal, Québec, Canada
2. Department of Radiology, Radio-Oncology and Nuclear Medicine, and Institute of Biomedical Engineering, University of Montreal, Montréal, Québec, Canada
3. University of Montreal Hospital Research Center (CRCHUM), Montréal, Québec, Canada
4. Laboratory of Biorheology and Medical Ultrasonics, University of Montreal Hospital Research Center (CRCHUM), Montréal, Québec, Canada
5. Department of Medicine, University of Montreal Hospital Center (CHUM), Montréal, Québec, Canada

The role of all authors of the submitted article is detailed below.

Cyrille Naïm: First author of this project. Performed: protocol modifications and approval by ethics research committee; clinical data collection, medical chart review and telephone interviews; MR image positioning and post-

contrast selections; MR image interpretation and segmentation; clinical, MRI and US-NIVE data collection, interpretation, and statistical analyses; optimization of QPlaque segmentation software with professionals from the Netherlands; literature review; presentation of project at multiple conferences in 2011 (Canadian Association of Radiologists (Montréal, QC), International Tissue Elasticity Conference (Dallas, TX); Journées Françaises de Radiologie, Société Française de Radiologie (Paris, France); and Radiological Society of North America (Chicago, IL); writer of manuscript submitted to *European Radiology*.

Guy Cloutier: Co-director and supervisor of my studies and this research project; correction of the manuscript for submission.

Elizabeth Mercure: Performed plaque segmentations on B-mode images from reconstructed raw radiofrequency (RF) signals; analyzed elastographies with Matlab (segmentation and computations); programming for output of strain parameters; statistical analyses for strain parameters; troubleshooting of technical issues for calculation of elastograms (correction of RF artefact signals by designing a filtering technique).

François Destrempes: Informatician who designed the semi-automatic segmentation technique of US images used in this study; contributed to troubleshooting of technical issues for calculation of elastograms (strain curve filtering).

Zhao Qin: Performed plaque segmentations on B-mode images from reconstructed raw radiofrequency (RF) signals; analyzed elastographies with Matlab (segmentation and computations); programming for output of strain parameters; statistical analyses for strain parameters; troubleshooting of technical issues for calculation of elastograms.

Walid El-Abyad: Research assistant who screened for eligible patients and performed recruitment for the study (first contact with research group); collected all pertinent clinical data; contact with patients except for follow-up telephone interviews of asymptomatic patients; administrative organization and preparation of documents, meetings, for ethics research committee requirements and research group requirements.

Sylvain Lanthier: Recruited eligible patients for our study from within his clinical practice in neurology; neurological evaluation of patients for whom eligibility was uncertain; correction of manuscript.

Marie-France Giroux: Performed elastography, color and pulsed Doppler US, and supervised MR imaging; review of interpretation of diagnostic imaging tests (MRI, US, angiography, and elastographies); correction of manuscript.

Gilles Soulez : Director and supervisor of my studies and this research project; performed elastography, color and pulsed Doppler US, and supervised MR imaging; review of interpretation of diagnostic imaging tests (MRI, US, angiography, and elastographies); correction of manuscript.

4.1.2. Thesis Format of Submitted Manuscript

In section 4.2, the manuscript submitted to *European Radiology* for publication is presented. The list of references following the conclusion of this manuscript is the same as what was submitted, and the article's reference numbers have been kept in round brackets and italicized "*(1)*" throughout the manuscript. In addition, for efficient navigation and homogeneity of this thesis, appropriate reference numbers in square brackets "[1]", with links to the reference section of this thesis, have been maintained.

4.2. *Manuscript submitted to European Radiology*

The manuscript starts on the following page.

TITLE PAGE

Title of manuscript:

"Characterization of Carotid Plaques with Ultrasound Non-Invasive Vascular Elastography (NIVE): Feasibility and Correlation with High-Resolution Magnetic Resonance Imaging"

Authors: Cyrille Naim, MD [1,2,3,4]
Guy Cloutier, PhD [2,3,4]
Elizabeth Mercure, MSc [3,4]
François Destrempes, PhD [3,4]
Zhao Qin, MSc [3,4]
Walid El-Abyad, MD, MSc [1,3]
Sylvain Lanthier, MD, MSc [1,3,5]
Marie-France Giroux, MD [1,2]
Gilles Soulez, MD, MSc [1,2,3]

Institutions :

1. Department of Radiology, University of Montreal Hospital Center (CHUM), Montréal, Québec, Canada
2. Department of Radiology, Radio-Oncology and Nuclear Medicine, and Institute of Biomedical Engineering, University of Montreal, Montréal, Québec, Canada
3. University of Montreal Hospital Research Center (CRCHUM), Montréal, Québec, Canada
4. Laboratory of Biorheology and Medical Ultrasonics, University of Montreal Hospital Research Center (CRCHUM), Montréal, Québec, Canada
5. Department of Medicine, University of Montreal Hospital Center (CHUM), Montréal, Québec, Canada

Corresponding Author: **Gilles Soulez, MD, MSc**
Work: +1-514-890-8000 extension 26522
Fax: +1-514-412-7547

Work address: Centre Hospitalier de l'Université de Montréal (CHUM)
Hôpital Notre-Dame—Pavillon Lachapelle (Room B1038-A)
1560 Sherbrooke East
Montréal (Québec)
Canada H2L 4M1

Conflicts of Interest and Source of Funding:
Dr Gilles Soulez holds a national scientist award from the Fonds de la Recherche en Santé du Québec.
This project was funded by the Natural Sciences and Engineering Research Council of Canada (CIHR-NSERC, grant # 06-07-164), the Canadian Institutes of Health Research (CIHR, grant # 05-06-0344), Gestion Univalor (VAL-358-CHUM) and a grant from Bracco Diagnostics.
The authors of this manuscript have no conflicts of interest to declare.

Short title:
"Carotid Plaque Ultrasound Elastography"

ABSTRACT

TITLE:

Characterization of Carotid Plaques with Ultrasound Non-Invasive Vascular Elastography (NIVE): Feasibility and Correlation with High-Resolution Magnetic Resonance Imaging

ABSTRACT:

OBJECTIVES: Evaluate the ability of ultrasound Non-Invasive Vascular Elastography (NIVE) strain analysis to characterize carotid plaque composition and vulnerability as determined by high resolution MRI.

METHODS: Thirty-one subjects with 50% or greater carotid stenosis underwent NIVE and high-resolution MRI of internal carotid arteries. Time-varying strain images (elastograms) of segmented plaques were generated from ultrasonic raw radiofrequency sequences. On MRI, corresponding plaques and components were segmented and quantified. Associations between strain parameters, plaque composition and symptomatology were estimated with curve-fitting regressions and Mann-Whitney tests.

RESULTS: Mean stenosis and age were 72.7% and 69.3 years. Of 31 plaques, 9 were symptomatic, 17 contained lipid and 7 were vulnerable on MRI. Strains were significantly lower in plaques containing a lipid core compared to those without lipid, with 77% to 100% sensitivity and 57% to 79% specificity ($p <$ 0.032). A statistically significant quadratic fit was found between strain and

lipid content ($p < 0.03$). Strains did not discriminate symptomatic patients or vulnerable plaques.

CONCLUSIONS: Ultrasound NIVE is feasible in patients with significant carotid stenosis and can detect the presence of a lipid core with high sensitivity and moderate specificity. Further studies of plaque progression with NIVE are required to identify vulnerable plaques.

KEY WORDS (from Medical Subject Headings):

Carotid Artery Plaque; Atherosclerotic Plaque; Elastography; Ultrasound; Magnetic Resonance Imaging (MRI).

KEY POINTS:

- Ultrasound NIVE is feasible in patients with significant carotid stenosis
- Ultrasound NIVE detects a lipid core with high sensitivity and moderate specificity
- Further plaque progression studies with NIVE are required to identify vulnerable plaques

ABBREVIATIONS AND ACRONYMS:

Ultrasound Non-Invasive Vascular Elastography (Ultrasound NIVE); Ultrasound (US); high-resolution Magnetic Resonance Imaging (high-resolution MRI); Radiofrequency (RF); Lagrangian Speckle Model Estimator (LSME); Mean Strain at Peak Systolic Compression (MSPSC); Mean Strain Amplitude (MSA); Maximal Strain Rate (MaxSR); Minimal Strain Rates (MinSR); Intraplaque Hemorrhage (IPH); lipid percentage of total plaque

volume (%Lipid volume) and calcium percentage of total plaque volume (%Calcium volume); Standard Deviation (SD); Intravascular Ultrasound Elastography (IVUS).

INTRODUCTION

It is estimated that up to 20% of strokes are caused by carotid atherosclerosis [10] *(1)*. Severity of carotid stenosis is a strong predictor of recurrent atheroembolic strokes in symptomatic patients with a significant stenosis [195] *(2)*, but it is not a reliable predictor of stroke incidence in asymptomatic patients [28] *(3)*. Hence, appropriate management of asymptomatic patients remains controversial, warranting further risk stratification.

According to the coronary artery literature, risk stratification should involve identification of the vulnerable plaque, that is, an atherosclerotic plaque at elevated risk of causing an ischemic event [33] *(4)*. Pathology of culprit coronary plaques has been shown to be similar to that of symptomatic carotid plaques [48] *(5)*. Thus, research in stroke prevention emphasizes the identification of vulnerable plaques in carotid arteries with a variety of imaging techniques that characterize plaque composition, morphology, molecular processes, or biomechanical properties. For instance, CT and PET-CT were proposed to evaluate plaque composition and inflammation, respectively [125,196] *(6, 7)*. B-mode echo-texture [86] *(8)* and plaque volume measurement by ultrasound [89] *(9)* were also tested to evaluate plaque vulnerability and evolution with statin therapy. Ultimately, multicontrast high-resolution MRI was found to be the most accurate non-invasive imaging technique to identify and quantify plaque components compared to histology [148,153] *(10, 11)*. In addition, MRI-detected intra-plaque hemorrhage and fibrous cap disruption were associated with plaque vulnerability [152,157] *(12, 13)*. Despite its high sensitivity and specificity for plaque morphology [144,147,148,153] *(10, 11, 14, 15)*, elevated costs and time requirements render implementation of MRI difficult for patient screening and follow-up. As a result, an affordable non-invasive imaging technique to characterize carotid plaque composition and its progression is yet to be determined.

To date, no single carotid plaque imaging feature is recognized as a reliable independent predictor of future ischemic events. Furthermore, there is no established technique analyzing plaque biomechanics non-invasively. Non-Invasive Vascular Elastography (NIVE) by ultrasound is a novel ultrasonic technique that characterizes plaque biomechanics by mapping carotid plaque strains [113] *(16)*. It is low-cost, implementable on clinical ultrasound scanners, and could potentially accompany routine carotid imaging examinations. A previous study assessed the feasibility of NIVE to analyze the strain of carotid walls in healthy subjects [114] *(17)*. The next step is to evaluate the ability of NIVE strain analysis to characterize atherosclerotic plaques in patients with a carotid stenosis. We hypothesized that lipid-rich and vulnerable plaques have different strains (deformations) than calcified and non-vulnerable plaques. Hence, we aimed to evaluate the ability of ultrasound NIVE strain analysis to characterize carotid plaque composition and vulnerability, using high resolution MRI as a reference standard. As a secondary endpoint, we aimed to determine the feasibility of NIVE to discriminate symptomatic from asymptomatic patients.

METHODS

This prospective study was compliant with the Health Insurance Portability and Accountability Act and approved by the institutional review board. All subjects gave their written informed consent. Subjects were recruited from the vascular and interventional radiology, vascular surgery, neurology, and vascular medicine clinics. Between January 2006 and December 2010, 44 non-consecutive patients referred to the radiology department for suspected significant carotid stenosis were enrolled. Indications for imaging carotid arteries were based on local standards of care. Men and women aged 40 to 85 years were eligible if they had a symptomatic or asymptomatic carotid artery stenosis of at least 50% diameter reduction documented on a previous angiography study if available [CT angiography (n=23), MR angiography

(n=4), digital subtraction angiography (n=1)] combined with duplex Doppler ultrasound, or based solely on duplex Doppler ultrasound (n=16). For angiography studies, stenosis was evaluated according to the NASCET criteria [21] *(18)*. One carotid artery per patient was selected for analysis ("index side"): the symptomatic side, and for asymptomatic patients, the most severely stenotic side. Subjects were excluded if they had any contraindication to ultrasound, MRI or gadolinium injection; incomplete MRI or ultrasound elastography examination; endarterectomy within the last 10 years; carotid stenting; total occlusion; or severe calcification that impeded proper ultrasound imaging.

At enrolment, a medical history and clinical examination were performed for all subjects. Baseline modified Rankin scale scores were recorded, and subjects were classified as symptomatic if they had a stroke or transient ischemic attack (TIA) attributed to their index carotid artery plaque in the previous three months. If there was any doubt on the relationship between the occurrence of neurologic symptoms and the index carotid, the patient was referred for an independent assessment by a neurologist. Serum fasting lipid profile and C-reactive protein were sampled. A color and pulsed Doppler ultrasound examination was performed using standardized criteria [76] *(19)* to confirm degree of stenosis, followed by an ultrasound acquisition for elastography and a high-resolution MRI of the index carotid artery. All imaging examinations were performed within the first month of participation.

Asymptomatic subjects were followed annually in order to determine if their index carotid plaque had become symptomatic or occluded, in the form of a stroke, a TIA, or a newly documented asymptomatic total artery occlusion. In that case, subjects were classified in the "symptomatic" group for analysis. Follow-up consisted of completion of a dedicated questionnaire with telephone interviews and medical and imaging file reviews.

Ultrasound Elastography Protocol

Ultrasound Non-Invasive Vascular Elastography (NIVE) estimates the local deformation of a plaque induced by its natural cardiac pulsation, as explained schematically in Figure 4.1.

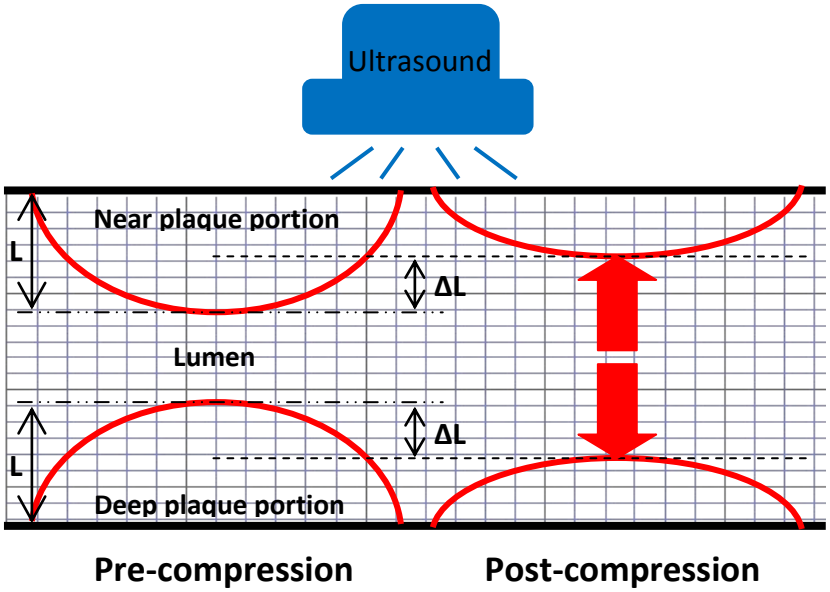

Figure 4.1. Schematic depiction of ultrasound NIVE. Blood pressure from the systolic carotid pulse induces a compression (axial stress denoted by large red arrows) and a deformation (axial strain denoted by ΔL/L X 100) of the atherosclerotic plaque. This is a simplified depiction, because axial strain is calculated for each individual window (1.54 X 2.99 mm), after which mean axial strain for the entire segmented plaque is calculated.

A single operator performed all ultrasonic raw radiofrequency (RF) data sequence acquisitions, with an ES500RP system (Ultrasonix, Vancouver, Canada) equipped with a L14-5/38 linear array transducer (20 MHz sampling frequency; 20-25 frames per second; 38.5 x 149.6 μm pixel size). B-mode images from reconstructed RF data were acquired longitudinally, centered on the plaque at the level of the carotid bulb, and in a time-varying sequence over approximately 10 seconds. Brachial blood pressure and heart rate were measured before, during, and after ultrasound acquisitions.

The implemented NIVE algorithm software consisted of two major steps to obtain an elastogram from consecutive RF images. First, manual segmentation of the plaque on the first image frame was followed by automatic adaptation of the initialized region through the time-varying sequence [118] *(20)*. The segmentation was performed by a technician and reviewed by a radiologist, both blinded to MRI. Second, the Lagrangian Speckle Model Estimator (LSME) algorithm [112] *(21)* was applied to compute axial strain of the time-varying sequence of the segmented plaque. This algorithm calculates speckle vector translations and morphological changes between consecutive image frames, thus providing values of relative axial strain over time. Hence, for each pair of image frames, an elastogram (color map of axial strain) was obtained, and strain parameters were computed from the average axial strain of the whole plaque (*i.e.*, both near and far plaque portions illustrated in Figure 4.1). Time-varying strain curves were filtered to eliminate respiratory and motion artefacts [119] *(22)*, and 2 to 5 consecutive cardiac cycles were chosen for analysis. A thorough biomechanical description of axial strain was obtained with four different strain parameters as outcome variables of NIVE: Mean Strain at Peak Systolic Compression (MSPSC), Mean Strain Amplitude (MSA), and Maximal and Minimal Strain Rates (MaxSR, MinSR). Figure 4.2 explains each parameter in detail.

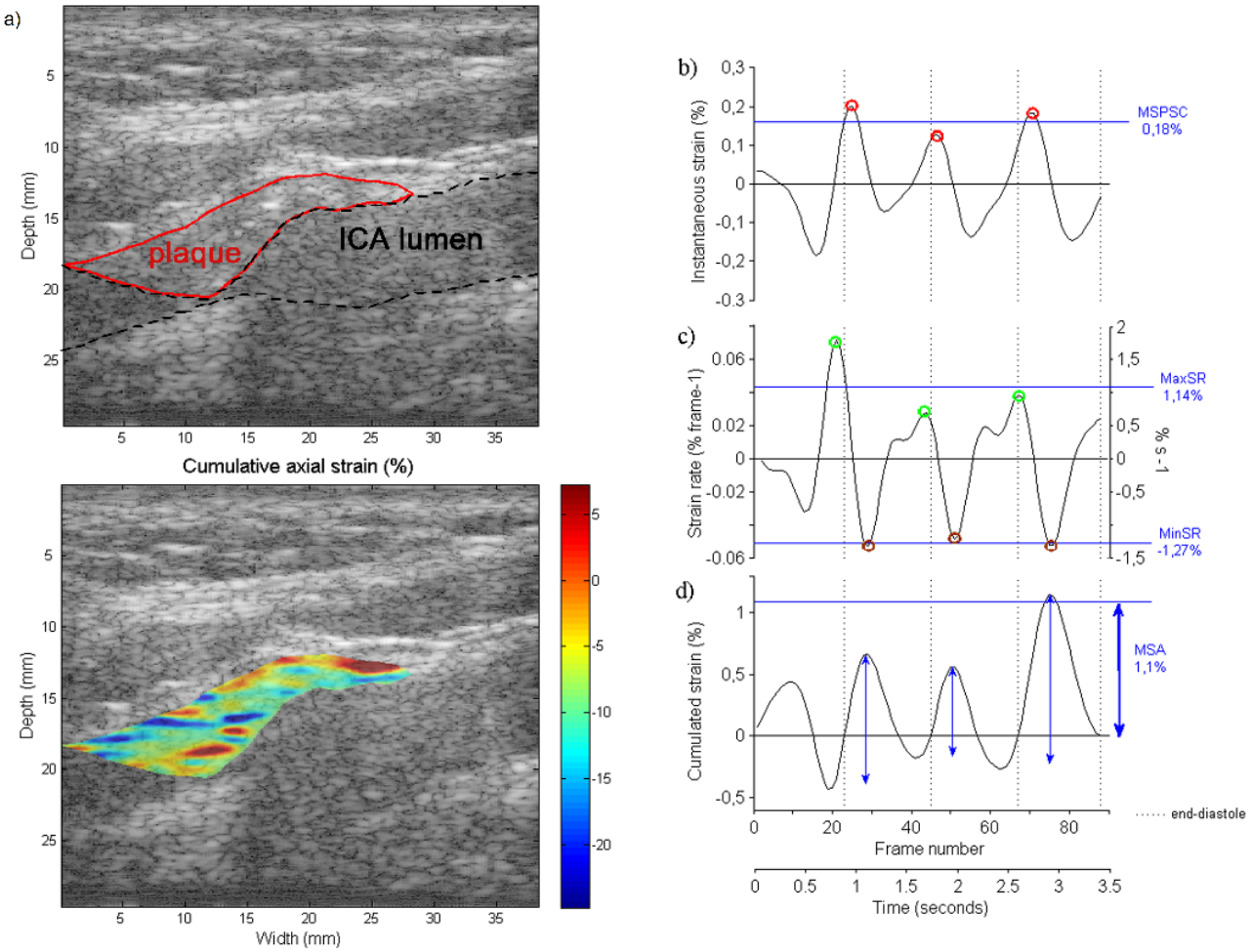
a)
plaque
ICA lumen
Depth (mm)
Cumulative axial strain (%)
Width (mm)
b)
Instantaneous strain (%)
MSPSC
0,18%
c)
Strain rate (% frame-1)
% s-1
MaxSR
1,14%
MinSR
-1,27%
d)
Cumulated strain (%)
MSA
1,1%
end-diastole
Frame number
Time (seconds)

Figure 4.2. Elastogram and strain curves of the left carotid plaque of a 70 year old man who presented with left-sided amaurosis fugax. (a) A two-dimensional longitudinal view B-mode image reconstructed from raw RF data showing the segmented plaque (red contour) on the anterior vascular wall of the internal carotid artery (ICA), and the same image with a superimposed elastogram (color map) representing cumulated axial strain at maximal systolic compression. The colors range from -20% (dark blue) to +20% (dark red), denoting areas of dilation and compression respectively. (b) A graph of instantaneous mean axial strain is obtained from the strain difference between two consecutive image frames, thus representing the variation of mean axial strain over time. Peak systolic compression is denoted by red circles. Mean Strain at Peak Systolic Compression (MSPSC) is the average of these peak values over the number of cardiac cycles. Dotted vertical lines represent end-diastole, estimated from B-mode videos and M-mode images. (c) Strain Rate is the slope of the instantaneous strain in (b). Maximum Strain Rate (MaxSR) is the mean of the greatest strain rate occurring at end-diastole (green circles). Minimum Strain Rate (MinSR) is the mean of the lowest strain rate, occurring at the onset of diastole (purple circles). In other words, MaxSR represents greatest tissue compression over time, and MinSR represents greatest tissue dilation over time, which explains why MinSR is a negative value. (d) A graph of cumulated mean axial strains is derived from (b). Double-sided blue arrows represent strain amplitude for each cardiac cycle. Mean Strain Amplitude (MSA) is the average of these three amplitudes. The peak of the third cardiac cycle corresponds to the elastogram in (a).

MR Imaging Protocol

Using a 1.5-Tesla MRI unit (Siemens, Avanto, Erlangen, Germany) and a dedicated 4-element radiofrequency surface coil, axial images of the index carotid artery were obtained from 10 mm below to 3 cm above the bifurcation. First, a 3D Time-of-Flight sequence was performed [repetition time (msec)/echo time (msec), 24/7.15; flip angle (FA), 25°; section thickness, 1 mm; field of view, 12 cm; resolution, 0.6 X 1 mm; number of signals averaged, 3]. Using the same field of view and positioning, as well as ECG-gating, fat-suppression, and 0.6 X 0.5 X 3 mm voxel size with 1 mm intersection gap, four black-blood double-inversion recovery turbo spin echo sequences were acquired with the following parameters: T2-weighted [repetition time (msec)/echo time (msec), 2 R-R intervals/78; number of signals averaged, 3]; proton density weighted [2 R-R intervals/11; 2]; and pre- and post-contrast T1-weighted [600-700/6.8; 2] sequences. Two adjacent slices containing the major portion of the plaque were selected for post-contrast imaging. Gadolinium-BOPTA (MultiHance, Bracco Diagnostics, Vaughan, ON, Canada) was injected at a rate of 2 ml/sec (0.1 mmol/kg), after which image acquisition was performed every minute for 10 minutes. Total imaging time was typically less than 45 minutes.

MR Image Review

Plaque image analysis and segmentation were performed by one junior reader (6 months training) and reviewed by a senior reader (20 year experience in MR vascular imaging). Both were blinded to plaque strain values and elastograms. All image sequences were used for interpretation and segmentation, including the post-contrast image sequence of the major plaque portion, which complemented plaque characterization. The post-contrast image sequence chosen for analysis was acquired at least 5 minutes after injection onset and displayed the best image quality and maximum enhancement. At each image

slice level, vessel contours and components were manually traced using a segmentation software (QPlaque MR 1.0.16, Medis, Netherlands) that allows simultaneous tracing on all sequences and provides volume and area measurements. Plaque components were identified using previously published criteria [131,144,155,164] *(14, 23-25)*, and included: lipid core, calcifications, intra-plaque hemorrhage, loose matrix, fibrous cap, and inflammation/neovasculature. Inflammation/neovasculature was defined as a region of enhancement on the post-contrast injection sequence [163,173,197] *(26-28)*. Fibrous tissue was not segmented; it was defined as the remainder of the plaque between inner and outer vessel wall contours, and only included fibrous cap and loose matrix segmented areas for volumetric analyses. A segmented plaque is illustrated as an example in Figure 4.3.

The carotid plaque was deemed vulnerable on MRI if it had one of the following features: thin fibrous cap with a large lipid core (≥25% surface area), ruptured fibrous cap, or intraplaque hemorrhage (Figure 4.3). The main outcome variables for high-resolution MRI were lipid and calcium proportions, in percentage of total plaque volume ("%Lipid volume" and "%Calcium volume").

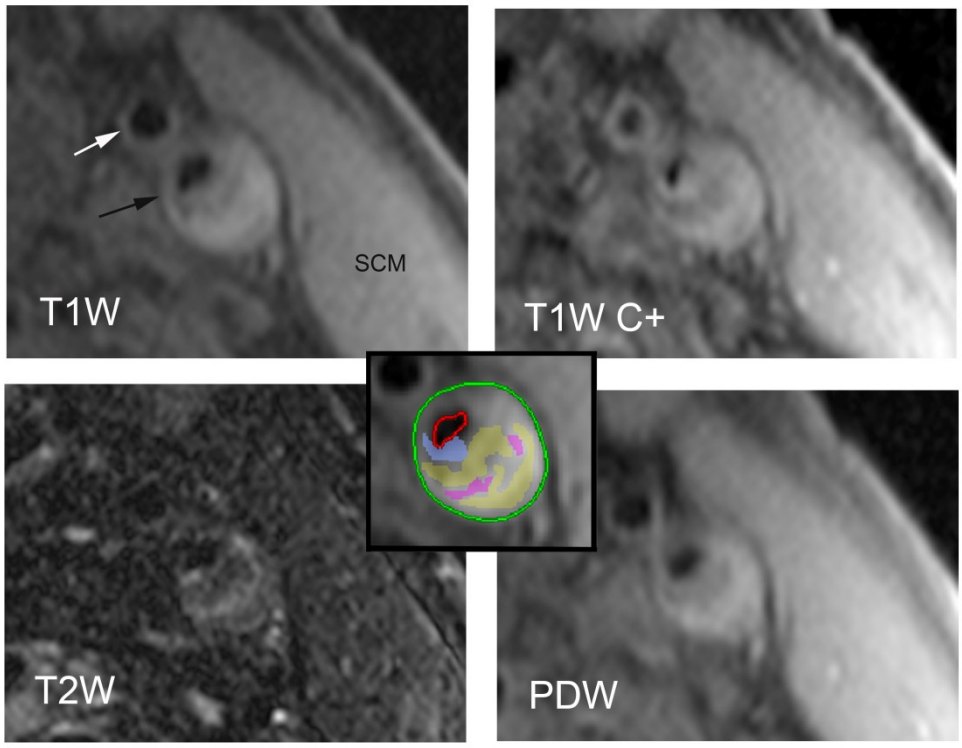

Figure 4.3. High-resolution MRI of the left internal carotid artery plaque of a 65 year old man who presented with a left hemispheric stroke (axial view). This is a vulnerable-appearing lipid-rich hemorrhagic plaque. The external and internal carotid arteries are indicated with a white and black arrow, respectively. The segmentation using the QPlaque software is shown superimposed on the T1-weighted image (framed inset at the center). The green and red contours designate the outer and inner vascular wall contours of the internal carotid artery. Yellow represents lipid, pink represents hemorrhage, and purple represents inflammation. T1W = T1-weighted; T2W = T2-weighted; PDW = Proton Density-weighted; T1WC+ = T1-weighted post-contrast injection.

RESULTS

Forty-four subjects were recruited. Thirty-one met inclusion criteria for analysis as the flowchart demonstrates (Figure 4.4). No adverse events occurred. Population baseline clinical, MRI and ultrasound characteristics are presented in Tables IV-I and IV-II. During a mean follow-up of 69.9 weeks (SD 82.4; range 0-253.6), one of the 23 asymptomatic subjects developed an asymptomatic total artery occlusion.

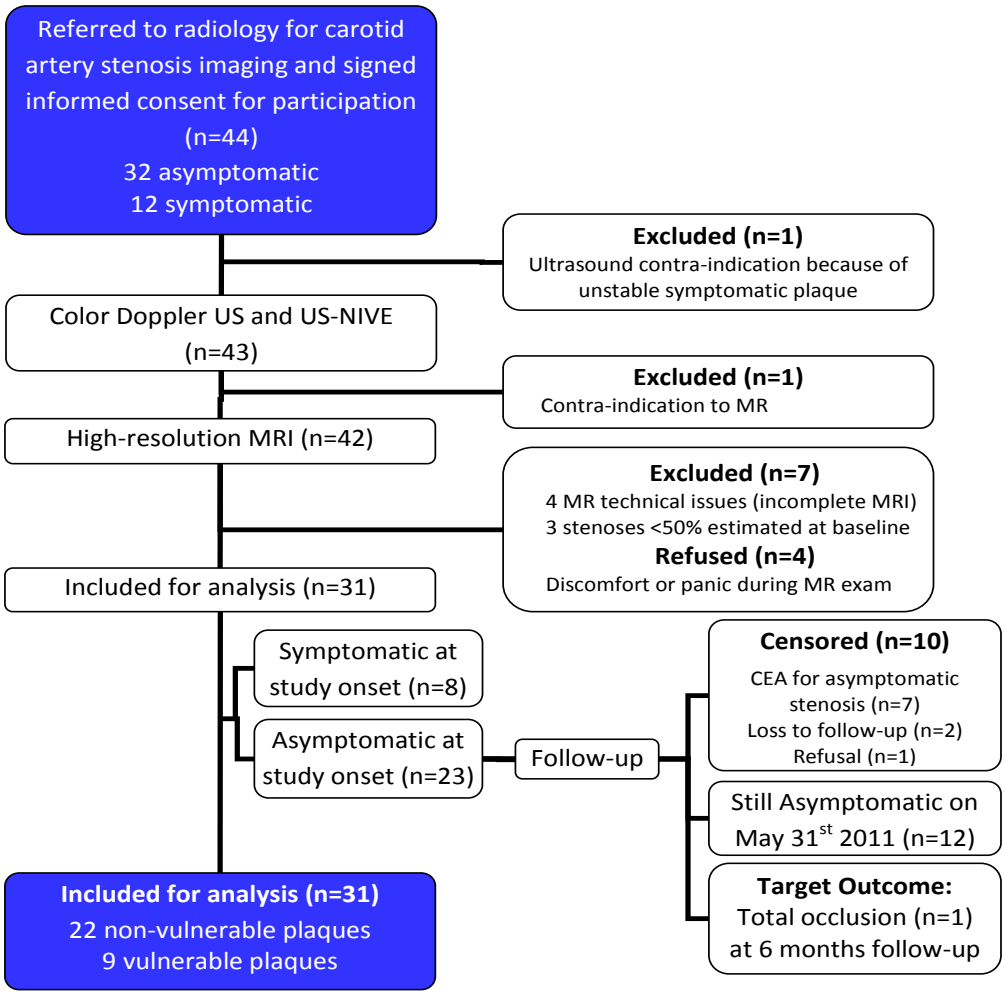

Figure 4.4. Flowchart of subject recruitment.

Table IV-I. Population Clinical Characteristics				
	Total n = 31	**Symptomatic n=9**	**Asymptomatic n=22**	***P*-value**
Clinical Characteristics				
Male (number) *	22 (71%)	8 (88.9%)	14 (63.6%)	0.160
Age (y) ‡	69.3 ± 7.8	69.3 ± 9.0	69.3 ± 7.5	0.793
Mean percent diameter stenosis (%)‡	72.7 ± 12.2	74.4 ± 12.4	72.1 ± 12.4	0.544
Left index carotid artery *	13 (41.9%)	6 (66.7%)	7 (31.8%)	0.074
Clinical history				
Symptomatic	9 (29%)			N/A
Amaurosis fugax	3			N/A
TIA	1			N/A
Completed stroke	3			N/A
Retinal infarct	1			N/A
Asymptomatic carotid occlusion	1			N/A
Body Mass Index (kg/m^2) †	26.6 ± 4.5	28.2 ± 6.0	26.0 ± 3.8	0.246
Peripheral vascular disease *	22 (71%)	2 (22.2%)	20 (90.9%)	0.0001¥
Ischemic heart disease *	12 (38.7%)	3 (33.3%)	9 (40.9%)	0.694
Diabetes Mellitus *	15 (48.4%)	5 (55.6%)	10 (45.5%)	0.609
Dyslipidemia *	27 (87.1%)	7 (77.8%)	20 (90.9%)	0.322
Hypertension *	27 (87.1%)	6 (66.7%)	21 (95.5%)	0.030¥
Smoking history *	25 (80.7%)	7 (77.8%)	18 (81.8%)	0.965

Table IV-I. Population Clinical Characteristics (cont'd)					
		Total n = 31	**Symptomatic n=9**	**Asymptomatic n=22**	***P*-value**
Rankin scale[a] *	0	23 (74.2%)	5 (55.6%)	18 (81.8%)	0.039¥
	1	4 (12.9%)	3 (33.3%)	1 (4.5%)	
	2	3 (9.7%)	0 (0.0%)	3 (13.6%)	
	3	1 (3.2%)	1 (11.1%)	0 (0.0%)	
Aspirin[§] *		26 (83.9%)	8 (88.9%)	18 (81.8%)	0.627
Antiplatelet[§] *		10 (32.3%)	6 (66.7%)	7 (31.8%)	0.935
Anticoagulant[§] *		2 (6.5%)	1 (11.1%)	1 (4.5%)	0.499
Statin[§] *		27 (87.1%)	8 (88.9%)	19 (86.4%)	0.849
Blood biochemistry ‡					
Total cholesterol (C) (mmol/L)		3.85 ± 0.82	3.87 ± 1.11	3.84 ± 0.71	0.826
LDL-C (mmol/L)		2.00 ± 0.70	2.11 ± 1.04	1.97 ± 0.54	0.807
C-Reactive Protein (mg/L)		4.01 ± 3.20	3.02 ± 1.72	4.30 ± 3.51	0.670
Mean sBP (mm Hg) †		132.3 ± 16.3	120.2 ± 12.2	137.1 ± 15.4	0.007¥
Mean dBP (mm Hg) †		67.3 ± 10.0	66.9 ± 10.3	69.3 ± 10.1	0.553
Mean heart rate (beats per minute) †		69.7 ± 14.8	73.6 ± 18.1	69.8 ± 13.5	0.530

N/A: not applicable; sBP: systolic blood pressure; dBP: diastolic blood pressure
* Pearson Chi-squared test
† Independent sample student T-test
‡ Mann-Whitney test
[a] Rankin scale at participation onset (includes residual symptoms from any previous stroke)
[§] Consistent use of medications for at least 3 months prior to participation
¥ Statistically significant

Table IV-II. Population MRI and Ultrasound Characteristics				
	Total n = 31	**Symptomatic n=9**	**Asymptomatic n=22**	***P*-value**
MRI characteristics				
Vulnerable by MR *	7 (22.6%)	4 (44.4%)	3 (13.6%)	0.063
Presence of:				
Lipid **	17 (54.8%)	7 (77.8%)	10 (45.5%)	0.132
Calcium **	27 (87.1%)	8 (88.9%)	19 (86.4%)	1.000
Fibrous cap *				
Thick intact	24 (77.4%)	5 (55.6%)	19 (86.4%)	0.019¥
Thin Intact	2 (6.5%)	0 (0%)	2 (9.1%)	
Ruptured	5 (16.1%)	4 (44.4%)	1 (4.5%)	
Intra-plaque hemorrhage **	2 (6.5%)	2 (22.2%)	0 (0%)	0.077
Contrast enhancement *	19 (61.3%)	6 (66.7%)	13 (59.1%)	0.694
Modified AHA criteria * [23] [131]				
Type IV-V, fibroatheroma	10 (32.3%)	3 (33.3%)	7 (31.8%)	0.019¥
Type VI, complicated	5 (16.1%)	4 (44.4%)	1 (4.5%)	
Type VII, calcified	9 (29.0%)	0 (0.0%)	9 (40.9%)	
Type VIII, fibrous	7 (22.6%)	2 (22.2%)	5 (22.7%)	
Plaque volume, mm^3 †	1529.2 ± 676.5	1598.5 ± 792.3	1500.9 ± 641.7	0.722
Max segmental wall thickness, mm‡	5.6 ± 2.0	6.1 ± 3.1	5.3 ± 1.4	0.896
Mean fibrous cap thickness, mm †	1.4 ± 0.5	1.5 ± 0.5	1.3 ± 0.6	0.516

Table IV-II. Population MRI and Ultrasound Characteristics (cont'd)

	Total n = 31	Symptomatic n=9	Asymptomatic n=22	*P*-value
Mean % volumes				
Lipid ‡	4.8 ± 9.3	9.4 ± 11.3	3.0 ± 7.9	0.022¥
Calcium †	5.1 ± 4.6	2.2 ± 2.5	6.3 ± 4.8	0.005¥
Contrast enhancement ‡	2.2 ± 2.9	3.0 ± 4.1	1.8 ± 2.3	0.638
Loose matrix ‡	1.3 ± 2.4	0.8 ± 1.4	1.5 ± 2.7	0.668
Fibrous tissue (loose matrix included) ‡	87.8 ± 9.4	85.2 ± 12.7	88.9 ± 7.7	0.828
Intra-plaque hemorrhage ‡	0.05 ± 0.2	0.2 ± 0.3	0.0 ± 0.0	0.025¥
Ultrasound characteristics				
Degree of calcification *				
0 = absent	7 (22.6%)	4 (44.4%)	3 (13.6%)	
1 = slight	5 (16.1%)	2 (22.2%)	3 (13.6%)	0.176
2 = moderate	9 (29.0%)	2 (22.2%)	7 (31.8%)	
3 = severe	10 (32.3%)	1 (11.1%)	9 (40.9%)	
Plaque echogenicity *				
1 = hypoechoic	8 (25.8%)	3 (33.3%)	5 (22.7%)	
2 = isoechoic	2 (6.5%)	2 (22.2%)	0 (0.0%)	0.0004¥
3 = hyperechoic	16 (51.6%)	0 (0.0%)	16 (72.7%)	
4 = heterogeneous	5 (16.1%)	4 (44.4%)	1 (4.5%)	

* Pearson Chi-squared test
** Fisher's exact test (bilateral)
† Independent sample student T-test
‡ Mann-Whitney test
¥ Statistically significant

For three NIVE parameters, absolute strain values were significantly lower in atherosclerotic plaques containing a lipid core compared to those devoid of lipid (Table IV-III). Figure 4.5 shows the Receiver Operating Characteristic (ROC) curve for the three significant NIVE parameters. Depending on chosen cut-off strain values to determine the presence or absence of a lipid core, sensitivities and specificities ranged from 77% to 100% and 57% to 79%, respectively. For indication of preventative medical therapy and regular follow-up, a greater sensitivity is required. Thus, for MSPSC, MaxSR and MinSR, maximum sensitivities of 88.2%, 94.1% and 100%, respectively, with corresponding specificities of 57.1%, were obtained for strain value thresholds of 0.254%, 1.834% $\times$ s^{-1}, and -2.380% $\times$ s^{-1}, respectively. On the other hand, for indication of surgical therapy, a greater specificity is preferred. Maximum specificities of 71.4%, 78.6%, and 78.6%, with corresponding sensitivities of 76.5%, 76.5%, and 94.1%, respectively, were obtained for strain value thresholds of 0.212%, 1.440% $\times$ s^{-1}, and -2.099% $\times$ s^{-1}.

Table IV-III. Bivariate Associations between Strain Parameters and Clinical Factors

Strain parameters	Strain values, Mean ± SD Median			*P*-value‡
	Total **n = 31**	**Lipid Present** **n = 17**	**Lipid Absent** **n = 14**	
MSPSC (%)	0.205 ± 0.120 0.193	0.163 ± 0.076 0.140	0.257 ± 0.144 0.259	0.032*
MSA (%)	1.248 ± 0.775 1.060	1.101 ± 0.677 0.806	1.428 ± 0.871 1.396	0.131
MaxSR (% s^{-1})	1.587 ± 1.004 1.407	1.110 ± 0.446 0.997	2.166 ± 1.193 2.020	0.003*
MinSR (% s^{-1})	-1.841 ± 1.199 -1.650	-1.234 ± 0.585 -1.139	-2.578 ± 1.354 -2.408	0.001*
		Calcium Present **n = 27**	**Calcium Absent** **n = 4**	
MSPSC (%)		0.213 ± 0.124 0.205	0.154 ± 0.086 0.166	0.346
MSA (%)		1.290 ± 0.804 1.060	0.971 ± 0.542 1.053	0.480
MaxSR (% s^{-1})		1.643 ± 1.042 1.407	1.212 ± 0.669 1.276	0.480
MinSR (% s^{-1})		-1.925 ± 1.241 -1.815	-1.275 ± 0.746 -1.349	0.263
		Symptomatic **n = 9**	**Asymptomatic** **n = 22**	
MSPSC (%)		0.193 ± 0.103 0.163	0.210 ± 0.128 0.206	0.761
MSA (%)		1.083 ± 0.613 0.963	1.316 ± 0.836 1.180	0.459

Table IV-III. Bivariate Associations… (cont'd)

MaxSR (% s^{-1})	1.624 ± 1.425 1.162	1.572 ± 0.816 1.488	0.514
MinSR (% s^{-1})	-1.815 ± 1.453 -1.278	-1.852 ± 1.118 -1.886	0.602
	Vulnerable on MRI n = 7	**Non-Vulnerable on MRI n = 24**	
MSPSC (%)	0.169 ± 0.098 0.128	0.216 ± 0.125 0.212	0.238
MSA (%)	0.921 ± 0.396 0.806	1.344 ± 0.837 1.337	0.219
MaxSR (% s^{-1})	1.593 ± 1.615 0.902	1.585 ± 0.796 1.488	0.345
MinSR (% s^{-1})	-1.639 ± 1.663 -0.849	-1.900 ± 1.067 -1.950	0.131
	Male n =22	**Female n = 9**	
MSPSC (%)	0.204 ± 0.131 0.155	0.207 ± 0.093 0.221	0.602
MSA (%)	1.320 ± 0.856 1.083	1.074 ± 0.531 0.938	0.663
MaxSR (% s^{-1})	1.545 ± 1.088 1.233	1.690 ± 0.810 1.736	0.384
MinSR (% s^{-1})	-1.792 ± 1.311 -1.418	-1.961 ± 0.927 -2.214	0.258

MSA = Mean Strain Amplitude; MSPSC = Mean Strain at Peak Systolic Compression; MaxSR = Maximal Strain Rate; MinSR = Minimal Strain Rate; sBP = systolic blood pressure; dBP = diastolic blood pressure.
‡ Mann-Whitney test
* Statistically significant

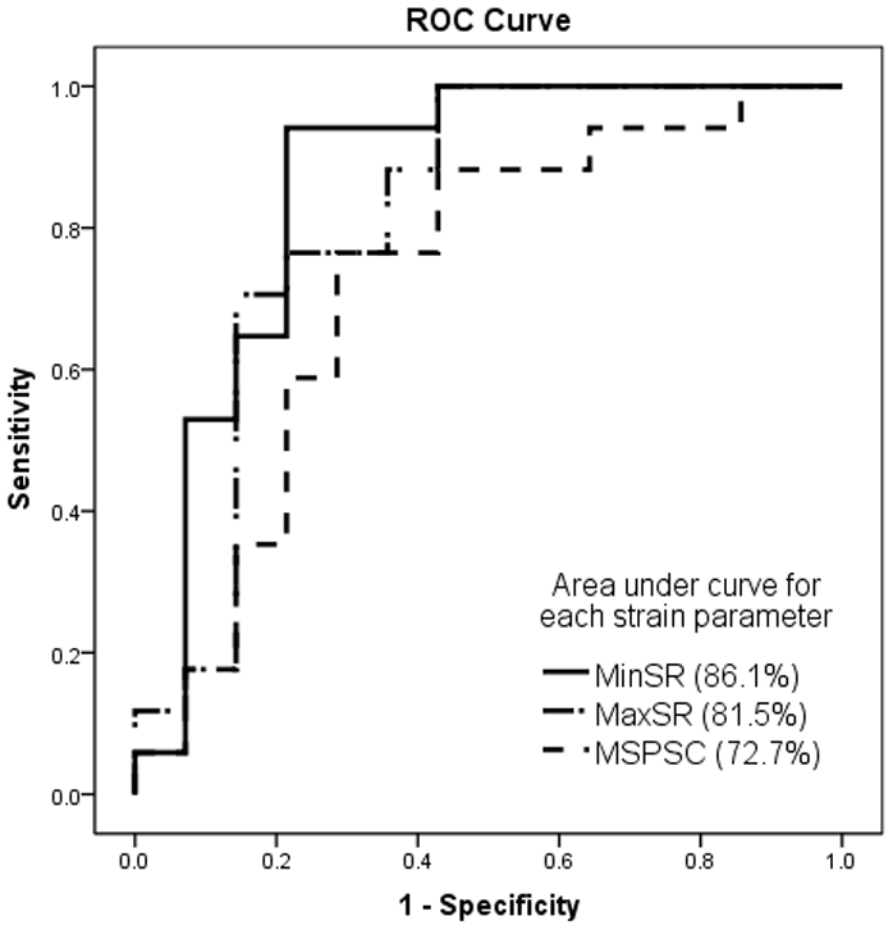

Figure 4.5. ROC curves for NIVE strain parameters to detect the presence of a lipid core.

NIVE strain parameters did not show a significant difference between symptomatic and asymptomatic groups, vulnerable and non-vulnerable plaques on MRI, genders, or presence and absence of calcium, inflammation, loose matrix, hemorrhage or ulceration (Figure 4.6, Table IV-III). There were no significant associations between strain parameters and modified Rankin scale score, degree of stenosis, age, heart rate, and mean diastolic and systolic blood pressures, except for a single strain parameter, MSA, correlating negatively with heart rate (Spearman correlation coefficient (r_s) = -0.385, p = 0.036).

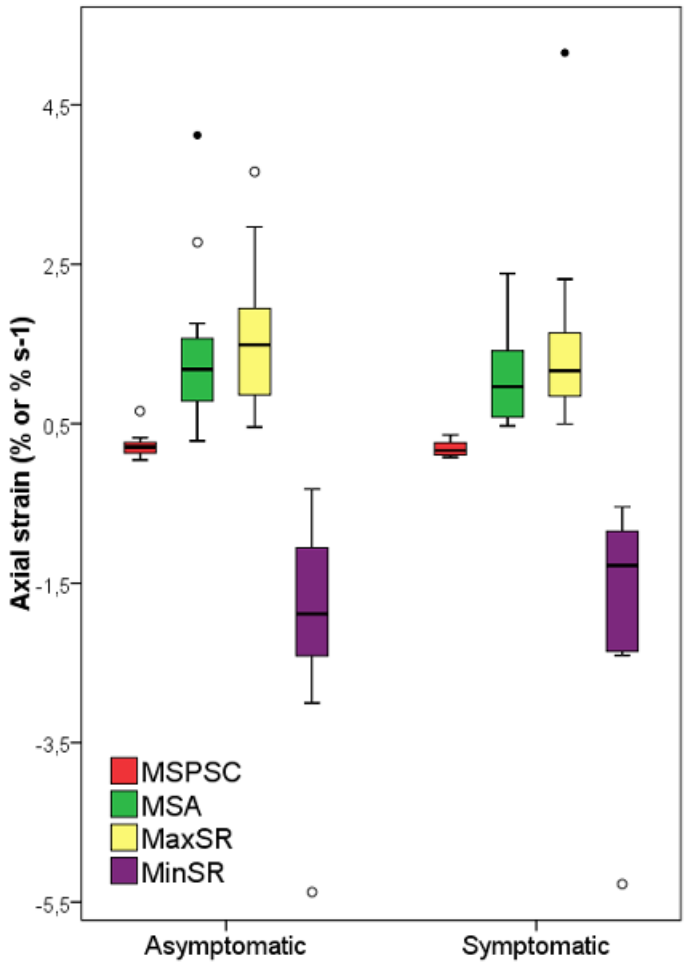

Figure 4.6. Distribution of axial strain parameters by presence of symptoms. MSPSC = Mean Strain at Peak Systolic Compression; MSA = Mean Strain Amplitude; MaxSR and MinSR = Maximal and Minimal Strain Rates.

There was a significant correlation between the %Lipid volume and each of the 4 NIVE parameters (Figure 4.7a). Curve-fitting analyses revealed a statistically significant quadratic fit, estimated with the addition of the quadratic term $(\%\text{Lipid volume})^2$ (Table IV-IV). On scatter plots, higher strains were observed with little to no lipid content, followed by an initial decrease in strain values until approximately 12% Lipid volume, after which strain values increased slightly with lipid content (the opposite was observed for MinSR) (Figure 4.7a). Only age and heart rate were found to have a confounding effect on these associations. Nevertheless, these associations were maintained at significance levels when controlling those two variables in multivariate analyses (Table IV-IV). An inverse correlation between %Calcium volume and %Lipid volume was found (r_s = - 0.624, p = 0.00009), but %Calcium volume did not significantly change the nature or strength of the association between %Lipid volume and each strain parameter.

There were borderline positive linear associations between %Calcium volume and two strain parameters, MSA and MinSR (Figure 4.7b); however these associations lost significance when controlling for confounding variables (Table IV-IV). Finally, there were no significant correlations between percentage volumes of other plaque components and strain parameters.

Figure 4.7:

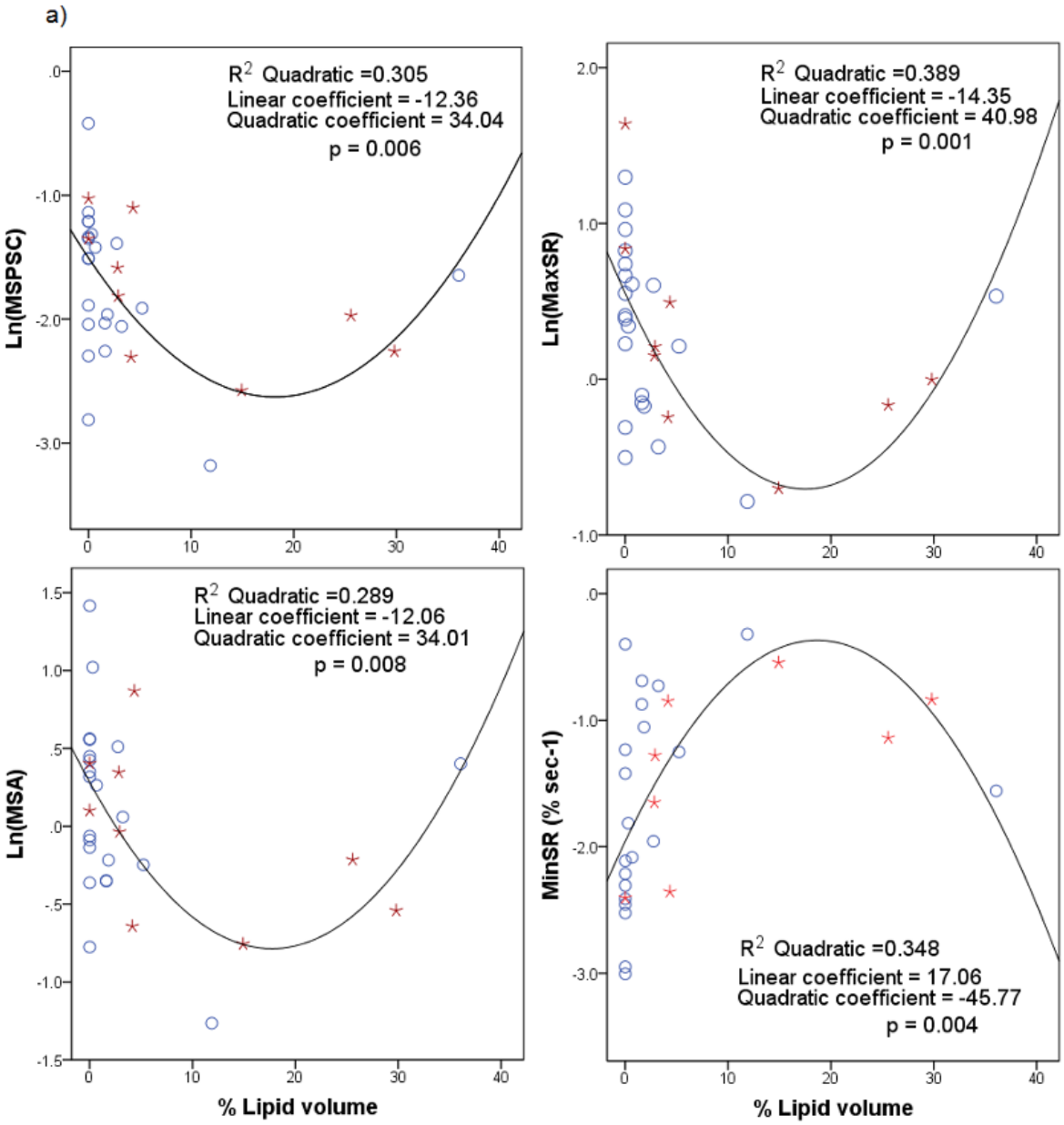
a)
R² Quadratic =0.305
Linear coefficient = -12.36
Quadratic coefficient = 34.04
p = 0.006
Ln(MSPSC)
R² Quadratic =0.389
Linear coefficient = -14.35
Quadratic coefficient = 40.98
p = 0.001
Ln(MaxSR)
R² Quadratic =0.289
Linear coefficient = -12.06
Quadratic coefficient = 34.01
p = 0.008
Ln(MSA)
R² Quadratic =0.348
Linear coefficient = 17.06
Quadratic coefficient = -45.77
p = 0.004
MinSR (% sec-1)
% Lipid volume
% Lipid volume

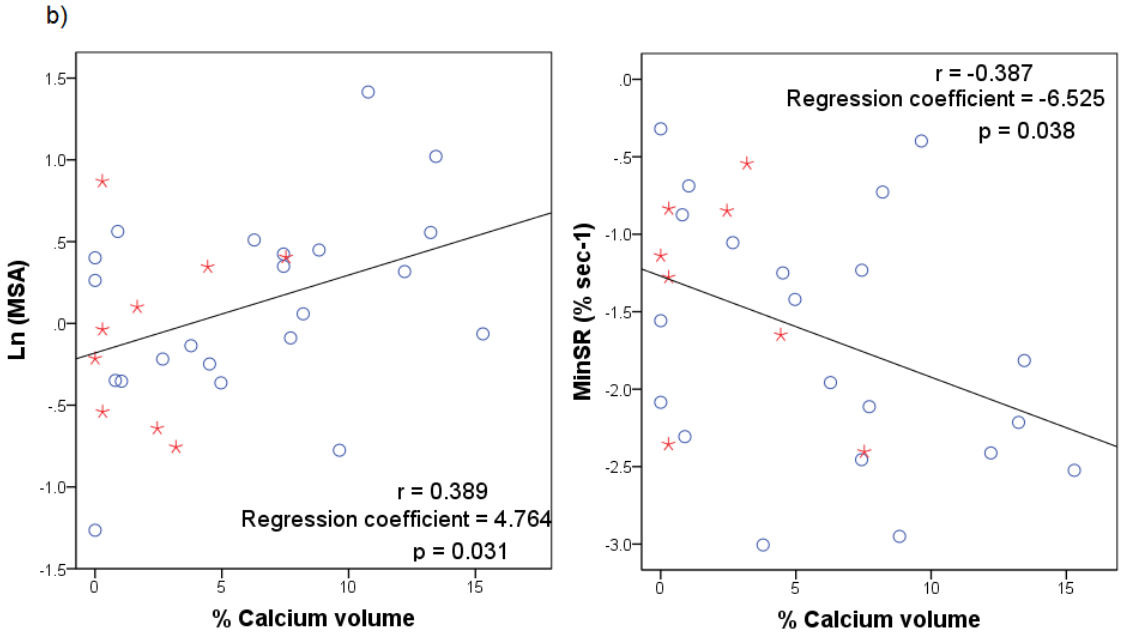

Figure 4.7. Scatter plots with curve fitting functions of the natural logarithm of strain parameters with (a) % Lipid volume and (b) % Calcium volume (bivariate analyses). Note that only for the MinSR parameter, 2 outliers were removed to normalize the distribution. For all other parameters, a natural logarithm was applied for normalization. MSPSC = Mean Strain at Peak Systolic Compression; MSA = Mean Strain Amplitude; MaxSR and MinSR = Maximal and Minimal Strain Rates.

Note: red stars = symptomatic group, blue circles = asymptomatic group

Table IV-IV. Multivariate Analyses for Each Strain Parameter				
Multivariate model	Estimate (linear or quadratic coefficient)	*p*-value	Joint *p*-value (F-test)	95% CI
Ln(MSPSC) *				
%Lipid volume	-10.98	0.008¥	0.0211¥	-18.78 ; -3.18
$(\%\text{Lipid volume})^2$	30.48	0.016¥		6.27 ; 54.68
Ln(MSA) **				
%Lipid volume	-11.33	0.0031¥	0.0105¥	-18.46 ; -4.21
$(\%\text{Lipid volume})^2$	32.29	0.0056¥		10.36 ; 54.23
Ln(MaxSR) **				
%Lipid volume	-11.67	0.0021¥	0.0078¥	-18.68 ; -4.50
$(\%\text{Lipid volume})^2$	34.04	0.0032¥		12.59 ; 55.62
MinSR *†				
%Lipid volume	16.98	0.0031¥	0.0068¥	6.34 ; 27.67
$(\%\text{Lipid volume})^2$	-45.53	0.0089¥		-78.66 ; -12.59
Ln(MSA) **				
%Calcium volume	3.62	0.0877	N/A	-0.58 ; 7.78
MinSR *†				
%Calcium volume	-6.25	0.0584	N/A	-12.71 ; 0.25

Ln( )= natural logarithmic of ( ) ; MSPSC = Mean Strain at Peak Systolic Compression; MSA = Mean Strain Amplitude; MaxSR = Maximal Strain Rate; MinSR = Minimal Strain Rate; %Lipid volume = percent of lipid contained in total plaque volume; $(\%\text{Lipid volume})^2$ = %Lipid volume X %Lipid volume (quadratic term); %Calcium volume = percent of calcium contained in total plaque volume; CI = confidence interval.

*Controlled for age

**Controlled for both age and heart rate

† Removal of 2 outlier negative values to obtain a normal distribution; these outliers are kept in Figure 4.7 scatter plots

¥ Statistically significant

DISCUSSION

This study demonstrated the clinical feasibility of NIVE to characterize plaque composition by strain analysis in patients with 50% or greater carotid stenosis. The NIVE algorithm used in our study is based on the Lagrangian Speckle Model Estimator that estimates the deformation of plaque components induced by the cardiac pulsation [112] *(21)*. It does not require external compression or creation of a radiation force. Acoustic radiation force impulse imaging was tested in phantoms, ex-vivo and in-vivo in carotid arteries but without clinical validation [198] *(29)*.

In this patient population, NIVE strain parameters (MSPSC, Max and MinSR) could detect the presence of a lipid core with sensitivities of up to 100% and corresponding specificities of up to 79%. The ability of non-invasively detecting a lipid core with NIVE in patients with 50% or greater stenosis can be valuable to detect plaque vulnerability and monitor the efficacy of medical treatment on plaque stabilization. Such a tool could also be helpful to help determine which asymptomatic patients would most benefit from medical versus surgical treatment.

We observed significantly lower strain values in carotid plaques that contained a lipid core. This contradicts findings from previous authors who observed higher strain values in early fatty plaques compared to non-fatty plaques using Intravascular Ultrasound Elastography (IVUS) in iliac and femoral arteries of pigs [199] *(30)*. In this last study, the types of atherosclerotic plaques were different than those of the present patient population: all fatty plaques were less than 30% stenotic, and all plaques were homogeneous and devoid of calcium. Conversely, the present study included mostly heterogeneous plaques with some degree of calcification, and at least 50% diameter reduction. Given that strain parameters were spatially averaged on the whole segmented plaque,

we interpret our findings with a “damper” hypothesis, whereby a lipid core embedded in a large stenotic plaque behaves as a damper reducing deformation of the whole plaque.

We observed a non-linear “U”-shaped association between axial strain indices and plaque lipid content (Figure 4.7a). This quadratic fit is explained by the above finding where plaques containing lipid had smaller strains than those devoid of lipid. As the lipid core further increased in size above a threshold of approximately 12% lipid volume, there was a slight and steady increase in strain, but with values that remained lower than strains of plaques devoid of lipid (Figures 4.7a). The latter part of the association relies on a very small number of subjects, but concurs with the observation of others [199] *(30)* that increasing lipid content will increase strain. Therefore, although NIVE can currently detect plaques that contain a lipid core, further technical optimisation and analysis may provide NIVE with the ability to determine which fatty plaque would become vulnerable. The assessment of Young’s modulograms with *a priori* information relying on elastography strain maps is an avenue deserving attention for such an objective [200,201] *(31, 32)*.

We observed a significant tendency for MSA to increase and MinSR to decrease with calcium content, despite wide variability (Figure 4.7b). In contrast, previous authors reported lower strain values in calcified areas on in vivo ultrasound elastograms [115] *(33)*. In a previous study on a few in vivo cases, we found that the effect of a rigid calcium annulus could cause a high mechanical stress on other plaque components and induce high strain values around it [113] *(16)*. Since we are averaging strain parameters within the whole plaque, this “hammer effect” may explain the large variability and slight rise in strain associated with calcium content. Detection of areas with elevated strain or high strain spatial variation may be valuable to identify areas of potential plaque rupture and elevated shear stress. Areas suspected of having these

features included the shoulders of a plaque or areas adjacent to superficial calcium nodules [33] *(4)*.

Strain parameters did not discriminate symptomatic subjects or vulnerable plaque according to MRI criteria. This can partially be explained by the spatial averaging of strain parameters as discussed above. In addition, we did not study more sensitive surrogate endpoints of vulnerability such as subclinical ischemic lesions on follow-up brain MRI or advanced neuropsychological testing [116] *(34)*, thus limiting the evaluation of vulnerability to hard clinical endpoints, which usually require a larger sample size to find meaningful differences. Finally, in contrast to the study by Maurice et al [114] *(17)* on normal subjects demonstrating higher strain values in women, we did not find gender differences. This may be attributed to our sample population, with a male predominance and advanced atherosclerotic disease.

Baseline clinical characteristics were similar among symptomatic and asymptomatic subjects, except for a higher prevalence of peripheral vascular disease, hypertension, and higher mean systolic blood pressure in asymptomatic subjects. This can be explained by the selection process of asymptomatic patients (mainly recruited from vascular surgery and interventional radiology clinics), and by the strong association between peripheral vascular disease and hypertension [202] *(35)*.

Other imaging results from the present study are consistent with previous studies. Symptomatic patients had a higher prevalence of plaque vulnerability features by MRI [157] *(12)*, higher lipid and lower calcium plaque content [152,203] *(13,36)* by MRI, and lower plaque echogenicity [80] *(37)* by ultrasound compared to asymptomatic patients.

Our study adds to earlier findings by providing a non-invasive technique, measurements averaged over more than one cardiac cycle, and four distinct

strain parameters that showed consistent associations with lipid content. The strain parameters MSPSC and MSA used in this study were similar to those used in other studies, both in computation methodology and strain magnitude [113-115,199,204] *(16, 17, 30, 33, 38)*. Finally, our study is the first to provide non-invasive strain analysis in vivo in patients with significant carotid stenosis due to atherosclerotic disease, with high-resolution multicontrast MRI as a reference standard for plaque composition.

The present ultrasound NIVE technique has limitations in the characterization of atherosclerotic plaques. First, as described above, given that most atherosclerotic plaques are heterogeneous structures made of lipid and calcium, areas with high and low deformations are pooled together to compute mean strain. This evens out strain parameter values and consequently decreases the ability of NIVE to discriminate plaques based on mechanical behavior. Second, most of the plaque consists of fibrous tissue. With a two-dimensional longitudinal acquisition, a limited B-mode image quality obtained from reconstructed RF signals, and no real time visualization of elastograms, we could not target specific regions of interest within the plaque during image acquisition and segmentation. This last drawback could be alleviated with further developments to obtain real-time imaging; it is comparable to performing color Doppler scanning without image feedback for probe positioning over the region of interest.

The present study provides a comprehensive evaluation of the current ultrasound NIVE technique and a better understanding of carotid plaque biomechanical behaviour in relation to plaque content. In addition, it demonstrates the need for technical optimisation of strain analysis in order to identify the lipid core, discriminate other plaque components, and ultimately detect vulnerability. Further studies with exploration of real-time imaging to visualize and target plaque components, echo-texture analysis based on raw RF

signals, and shear strain mapping could be valuable to improve plaque characterization and detect vulnerability.

In conclusion, ultrasound NIVE determines time-varying atherosclerotic plaque strains. This technique is feasible and can detect the presence of a lipid core in subjects with 50% or greater carotid stenosis with high sensitivity and moderate specificity. Larger patient populations and further technical optimization of ultrasound NIVE with plaque subcomponent analysis are required to better characterize the biomechanical behaviour of carotid atherosclerotic plaques.

ACKNOWLEDGEMENTS:

The authors are grateful to Mrs Vicky Thiffault, Louise Allard and Andrée Cliche for their dedication in study coordination, IRB documentation preparation and patient recruitment. We would like to also acknowledge the contributions of Drs Stéphane Elkouri, Nathalie Beaudoin, Jean-Francois Blair and Eric Therasse in patient recruitment and useful advices. We would also like to thank Madame Marie-Pierre Sylvestre, biostatistician, who guided us through statistical analyses.

The authors are also grateful to the Natural Sciences and Engineering Research Council of Canada, the Canadian Institutes of Health Research, Gestion Univalor and Bracco Diagnostics who provided grants to help fund this project.

REFERENCES

1. *Pasternak RC, Criqui MH, Benjamin EJ, et al. (2004) Atherosclerotic Vascular Disease Conference: Writing Group I: Epidemiology. Circulation, 109(21):2605-2612.*
2. *Rothwell PM, Eliasziw M, Gutnikov SA, et al. (2003) Analysis of pooled data from the randomised controlled trials of endarterectomy for symptomatic carotid stenosis. Lancet, 361(9352):107-116.*
3. *Halliday A, Harrison M, Hayter E, et al. (2010) 10-year stroke prevention after successful carotid endarterectomy for asymptomatic stenosis (ACST-1): a multicentre randomised trial. Lancet, 376(9746):1074-1084.*
4. *Naghavi M, Libby P, Falk E, et al. (2003) From vulnerable plaque to vulnerable patient: a call for new definitions and risk assessment strategies: Part I. Circulation, 108(14):1664-1672.*
5. *Redgrave JNE, Lovett JK, Gallagher PJ, Rothwell PM (2006) Histological Assessment of 526 Symptomatic Carotid Plaques in Relation to the Nature and Timing of Ischemic Symptoms: The Oxford Plaque Study. Circulation, 113(19):2320-2328.*
6. *de Weert TT, Ouhlous M, Meijering E, et al. (2006) In Vivo Characterization and Quantification of Atherosclerotic Carotid Plaque Components With Multidetector Computed Tomography and Histopathological Correlation. Arterioscler Thromb Vasc Biol, 26(10):2366-2372.*

7. *Tawakol A, Migrino RQ, Bashian GG, et al. (2006) In Vivo 18F-Fluorodeoxyglucose Positron Emission Tomography Imaging Provides a Noninvasive Measure of Carotid Plaque Inflammation in Patients. J Am Coll Cardiol, 48(9):1818-1824.*

8. *Christodoulou CI, Pattichis CS, Pantziaris M, Nicolaides A (2003) Texture-based classification of atherosclerotic carotid plaques. IEEE Trans Med Imaging, 22(7):902-912.*

9. *Ainsworth CD, Blake CC, Tamayo A, Beletsky V, Fenster A, Spence JD (2005) 3D ultrasound measurement of change in carotid plaque volume: a tool for rapid evaluation of new therapies. Stroke, 36(9):1904-1909.*

10. *Cai J, Hatsukami TS, Ferguson MS, et al. (2005) In vivo quantitative measurement of intact fibrous cap and lipid-rich necrotic core size in atherosclerotic carotid plaque: comparison of high-resolution, contrast-enhanced magnetic resonance imaging and histology. Circulation, 112(22):3437-3444.*

11. *Cappendijk VC, Cleutjens KBJM, Kessels AGH, et al. (2005) Assessment of Human Atherosclerotic Carotid Plaque Components with Multisequence MR Imaging: Initial Experience. Radiology, 234(2):487-492.*

12. *Saam T, Cai J, Ma L, et al. (2006) Comparison of symptomatic and asymptomatic atherosclerotic carotid plaque features with in vivo MR imaging. Radiology, 240(2):464-472.*

13. *Takaya N, Yuan C, Chu B, et al. (2006) Association between carotid plaque characteristics and subsequent ischemic cerebrovascular events: a prospective assessment with MRI--initial results. Stroke, 37(3):818-823.*

14. *Yuan C, Mitsumori LM, Ferguson MS, et al. (2001) In vivo accuracy of multispectral magnetic resonance imaging for identifying lipid-rich necrotic cores and intraplaque hemorrhage in advanced human carotid plaques. Circulation, 104(17):2051-2056.*

15. *Saam T, Ferguson MS, Yarnykh VL, et al. (2005) Quantitative evaluation of carotid plaque composition by in vivo MRI. Arterioscler Thromb Vasc Biol, 25(1):234-239.*

16. *Schmitt C, Soulez G, Maurice RL, Giroux MF, Cloutier G (2007) Noninvasive vascular elastography: toward a complementary characterization tool of atherosclerosis in carotid arteries. Ultrasound Med Biol, 33(12):1841-1858.*

17. *Maurice RL, Soulez G, Giroux MF, Cloutier G (2008) Noninvasive vascular elastography for carotid artery characterization on subjects without previous history of atherosclerosis. Med Phys, 35(8):3436-3443.*

18. *(1991) Beneficial effect of carotid endarterectomy in symptomatic patients with high-grade carotid stenosis. North American Symptomatic Carotid Endarterectomy Trial Collaborators. N Engl J Med, 325(7):445-453.*

19. *Grant EG, Benson CB, Moneta GL, et al. (2003) Carotid Artery Stenosis: Gray-Scale and Doppler US Diagnosis--Society of Radiologists in Ultrasound Consensus Conference. Radiology, 229(2):340-346.*

20. *Destrempes F, Meunier J, Giroux MF, Soulez G, Cloutier G (2011) Segmentation of Plaques in Sequences of Ultrasonic B-Mode Images of Carotid Arteries Based on Motion Estimation and a Bayesian Model. IEEE Trans Biomed Eng, 58(8):2202-2211.*

21. *Maurice RL, Ohayon J, Fretigny Y, Bertrand M, Soulez G, Cloutier G (2004) Noninvasive vascular elastography: theoretical framework. IEEE Trans Med Imaging, 23(2):164-180.*

22. *Mercure E, Destrempes F, Ohayon J, Soulez G, Cloutier G (In press, 2012.) Quantitative parameter extraction from axial strain maps in non-invasive vascular elastography of carotid arteries(ed)^(eds) 3rd MICCAI Workshop on Computing and Visualization for (Intra) Vascular Imaging, 9 pages.*

23. *Cai J-M, Hatsukami TS, Ferguson MS, Small R, Polissar NL, Yuan C (2002) Classification of Human Carotid Atherosclerotic Lesions With In Vivo Multicontrast Magnetic Resonance Imaging. Circulation, 106(11):1368-1373.*

24. *Wasserman BA, Smith WI, Trout HH, Cannon RO, Balaban RS, Arai AE (2002) Carotid Artery Atherosclerosis: In Vivo Morphologic*

Characterization with Gadolinium-enhanced Double-oblique MR Imaging—Initial Results. Radiology, 223(2):566-573.

25. *Chu B, Kampschulte A, Ferguson MS, et al. (2004) Hemorrhage in the Atherosclerotic Carotid Plaque: A High-Resolution MRI Study. Stroke, 35(5):1079-1084.*

26. *Yuan C, Kerwin WS, Ferguson MS, et al. (2002) Contrast-enhanced high resolution MRI for atherosclerotic carotid artery tissue characterization. J Magn Reson Imaging, 15(1):62-67.*

27. *Kerwin WS, O'Brien KD, Ferguson MS, Polissar N, Hatsukami TS, Yuan C (2006) Inflammation in carotid atherosclerotic plaque: a dynamic contrast-enhanced MR imaging study. Radiology, 241(2):459-468.*

28. *Kerwin WS, Oikawa M, Yuan C, Jarvik GP, Hatsukami TS (2008) MR imaging of adventitial vasa vasorum in carotid atherosclerosis. Magn Reson Med, 59(3):507-514.*

29. *Allen JD, Ham KL, Dumont DM, Sileshi B, Trahey GE, Dahl JJ (2011) The development and potential of acoustic radiation force impulse (ARFI) imaging for carotid artery plaque characterization. Vasc Med, 16(4):302-311.*

30. *de Korte CL, Sierevogel MJ, Mastik F, et al. (2002) Identification of Atherosclerotic Plaque Components With Intravascular Ultrasound Elastography In Vivo. Circulation, 105(14):1627-1630.*

31. *Baldewsing RA, Danilouchkine MG, Mastik F, Schaar JA, Serruys PW, van der Steen AF (2008) An inverse method for imaging the local elasticity of atherosclerotic coronary plaques. IEEE transactions on information technology in biomedicine : a publication of the IEEE Engineering in Medicine and Biology Society, 12(3):277-289.*

32. *Le Floc'h S, Ohayon J, Tracqui P, et al. (2009) Vulnerable atherosclerotic plaque elasticity reconstruction based on a segmentation-driven optimization procedure using strain measurements: theoretical framework. IEEE Trans Med Imaging, 28(7):1126-1137.*

33. *Shi H, Mitchell CC, McCormick M, Kliewer MA, Dempsey RJ, Varghese T (2008) Preliminary in vivo atherosclerotic carotid plaque characterization using the accumulated axial strain and relative lateral shift strain indices. Phys Med Biol, 53(22):6377-6394.*

34. *Dempsey RJ, Vemuganti R, Varghese T, Hermann BP (2010) A review of carotid atherosclerosis and vascular cognitive decline: a new understanding of the keys to symptomology. Neurosurgery, 67(2):484-493; discussion 493-494.*

35. *Selvin E, Erlinger TP (2004) Prevalence of and risk factors for peripheral arterial disease in the United States: results from the National Health and Nutrition Examination Survey, 1999-2000. Circulation, 110(6):738-743.*

36. *Nandalur KR, Baskurt E, Hagspiel KD, Phillips CD, Kramer CM (2005) Calcified carotid atherosclerotic plaque is associated less with ischemic symptoms than is noncalcified plaque on MDCT. Am J Roentgenol, 184(1):295-298.*

37. *Mathiesen EB, Bonaa KH, Joakimsen O (2001) Echolucent plaques are associated with high risk of ischemic cerebrovascular events in carotid stenosis: the tromso study. Circulation, 103(17):2171-2175.*

38. *Larsson M, Kremer F, Claus P, Kuznetsova T, Brodin LA, D'Hooge J (2011) Ultrasound-based radial and longitudinal strain estimation of the carotid artery: a feasibility study. IEEE Trans Ultrason Ferroelectr Freq Control, 58(10):2244-2251.*

4.3. *Further discussion and future perspectives*

This postscript provides further discussion on methodology, results, and prospects of ultrasound non-invasive vascular elastography (US NIVE).

4.3.1. Study Methodology

The methodology of this study can be divided into three main components: clinical, MRI, and US NIVE.

The clinical methodology is focused on determining which patient is symptomatic and which is asymptomatic. This touches upon an important distinction between clinical and surrogate endpoints. Clinical endpoints are based on signs and symptoms that a patient presents with, whereas surrogate endpoints are based on pathological or indirect evidence of disease that does not necessarily cause apparent signs or symptoms (e.g. presence of an ulcerated plaque on an imaging study of an asymptomatic patient). Hence, as previously discussed in Chapter 2, not all vulnerable plaques are symptomatic. A vulnerable plaque may rupture and send a microembolus to the brain; the patient could have absolutely no new symptoms or complaints despite a small infarcted area in the brain. Moreover, a vulnerable plaque may rupture and occlude the internal carotid artery without causing clinical symptoms if the patient has an effective collateral circulation. It follows that classifying patients into symptomatic and asymptomatic for the purpose of detecting the vulnerable plaque must be done carefully and also consider silent manifestations of plaque vulnerability.

Cerebral ischemia due to a vulnerable carotid plaque occurs only in the anterior cerebral circulation. Lacunar infarcts in the basal ganglia region imply small penetrating artery disease; they are not caused by carotid plaque. A

patient who presents with stroke symptoms could have any type of stroke; the type of stroke must be defined before assuming it is caused by an ipsilateral carotid plaque.

In the present study, careful investigation as to the cause of stroke or TIA was performed for every patient by consulting medical records and the patient's physician if needed. Imaging studies were verified to confirm cerebral infarction (CT or MRI of the brain), cardiac thrombus (echocardiography), and large-vessel atherosclerotic disease (US color pulsed Doppler, CTA, MRA, or conventional angiography). The location of stroke and atherosclerotic plaque were well noted. Thus, symptomatic patients were classified as such when symptomatic from their ipsilateral carotid plaque. Asymptomatic patients were followed to determine if their carotid plaque was indeed vulnerable, either by developing future cerebral ischemic events from their carotid plaque or a total carotid occlusion from rapid plaque progression. If one of these situations occurred, the asymptomatic patient was classified as "symptomatic" regardless of presence or absence of clinical symptoms. Despite annual follow-up of asymptomatic patients with telephone interviews, dedicated questionnaires (Appendix 3) and thorough review of medical records and imaging examinations, valuable information could have been lost. Asymptomatic patients did not systematically have annual brain or carotid artery imaging; prescription of imaging studies was at the discretion of their physician, based on clinical indications. Therefore, some asymptomatic patients with microembolic strokes from their carotid artery or asymptomatic total carotid occlusion could have been missed.

The MRI protocol of the present study was based on an extensive literature review validating MRI against histopathology. In order to appropriately identify all major plaque components (lipid rich necrotic core, fibrous cap, intraplaque hemorrhage, loose and dense fibrous matrix, neovascularisation/inflammation, and calcifications), black-blood T1, T2,

proton density weighting, and T1 post-gadolinium contrast injection images are required, along with bright-blood 3D-TOF. Image slices for each of these pulse sequences had to be exactly at the same distances from the bifurcation and have the exact same plane for appropriate analysis. The detailed MRI protocol is based on protocols from validation studies and is described in the manuscript. High-resolution MRI of carotid plaque is a technically demanding examination that requires cooperation among investigators, radiology technicians, and frequent quality control of standardized technique, especially in our setting where the study was on-going for years with a small sample of recruited patients and changing staff. When data analysis began in 2010, there was already over 3 years of patient recruitment. During those 3 years, MRI acquisition methods differed slightly across patients and scanner operators. According to the study protocol, ten 3 mm-thick slices had to be acquired per image sequence, and these 10 slices had to concord in location and plane across all sequences. In reality, a few MRI studies had, for example, 12 slices in the T2 sequence, and 11 slices in T1 and proton density sequences, with an overlap of only 9 slices (Figure 4.8). In these patients, this partial overlap of image slices prevented full coverage of the plaque by all MR sequences. There are rational explanations for this: some plaques were too extensive to be covered by 10 slices, and some patients moved a few millimeters up or down in between sequence acquisitions. In such cases, the following was performed:

1. Image registration for proper positioning of slices
2. For quantitative analysis such as plaque volume, if plaque coverage was incomplete on the T1-weighted acquisition, available slices on other sequences (proton density or T2-weighted) were used. For instance, in Figure 4.8, a total of 14 slices would be used to quantify plaque volume and vessel wall areas.
3. For plaque morphology and AHA classification, interpretation was based on the overlapping slices, since they included the bulk of the plaque and all image sequences were available for proper plaque component identification.

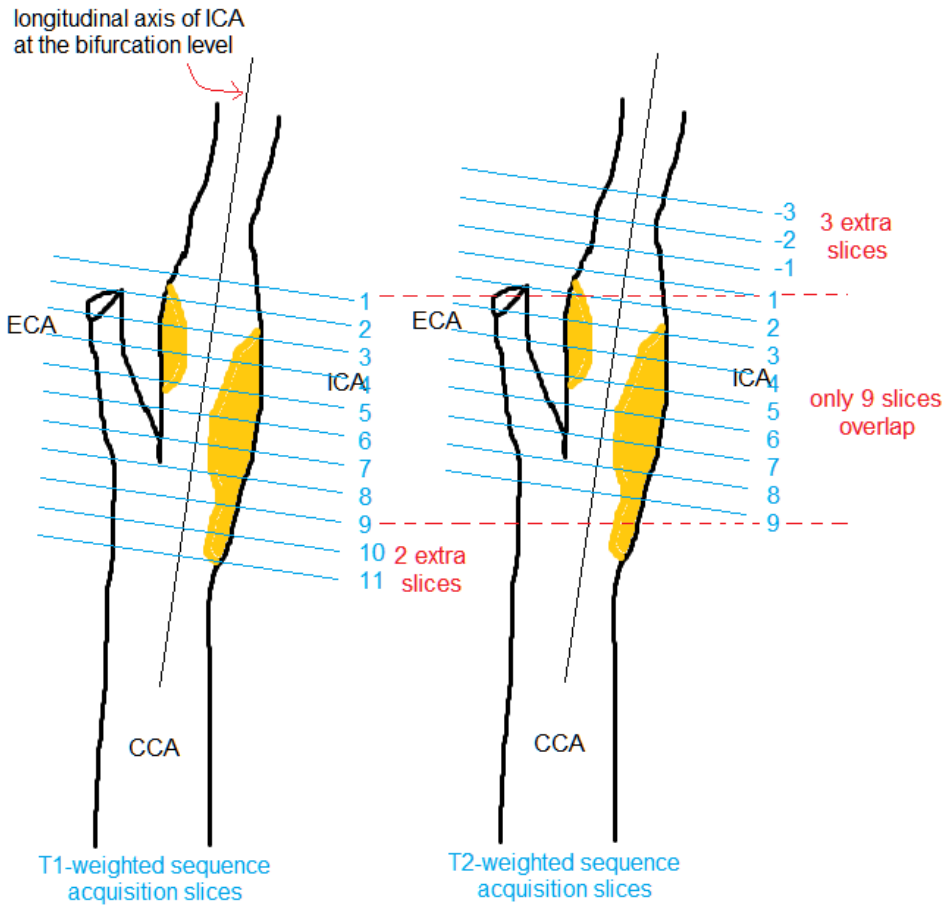

Figure 4.8. Common issue of slice acquisition overlap between image sequences.

Another common problem that occurred was a missing sequence, especially 3D TOF, which was not acquired in all patients for variable reasons (time constraints, unintentional oversight). Also, some sequences had poor image quality due to motion artefacts and could not be used for analysis. Based on a previous image quality assessment protocol [144], we required the following for MRI analysis to be valid:

1. At least 2 image sequences (among T1, T2, proton density, T1 post contrast, and 3D TOF) had to have an image quality of at least grade 2.
2. Image quality rating depends on overall SNR. Rating is from 1 (poor) to 5 (excellent):

Grade 1: low SNR limits use, arterial wall and vessel margins are unidentifiable

Grade 2: marginal SNR, arterial wall is visible, but the substructure, lumen, and outer boundaries are indistinct

Grade 3: marginal SNR, wall structures are identifiable, but lumen and outer boundaries are partially obscured

Grade 4: high SNR with minimal artefacts, vessel wall, lumen, and adventitial boundary are clearly defined

Grade 5: high SNR without artefacts, wall architecture depicted in detail, lumen and adventitial boundary are clearly defined.

Measurements of plaque burden and components were obtained with a semi-automatic segmentation software, QPlaque MR (Medis medical imaging systems, Leiden, Netherlands), dedicated to segmenting carotid plaque images in the transverse plane. Thus, image interpretation and segmentation was facilitated with image registration (placing all 5 image sequences at the corresponding spatial coordinates in all three x, y, and z dimensions), ability to adjust window-level, and zooming to pixel level for precise segmentation. Segmentation could be performed on any sequence because it appeared simultaneously on all other sequences, allowing for direct comparison and precise spatial registration. The main limitation of the QPlaqueMR software was the lack of an option to measure SNR, CNR, and relative signal intensity (rSI) compared to sternocleidomastoid muscle. Therefore, image interpretation was based on a subjective evaluation of rSI's.

The US NIVE methodology was complex and evolved considerably with techniques to decrease artefactual RF signals. First, a semi-automatic segmentation algorithm [118] provided improvements over manual segmentation: segmentation time decreased considerably and segmentation contours became less subjected to bias due to "copy-pasting" segmentation masks over multiple image frames and manual modifications per frame.

Second, a method to minimize noise and filter strain curves was proposed and applied [119]. The goals were to resolve issues of reproducibility of identification of peak strain values in noisy strain curves and to decrease noise related to respiratory motion and heart rate. The technique consisted of frequency spectrum analysis of initial raw strain curves, followed by elimination of frequencies below 0.3 Hz (representing a respiratory rate below approximately 20 per minute) and harmonic frequencies above 1.5 times the patient's heart rate. Thus, only frequencies in between, including the fundamental frequency corresponding to the heart rate, were sampled for analysis. After sampling, a reverse transformation back into time-varying strain curves was performed with the selected frequencies, resulting in smoother less noisy filtered strain curves. Associations of MRI plaque measurements with peak strain values from filtered strain curves were similar to those with peak strain values from raw noisy curves. Thus, this technique of filtering strain curves was adopted for analysis of all patients in the present study. Cardiac-gating with electrocardiography (ECG) during US NIVE acquisition would have been a good alternative to eliminate noise related to pulse rate, but the machine used in this study, SonixRP, did not include this option.

Another issue arose pertaining to computation of strain parameters of carotid plaques. Since two-dimensional B-mode US imaging was performed, the longitudinal views of carotid arteries often demonstrated both a near plaque portion (i.e. on the anterior carotid wall) and a far plaque portion (i.e. on the posterior carotid wall). Strain parameters of near plaque portions did not differ significantly from those of far plaque portions; hence, a weighted average strain value was computed based on plaque portion area. The following equation describes computation of the weighted average for total plaque strain:

$$S_{TOT} = S_N * (A_N / A_{TOT}) + S_F * (A_F / A_{TOT})$$

Where S_{TOT} = Total plaque Strain; S_N = Strain of Near plaque portion; S_F = Strain of Far plaque portion; A_N = Near plaque Area; A_F = Far plaque Area; and A_{TOT} = Total plaque Area.

4.3.2. Quadratic Correlation

The quadratic correlation found in this study relies on only 31 subjects, of which approximately 5 subjects with greater lipid volumes make it a U-shaped association. Although the discussion section in the above manuscript provides a rational explanation for this type of association, the conclusions drawn from it must be taken with a grain of salt. First, the sample population was too small to provide a sufficient power for this analysis. Second, high-resolution MRI has important limitations involving image quality, reproducibility of interpretation and measures, and specificity for precise segmentation of each individual component. Furthermore, our study used a 1.5T magnet; a 3.0T magnet may have provided a more robust quantification of plaque components. Quantification of plaque components on histological samples of carotid plaques would have been ideal; however, given the size and prospective nature of this study, in addition to a majority of asymptomatic patients not undergoing carotid endarterectomy, histological analysis could not be performed.

4.3.3. Clinical Correlations

In this study, clinical correlations depended on a slightly heterogeneous follow-up of subjects enrolled in this study. Symptomatic patients were more readily identified as such, since their clinical presentation and subsequent brain and cardiovascular imaging provided relatively concrete evidence of their carotid plaque vulnerability. Asymptomatic patients, on the other hand, were recruited through the Picture Archiving and Communication System (PACS) of the CHUM (Centre Hospitalier de l'Université de Montréal). Patients who had any type of carotid imaging that showed a 50% or greater carotid stenosis were contacted and asked if they were interested in participating. A portion of these patients were followed by a neurologist for remote symptoms, whereas

others were not because they never had any history of neurological symptoms. All asymptomatic patients were followed by the principle investigator (myself) by telephone to determine if patients developed neurological symptoms. Patients did not have serial brain imaging or serial neurological exams; hence the follow-up of this study was subject to information bias. Ideally, this study would have involved a neurological consultation and regular follow-ups in an equal manner for all asymptomatic patients (for example, with a single neurologist or a few that are trained to follow the same study protocol and indications for brain imaging). These measures could have decreased loss to follow-up and provided more accurate clinical information than telephone interviews and chart reviews. However, given the small sample population, it is unclear whether a more robust follow-up would have significantly changed results.

4.3.4. US Elastography Technical Optimization

The US elastography technique used in this study is still in its developmental stages. First, the frame-rate of imaging acquisition was only occasionally known; this could have contributed to the variability of strains observed from one subject's plaque to the next, although the use of cumulative strain values (such as for MSA) should have minimized this variability. Second, correction for artefacts (respiratory and motion artefacts, angle correction) was gradually implemented with power spectrum analysis and an algorithm for angle correction. At the time of publishing results, we found that only power spectrum analysis correcting for respiratory and motion artefacts caused a significant change in strain results; angle correction did not. Furthermore, the method of angle correction was not yet established for significantly stenotic carotid arteries. Hence we only "filtered" strain curves to eliminate motion artefacts from heart rate and respiration; this was performed uniformly across all 31 plaques, without any angle correction. Third, only axial strain was computed by the LSME algorithm, not lateral strain, because lateral resolution

of the ultrasound beam was twice as low as axial resolution (see Figure 4.1). Thus, whereas some plaques experienced more lateral strain than others, our data could not elucidate this information. Fourth, although two physicians performed US elastography acquisitions for each patient, only acquisitions performed by a single observer were analyzed and no study of interobserver reproducibility was performed. Fifth, B-mode images from reconstructed raw RF data were of poor quality; comparison with clinical B-mode US images had to be performed to appropriately localize and segment all plaques in a subjective manner. Individual plaque components and regions of interest could not be readily identified during imaging acquisition or during segmentation. It followed that we could not perform subsegmental analysis of individual plaque components to analyze their individual strains. Currently, however, an algorithm is being developed in our lab (LBUM) to help identify plaque subcomponents based on statistical distributions of signal echogenicity. In addition to modulography, this may contribute to detecting vulnerable plaque areas. Still, the most efficient manner of identifying subcomponents would be interactively during US NIVE acquisition; that is, with improved image quality on real-time imaging.

4.3.5. Final Conclusion

Ultrasound Non-Invasive Vascular Elastography is a novel technique that deserves attention in vascular medicine. Although it is at its developmental stages, technical optimization can be readily implemented, and US NIVE could be easily incorporated as an adjunct to routine carotid Doppler ultrasound examinations to help determine which plaques are vulnerable to biomechanical rupture. The results of the present pilot study on large carotid plaques presented in this thesis open an important door for this avenue.

This page is left intentionally blank

Section III

References

REFERENCES

1. (2006) Incidence and Prevalence: 2006 Chart Book on Cardiovascular and Lung Diseases.(ed)^(eds). National Heart, Lung, and Blood Institute, Bethesda, MD,

2. Azevedo FAC, Carvalho LRB, Grinberg LT, et al. (2009) Equal numbers of neuronal and nonneuronal cells make the human brain an isometrically scaled-up primate brain. The Journal of Comparative Neurology, 513(5):532-541.

3. Smith WS, English JD, Johnston SC (2012) Chapter 370. Cerebrovascular Diseases. In: D.L. Longo, A.S. Fauci, D.L. Kasper, S.L. Hauser, J.L. Jameson, J. Loscalzo, (eds) Harrison's Principles of Internal Medicine, 18th edn. McGraw-Hill, New York,

4. Hankey GJ (1996) Impact of treatment of people with transient ischemic attack on stroke incidence and public health. Cerebrovasc Dis, 6 (suppl 1):26-33.

5. Wu CM, McLaughlin K, Lorenzetti DL, Hill MD, Manns BJ, Ghali WA (2007) Early risk of stroke after transient ischemic attack: a systematic review and meta-analysis. Arch Intern Med, 167(22):2417-2422.

6. Giles MF, Rothwell PM (2007) Risk of stroke early after transient ischaemic attack: a systematic review and meta-analysis. Lancet neurology, 6(12):1063-1072.

7. Eliasziw M, Kennedy J, Hill MD, Buchan AM, Barnett HJ (2004) Early risk of stroke after a transient ischemic attack in patients with internal carotid artery disease. CMAJ, 170(7):1105-1109.

8. Johnston SC, Fayad PB, Gorelick PB, et al. (2003) Prevalence and knowledge of transient ischemic attack among US adults. Neurology, 60(9):1429-1434.

9. Hart RG, Benavente O (1999) Stroke: part I. A clinical update on prevention. Am Fam Physician, 59(9):2475-2482, 2485.

10. Pasternak RC, Criqui MH, Benjamin EJ, et al. (2004) Atherosclerotic Vascular Disease Conference: Writing Group I: Epidemiology. Circulation, 109(21):2605-2612.

11. Roger VL, Go AS, Lloyd-Jones DM, et al. (2011) Heart Disease and Stroke Statistics--2011 Update: A Report From the American Heart Association. Circulation, 123(4):e18-209.

12. (2009) Centers for Disease Control and Prevention. Prevalence and Most Common Causes of Disability Among Adults: United States, 2005.(ed)^(eds) MMWR Morbidity and Mortality Weekly Report pp 421-426

13. Xu JQ, Kochanek KD, Murphy SL, Tejada-Vera B (2010) Deaths: Final data for 2007. National vital statistics reports(ed)^(eds). National Center for Health Statistics, Hyattsville, MD,

14. Rosamond WD, Folsom AR, Chambless LE, et al. (1999) Stroke incidence and survival among middle-aged adults: 9-year follow-up of the Atherosclerosis Risk in Communities (ARIC) cohort. Stroke, 30(4):736-743.

15. El-Saed A, Kuller LH, Newman AB, et al. (2006) Geographic variations in stroke incidence and mortality among older populations in four US communities. Stroke, 37(8):1975-1979.

16. Asplund K, Stegmayr B, Peltonen M (1998) From the twentieth to the twenty-first century: a public health perspective on stroke. . Blackwell Science, Malden, Massachussetts

17. Bryan RN, Wells SW, Miller TJ, et al. (1997) Infarctlike lesions in the brain: prevalence and anatomic characteristics at MR imaging of the elderly--data from the Cardiovascular Health Study. Radiology, 202(1):47-54.

18. Howard G, Wagenknecht LE, Cai J, Cooper L, Kraut MA, Toole JF (1998) Cigarette smoking and other risk factors for silent cerebral infarction in the general population. Stroke, 29(5):913-917.

19. (Revised October 2003) National Institutes of Health NIH Stroke Scale. .

20. (2000) Part 3: Adult Basic Life Support. Circulation, 102(suppl 1):I-22-I-59.

21. (1991) Beneficial effect of carotid endarterectomy in symptomatic patients with high-grade carotid stenosis. North American Symptomatic Carotid Endarterectomy Trial Collaborators. N Engl J Med, 325(7):445-453.

22. Ota H, Takase K, Rikimaru H, et al. (2005) Quantitative Vascular Measurements in Arterial Occlusive Disease1. Radiographics, 25(5):1141-1158.

23. (1991) Beneficial effect of carotid endarterectomy in symptomatic patients with high-grade carotid stenosis. North American Symptomatic Carotid Endarterectomy Trial Collaborators.[see comment]. New England Journal of Medicine, 325(7):445-453.

24. Barnett HJM, Taylor DW, Eliasziw M, et al. (1998) Benefit of Carotid Endarterectomy in Patients with Symptomatic Moderate or Severe Stenosis. N Engl J Med, 339(20):1415-1425.

25. (1991) MRC European Carotid Surgery Trial: interim results for symptomatic patients with severe (70-99%) or with mild (0-29%) carotid stenosis. European Carotid Surgery Trialists' Collaborative Group.[see comment]. Lancet, 337(8752):1235-1243.

26. (1995) Endarterectomy for asymptomatic carotid artery stenosis. Executive Committee for the Asymptomatic Carotid Atherosclerosis Study. JAMA, 273(18):1421-1428.

27. Halliday A MA, Marro J, et al (2004) Prevention of disabling and fatal strokes by successful carotid endarterectomy in patients without recent neurological symptoms: randomised controlled trial. The Lancet, 363(9420):1491-1502.

28. Halliday A, Harrison M, Hayter E, et al. (2010) 10-year stroke prevention after successful carotid endarterectomy for asymptomatic stenosis (ACST-1): a multicentre randomised trial. Lancet, 376(9746):1074-1084.

29. Goessens BMB, Visseren FLJ, Kappelle LJ, Algra A, van der Graaf Y, for the SMART Study Group (2007) Asymptomatic Carotid Artery Stenosis and the Risk of New Vascular Events in Patients With Manifest Arterial Disease: The SMART Study. Stroke, 38(5):1470-1475.

30. Abbott AL, Chambers BR, Stork JL, Levi CR, Bladin CF, Donnan GA (2005) Embolic Signals And Prediction of Ipsilateral Stroke or Transient Ischemic Attack in Asymptomatic Carotid Stenosis: A Multicenter Prospective Cohort Study. Stroke, 36(6):1128-1133.

31. Nicolaides AN, Kakkos SK, Griffin M, et al. (2005) Severity of asymptomatic carotid stenosis and risk of ipsilateral hemispheric ischaemic events: results from the ACSRS study. Eur J Vasc Endovasc Surg, 30(3):275-284.

32. Abbott AL, Donnan GA (2008) Does the 'High Risk' Patient with Asymptomatic Carotid Stenosis Really Exist? European journal of vascular and endovascular surgery : the official journal of the European Society for Vascular Surgery, 35(5):524-533.

33. Naghavi M, Libby P, Falk E, et al. (2003) From vulnerable plaque to vulnerable patient: a call for new definitions and risk assessment strategies: Part I. Circulation, 108(14):1664-1672.

34. Lusis AJ (2000) Atherosclerosis. Nature, 407(6801):233-241.

35. Chambless LE, Folsom AR, Sharrett AR, et al. (2003) Coronary heart disease risk prediction in the Atherosclerosis Risk in Communities (ARIC) study. J Clin Epidemiol, 56(9):880-890.

36. Wilson PWF, D'Agostino RB, Levy D, Belanger AM, Silbershatz H, Kannel WB (1998) Prediction of Coronary Heart Disease Using Risk Factor Categories. Circulation, 97(18):1837-1847.

37. Pober JS, Min W, Bradley JR (2009) Mechanisms of Endothelial Dysfunction, Injury, and Death. Annual Review of Pathology: Mechanisms of Disease, 4(1):71-95.

38. Ross R (1999) Atherosclerosis — An Inflammatory Disease. N Engl J Med, 340(2):115-126.

39. Badimón L, Vilahur G, Padró T (2009) Lipoproteins, Platelets and Atherothrombosis. Rev Esp Cardiol, 62(10):1161-1178.

40. Chatzizisis YS, Coskun AU, Jonas M, Edelman ER, Feldman CL, Stone PH (2007) Role of Endothelial Shear Stress in the Natural History of Coronary Atherosclerosis and Vascular Remodeling: Molecular, Cellular, and Vascular Behavior. J Am Coll Cardiol, 49(25):2379-2393.

41. Gimbrone MA, Jr. (1999) Vascular endothelium, hemodynamic forces, and atherogenesis. Am J Pathol, 155(1):1-5.

42. Stary HC, Chandler AB, Dinsmore RE, et al. (1995) A definition of advanced types of atherosclerotic lesions and a histological classification of atherosclerosis. A report from the Committee on Vascular Lesions of the Council on Arteriosclerosis, American Heart Association. Arterioscler Thromb Vasc Biol, 15(9):1512-1531.

43. Stary HC (2000) Natural history and histological classification of atherosclerotic lesions: an update. Arterioscler Thromb Vasc Biol, 20(5):1177-1178.

44. Virmani R, Kolodgie FD, Burke AP, Farb A, Schwartz SM (2000) Lessons From Sudden Coronary Death : A Comprehensive Morphological Classification Scheme for Atherosclerotic Lesions. Arterioscler Thromb Vasc Biol, 20(5):1262-1275.

45. Virmani R, Burke A, Farb A, Kolodgie FD, Finn AV, Gold HK (2007) Pathology of the vulnerable plaque. In: R. Waksman, P.W. Serruys, J. Schaar, (eds) The Vulnerable Plaque, 2nd edn. Informa Healthcare, Oxon, United Kingdom,

46. Muller J, Tofler G, Stone P (1989) Circadian variation and triggers of onset of acute cardiovascular disease. Circulation, 79(4):733-743.

47. Schaar JA, Muller JE, Falk E, et al. (2004) Terminology for high-risk and vulnerable coronary artery plaques. Eur Heart J, 25(12):1077-1082.

48. Redgrave JNE, Lovett JK, Gallagher PJ, Rothwell PM (2006) Histological Assessment of 526 Symptomatic Carotid Plaques in Relation to the Nature and Timing of Ischemic Symptoms: The Oxford Plaque Study. Circulation, 113(19):2320-2328.

49. Spagnoli LG, Mauriello A, Sangiorgi G, et al. (2004) Extracranial thrombotically active carotid plaque as a risk factor for ischemic stroke. JAMA, 292(15):1845-1852.

50. Thim T, Hagensen MK, Bentzon JF, Falk E (2010) Pathology of Vulnerability Caused by High-Risk (Vulnerable) Arteries and Plaque. In: M. Naghavi, (ed) Asymptomatic Atherosclerosis: Pathophysiology, Detection, and Treatment. Springer, New York, NY,

51. Gronholdt ML, Nordestgaard BG, Bentzon J, et al. (2002) Macrophages are associated with lipid-rich carotid artery plaques, echolucency on B-mode imaging, and elevated plasma lipid levels. J Vasc Surg, 35(1):137-145.

52. Kolodgie FD, Gold HK, Burke AP, et al. (2003) Intraplaque hemorrhage and progression of coronary atheroma. N Engl J Med, 349(24):2316-2325.

53. Trostdorf F, Buchkremer M, Harmjanz A, et al. (2005) Fibrous cap thickness and smooth muscle cell apoptosis in high-grade carotid artery stenosis. Eur J Vasc Endovasc Surg, 29(5):528-535.

54. Redgrave JN, Gallagher P, Lovett JK, Rothwell PM (2008) Critical cap thickness and rupture in symptomatic carotid plaques: the oxford plaque study. Stroke, 39(6):1722-1729.

55. Libby P (2002) Inflammation in atherosclerosis. Nature, 420(6917):868-874.

56. Hansson GK (2005) Inflammation, atherosclerosis, and coronary artery disease. N Engl J Med, 352(16):1685-1695.

57. Lutgens E, de Muinck ED, Kitslaar PJ, Tordoir JH, Wellens HJ, Daemen MJ (1999) Biphasic pattern of cell turnover characterizes the progression from fatty streaks to ruptured human atherosclerotic plaques. Cardiovasc Res, 41(2):473-479.

58. Burke AP, Kolodgie FD, Farb A, Weber D, Virmani R (2002) Morphological predictors of arterial remodeling in coronary atherosclerosis. Circulation, 105(3):297-303.

59. Varnava AM, Mills PG, Davies MJ (2002) Relationship between coronary artery remodeling and plaque vulnerability. Circulation, 105(8):939-943.

60. Feldman CL, Chatzizisis YS, Coskun AU, Koskinas C, Naghavi M, Stone PH (2010) Vulnerable Anatomy; The Role of Coronary Anatomy and Endothelial Shear Stress in

the Progression and Vulnerability of Coronary Artery Lesions: Is Anatomy Destiny? In: M. Naghavi, (ed) Asymptomatic Atherosclerosis: Pathophysiology, Detection, and Treatment. Springer, New York, NY,

61. Falk E, Shah PK, Fuster V (1995) Coronary plaque disruption. Circulation, 92(3):657-671.

62. Wald NJ, Hackshaw AK, Frost CD (1999) When can a risk factor be used as a worthwhile screening test? BMJ, 319(7224):1562-1565.

63. Wald NJ, Morris JK, Rish S (2005) The efficacy of combining several risk factors as a screening test. J Med Screen, 12(4):197-201.

64. Ware JH (2006) The limitations of risk factors as prognostic tools. N Engl J Med, 355(25):2615-2617.

65. Lauer MS (2007) Primary prevention of atherosclerotic cardiovascular disease: the high public burden of low individual risk. JAMA, 297(12):1376-1378.

66. Naghavi M, Falk E, Hecht HS, et al. (2006) From vulnerable plaque to vulnerable patient--Part III: Executive summary of the Screening for Heart Attack Prevention and Education (SHAPE) Task Force report. Am J Cardiol, 98(2A):2H-15H.

67. Lanza GM, Wallace KD, Scott MJ, et al. (1996) A novel site-targeted ultrasonic contrast agent with broad biomedical application. Circulation, 94(12):3334-3340.

68. Demos SM, Alkan-Onyuksel H, Kane BJ, et al. (1999) In vivo targeting of acoustically reflective liposomes for intravascular and transvascular ultrasonic enhancement. J Am Coll Cardiol, 33(3):867-875.

69. Charles W (1991) MRC European Carotid Surgery Trial: interim results for symptomatic patients with severe (70-99%) or with mild (0-29%) carotid stenosis. The Lancet, 337(8752):1235-1243.

70. (1998) Randomised trial of endarterectomy for recently symptomatic carotid stenosis: final results of the MRC European Carotid Surgery Trial (ECST). Lancet, 351(9113):1379-1387.

71. Tahmasebpour HR, Buckley AR, Cooperberg PL, Fix CH (2005) Sonographic examination of the carotid arteries. Radiographics, 25(6):1561-1575.

72. AbuRahma AF, Kyer Iii PD, Robinson PA, Hannay RS (1998) The correlation of ultrasonic carotid plaque morphology and carotid plaque hemorrhage: clinical implications. Surgery, 124(4):721-728.

73. Hatsukami TS, Thackray BD, Primozich JF, et al. (1994) Echolucent regions in carotid plaque: preliminary analysis comparing three-dimensional histologic reconstructions to sonographic findings. Ultrasound Med Biol, 20(8):743-749.

74. Sabetai MM, Tegos TJ, Nicolaides AN, et al. (2000) Hemispheric symptoms and carotid plaque echomorphology. J Vasc Surg, 31(1 Pt 1):39-49.

75. Prabhakaran S, Rundek T, Ramas R, et al. (2006) Carotid plaque surface irregularity predicts ischemic stroke: the northern Manhattan study. Stroke, 37(11):2696-2701.

76. Grant EG, Benson CB, Moneta GL, et al. (2003) Carotid Artery Stenosis: Gray-Scale and Doppler US Diagnosis--Society of Radiologists in Ultrasound Consensus Conference. Radiology, 229(2):340-346.

77. Furst H, Hartl WH, Jansen I, Liepsch D, Lauterjung L, Schildberg FW (1992) Color-flow Doppler sonography in the identification of ulcerative

plaques in patients with high-grade carotid artery stenosis. AJNR Am J Neuroradiol, 13(6):1581-1587.

78. Gronholdt ML, Nordestgaard BG, Schroeder TV, Vorstrup S, Sillesen H (2001) Ultrasonic echolucent carotid plaques predict future strokes. Circulation, 104(1):68-73.

79. Polak JF, Shemanski L, O'Leary DH, et al. (1998) Hypoechoic plaque at US of the carotid artery: an independent risk factor for incident stroke in adults aged 65 years or older. Cardiovascular Health Study. Radiology, 208(3):649-654.

80. Mathiesen EB, Bonaa KH, Joakimsen O (2001) Echolucent plaques are associated with high risk of ischemic cerebrovascular events in carotid stenosis: the tromso study. Circulation, 103(17):2171-2175.

81. Reiter M, Effenberger I, Sabeti S, et al. (2008) Increasing carotid plaque echolucency is predictive of cardiovascular events in high-risk patients. Radiology, 248(3):1050-1055.

82. Joakimsen O, Bonaa KH, Stensland-Bugge E (1997) Reproducibility of ultrasound assessment of carotid plaque occurrence, thickness, and morphology. The Tromso Study. Stroke, 28(11):2201-2207.

83. Grogan JK, Shaalan WE, Cheng H, et al. (2005) B-mode ultrasonographic characterization of carotid atherosclerotic plaques in symptomatic and asymptomatic patients. J Vasc Surg, 42(3):435-441.

84. el-Barghouty N, Geroulakos G, Nicolaides A, Androulakis A, Bahal V (1995) Computer-assisted carotid plaque characterisation. Eur J Vasc Endovasc Surg, 9(4):389-393.

85. Takiuchi S, Rakugi H, Honda K, et al. (2000) Quantitative ultrasonic tissue characterization can identify high-risk atherosclerotic alteration in human carotid arteries. Circulation, 102(7):766-770.

86. Christodoulou CI, Pattichis CS, Pantziaris M, Nicolaides A (2003) Texture-based classification of atherosclerotic carotid plaques. IEEE Trans Med Imaging, 22(7):902-912.

87. Kakkos SK, Nicolaides AN, Kyriacou E, et al. (2011) Computerized Texture Analysis of Carotid Plaque Ultrasonic Images Can Identify Unstable Plaques Associated With Ipsilateral Neurological Symptoms. Angiology, 62(4):317-328.

88. Spence JD, Eliasziw M, DiCicco M, Hackam DG, Galil R, Lohmann T (2002) Carotid plaque area: a tool for targeting and evaluating vascular preventive therapy. Stroke, 33(12):2916-2922.

89. Ainsworth CD, Blake CC, Tamayo A, Beletsky V, Fenster A, Spence JD (2005) 3D ultrasound measurement of change in carotid plaque volume: a tool for rapid evaluation of new therapies. Stroke, 36(9):1904-1909.

90. Egger M, Spence JD, Fenster A, Parraga G (2007) Validation of 3D ultrasound vessel wall volume: an imaging phenotype of carotid atherosclerosis. Ultrasound Med Biol, 33(6):905-914.

91. Fenster A, Blake C, Gyacskov I, Landry A, Spence JD (2006) 3D ultrasound analysis of carotid plaque volume and surface morphology. Ultrasonics, 44 Suppl 1:e153-157.

92. Ukwatta E, Awad J, Ward AD, et al. (2011) Three-dimensional ultrasound of carotid atherosclerosis: semiautomated segmentation using a level set-based method. Med Phys, 38(5):2479-2493.

93. Yamaguchi M, Sasaki M, Ohba H, et al. Quantitative assessment of changes in carotid plaques during cilostazol administration using three-dimensional ultrasonography and non-gated magnetic resonance plaque imaging. Neuroradiology, 10.1007/s00234-012-1011-2:1-7.

94. Krasinski A, Chiu B, Spence JD, Fenster A, Parraga G (2009) Three-dimensional ultrasound quantification of intensive statin treatment of carotid atherosclerosis. Ultrasound Med Biol, 35(11):1763-1772.

95. Heliopoulos J, Vadikolias K, Piperidou C, Mitsias P (2011) Detection of Carotid Artery Plaque Ulceration Using 3-Dimensional Ultrasound. J Neuroimaging, 21(2):126-131.

96. Kono Y, Pinnell SP, Sirlin CB, et al. (2004) Carotid arteries: contrast-enhanced US angiography--preliminary clinical experience. Radiology, 230(2):561-568.

97. Shah F, Balan P, Weinberg M, et al. (2007) Contrast-enhanced ultrasound imaging of atherosclerotic carotid plaque neovascularization: a new surrogate marker of atherosclerosis? Vasc Med, 12(4):291-297.

98. Coli S, Magnoni M, Sangiorgi G, et al. (2008) Contrast-enhanced ultrasound imaging of intraplaque neovascularization in carotid arteries: correlation with histology and plaque echogenicity. J Am Coll Cardiol, 52(3):223-230.

99. Hoogi A, Adam D, Hoffman A, Kerner H, Reisner S, Gaitini D (2011) Carotid Plaque Vulnerability: Quantification of Neovascularization on Contrast-Enhanced Ultrasound With Histopathologic Correlation. Am J Roentgenol, 196(2):431-436.

100. Xiong L, Deng YB, Zhu Y, Liu YN, Bi XJ (2009) Correlation of carotid plaque neovascularization detected by using contrast-enhanced US with clinical symptoms. Radiology, 251(2):583-589.

101. Faggioli GL, Pini R, Mauro R, et al. (2011) Identification of Carotid 'Vulnerable Plaque' by Contrast-enhanced Ultrasonography: Correlation with Plaque Histology, Symptoms and Cerebral Computed Tomography. Eur J Vasc Endovasc Surg, 41(2):238-248.

102. Staub D, Patel MB, Tibrewala A, et al. (2010) Vasa Vasorum and Plaque Neovascularization on Contrast-Enhanced Carotid Ultrasound Imaging Correlates With Cardiovascular Disease and Past Cardiovascular Events. Stroke, 41(1):41-47.

103. Staub D, Partovi S, Schinkel AFL, et al. (2011) Correlation of Carotid Artery Atherosclerotic Lesion Echogenicity and Severity at Standard US with Intraplaque Neovascularization Detected at Contrast-enhanced US. Radiology, 258(2):618-626.

104. Kaufmann BA, Sanders JM, Davis C, et al. (2007) Molecular imaging of inflammation in atherosclerosis with targeted ultrasound detection of vascular cell adhesion molecule-1. Circulation, 116(3):276-284.

105. Kaufmann BA, Carr CL, Belcik JT, et al. (2010) Molecular imaging of the initial inflammatory response in atherosclerosis: implications for early detection of disease. Arterioscler Thromb Vasc Biol, 30(1):54-59.

106. Yan F, Li X, Jin Q, et al. (2012) Ultrasonic Imaging of Endothelial CD81 Expression Using CD81-Targeted Contrast Agents in In Vitro and In Vivo Studies. Ultrasound in Medicine & Biology, 38(4):670-680.

107. Chen J, Tung CH, Mahmood U, et al. (2002) In vivo imaging of proteolytic activity in atherosclerosis. Circulation, 105(23):2766-2771.

108. Shalhoub J, Monaco C, Owen DRJ, et al. (2011) Late-Phase Contrast-Enhanced Ultrasound Reflects Biological Features of Instability in Human Carotid Atherosclerosis. Stroke, 42(12):3634-3636.

109. (2006) Sonovue - Summary of Product Characteristics(ed)^(eds). Bracco International B.V.,

110. Yoshida J, Ohmori K, Takeuchi H, et al. (2005) Treatment of ischemic limbs based on local recruitment of vascular endothelial growth factor-producing inflammatory cells with ultrasonic microbubble destruction. J Am Coll Cardiol, 46(5):899-905.

111. Ophir J, Cespedes I, Ponnekanti H, Yazdi Y, Li X (1991) Elastography: a quantitative method for imaging the elasticity of biological tissues. Ultrason Imaging, 13(2):111-134.

112. Maurice RL, Ohayon J, Fretigny Y, Bertrand M, Soulez G, Cloutier G (2004) Noninvasive vascular elastography: theoretical framework. IEEE Trans Med Imaging, 23(2):164-180.

113. Schmitt C, Soulez G, Maurice RL, Giroux MF, Cloutier G (2007) Noninvasive vascular elastography: toward a complementary characterization tool of atherosclerosis in carotid arteries. Ultrasound Med Biol, 33(12):1841-1858.

114. Maurice RL, Soulez G, Giroux MF, Cloutier G (2008) Noninvasive vascular elastography for carotid artery characterization on subjects without previous history of atherosclerosis. Med Phys, 35(8):3436-3443.

115. Shi H, Mitchell CC, McCormick M, Kliewer MA, Dempsey RJ, Varghese T (2008) Preliminary in vivo atherosclerotic carotid plaque characterization using the accumulated axial strain and relative lateral shift strain indices. Phys Med Biol, 53(22):6377-6394.

116. Dempsey RJ, Vemuganti R, Varghese T, Hermann BP (2010) A review of carotid atherosclerosis and vascular cognitive decline: a new understanding of the keys to symptomology. Neurosurgery, 67(2):484-493; discussion 493-494.

117. Mercure E, Cloutier G, Schmitt C, Maurice RL (2008) Performance evaluation of different implementations of the Lagrangian speckle model estimator for non-invasive vascular ultrasound elastography. Med Phys, 35(7):3116-3126.

118. Destrempes F, Meunier J, Giroux MF, Soulez G, Cloutier G (2011) Segmentation of Plaques in Sequences of Ultrasonic B-Mode Images of Carotid Arteries Based on Motion Estimation and a Bayesian Model. IEEE Trans Biomed Eng, 58(8):2202-2211.

119. Mercure E, Destrempes F, Ohayon J, Soulez G, Cloutier G (In press, 2012.) Quantitative parameter extraction from axial strain maps in non-invasive vascular elastography of carotid arteries(ed)^(eds) 3rd MICCAI Workshop on Computing and Visualization for (Intra) Vascular Imaging, pp 9 pages

120. Allen JD, Ham KL, Dumont DM, Sileshi B, Trahey GE, Dahl JJ (2011) The development and potential of acoustic radiation force impulse (ARFI) imaging for carotid artery plaque characterization. Vasc Med, 16(4):302-311.

121. Couade M, Pernot M, Prada C, et al. (2010) Quantitative Assessment of Arterial Wall Biomechanical Properties Using Shear Wave Imaging. Ultrasound in Medicine & Biology, 36(10):1662-1676.

122. Walker LJ, Ismail A, McMeekin W, Lambert D, Mendelow AD, Birchall D (2002) Computed Tomography Angiography for the Evaluation of Carotid Atherosclerotic Plaque. Stroke, 33(4):977-981.

123. Wintermark M, Jawadi SS, Rapp JH, et al. (2008) High-resolution CT imaging of carotid artery atherosclerotic plaques. AJNR Am J Neuroradiol, 29(5):875-882.

124. Saba L, Caddeo G, Sanfilippo R, Montisci R, Mallarini G (2007) CT and ultrasound in the study of ulcerated carotid plaque compared with surgical results: potentialities and advantages of multidetector row CT angiography. AJNR Am J Neuroradiol, 28(6):1061-1066.

125. de Weert TT, Ouhlous M, Meijering E, et al. (2006) In Vivo Characterization and Quantification of Atherosclerotic Carotid Plaque Components With Multidetector Computed Tomography and Histopathological Correlation. Arterioscler Thromb Vasc Biol, 26(10):2366-2372.

126. de Weert TT, de Monye C, Meijering E, et al. (2008) Assessment of atherosclerotic carotid plaque volume with multidetector computed tomography angiography. The international journal of cardiovascular imaging, 24(7):751-759.

127. Saba L, Montisci R, Sanfilippo R, Mallarini G (2009) Multidetector row CT of the brain and carotid artery: a correlative analysis. Clin Radiol, 64(8):767-778.

128. Das M, Braunschweig T, Mühlenbruch G, et al. (2009) Carotid Plaque Analysis: Comparison of Dual-Source Computed Tomography (CT) Findings and Histopathological Correlation. European journal of vascular and endovascular surgery : the official journal of the European Society for Vascular Surgery, 38(1):14-19.

129. Ajduk M, Pavić L, Bulimbašić S, et al. (2009) Multidetector-Row Computed Tomography in Evaluation of Atherosclerotic Carotid Plaques Complicated with Intraplaque Hemorrhage. Ann Vasc Surg, 23(2):186-193.

130. U-King-Im JM, Fox AJ, Aviv RI, et al. (2010) Characterization of Carotid Plaque Hemorrhage. Stroke, 41(8):1623-1629.

131. Cai J-M, Hatsukami TS, Ferguson MS, Small R, Polissar NL, Yuan C (2002) Classification of Human Carotid Atherosclerotic Lesions With In Vivo Multicontrast Magnetic Resonance Imaging. Circulation, 106(11):1368-1373.

132. Nandalur KR, Baskurt E, Hagspiel KD, Phillips CD, Kramer CM (2005) Calcified carotid atherosclerotic plaque is associated less with ischemic symptoms than is noncalcified plaque on MDCT. AJR Am J Roentgenol, 184(1):295-298.

133. Saba L, Lai M, Montisci R, et al. (2012) Association between carotid plaque enhancement shown by multidetector CT angiography and histologically validated microvessel density. Eur Radiol, 10.1007/s00330-012-2467-5:1-9.

134. Romero JM, Babiarz LS, Forero NP, et al. (2009) Arterial Wall Enhancement Overlying Carotid Plaque on CT Angiography Correlates

With Symptoms in Patients With High Grade Stenosis. Stroke, 40(5):1894-1896.

135. Saba L, Mallarini G (2011) Carotid Plaque Enhancement and Symptom Correlations: An Evaluation by Using Multidetector Row CT Angiography. American Journal of Neuroradiology, 32(10):1919-1925.

136. Horie N, Morikawa M, Ishizaka S, et al. (2012) Assessment of Carotid Plaque Stability Based on the Dynamic Enhancement Pattern in Plaque Components With Multidetector CT Angiography. Stroke, 43(2):393-398.

137. Saba L, Piga M, Raz E, Farina D, Montisci R (2012) Carotid Artery Plaque Classification: Does Contrast Enhancement Play a Significant Role? American Journal of Neuroradiology, 10.3174/ajnr.A3073.

138. Schroeder S, Kopp AF, Ohnesorge B, et al. (2001) Accuracy and reliability of quantitative measurements in coronary arteries by multi-slice computed tomography: experimental and initial clinical results. Clin Radiol, 56(6):466-474.

139. Cademartiri F, Mollet NR, Runza G, et al. (2005) Influence of intracoronary attenuation on coronary plaque measurements using multislice computed tomography: observations in an ex vivo model of coronary computed tomography angiography. Eur Radiol, 15(7):1426-1431.

140. Hyafil F, Cornily JC, Feig JE, et al. (2007) Noninvasive detection of macrophages using a nanoparticulate contrast agent for computed tomography. Nat Med, 13(5):636-641.

141. Hyafil F, Cornily J-C, Rudd JHF, Machac J, Feldman LJ, Fayad ZA (2009) Quantification of Inflammation Within Rabbit Atherosclerotic Plaques Using the Macrophage-Specific CT Contrast Agent N1177: A Comparison with 18F-FDG PET/CT and Histology. J Nucl Med, 50(6):959-965.

142. Van Herck J, De Meyer G, Martinet W, et al. (2010) Multi-slice computed tomography with N1177 identifies ruptured atherosclerotic plaques in rabbits. Basic Res Cardiol, 105(1):51-59.

143. Toussaint JF, Southern JF, Fuster V, Kantor HL (1995) T2-weighted contrast for NMR characterization of human atherosclerosis. Arterioscler Thromb Vasc Biol, 15(10):1533-1542.

144. Yuan C, Mitsumori LM, Ferguson MS, et al. (2001) In vivo accuracy of multispectral magnetic resonance imaging for identifying lipid-rich necrotic cores and intraplaque hemorrhage in advanced human carotid plaques. Circulation, 104(17):2051-2056.

145. Hatsukami TS, Ross R, Polissar NL, Yuan C (2000) Visualization of fibrous cap thickness and rupture in human atherosclerotic carotid plaque in vivo with high-resolution magnetic resonance imaging. Circulation, 102(9):959-964.

146. Clarke SE, Hammond RR, Mitchell JR, Rutt BK (2003) Quantitative assessment of carotid plaque composition using multicontrast MRI and registered histology. Magn Reson Med, 50(6):1199-1208.

147. Saam T, Ferguson MS, Yarnykh VL, et al. (2005) Quantitative evaluation of carotid plaque composition by in vivo MRI. Arterioscler Thromb Vasc Biol, 25(1):234-239.

148. Cai J, Hatsukami TS, Ferguson MS, et al. (2005) In vivo quantitative measurement of intact fibrous cap and lipid-rich necrotic core size in atherosclerotic carotid plaque: comparison of high-resolution, contrast-enhanced magnetic resonance imaging and histology. Circulation, 112(22):3437-3444.

149. Saam T, Underhill HR, Chu B, et al. (2008) Prevalence of American Heart Association type VI carotid atherosclerotic lesions identified by magnetic resonance imaging for different levels of stenosis as measured by duplex ultrasound. J Am Coll Cardiol, 51(10):1014-1021.

150. Mitsumori LM, Hatsukami TS, Ferguson MS, Kerwin WS, Cai J, Yuan C (2003) In vivo accuracy of multisequence MR imaging for identifying unstable fibrous caps in advanced human carotid plaques. J Magn Reson Imaging, 17(4):410-420.

151. Yuan C, Zhang SX, Polissar NL, et al. (2002) Identification of fibrous cap rupture with magnetic resonance imaging is highly associated with recent transient ischemic attack or stroke. Circulation.

152. Takaya N, Yuan C, Chu B, et al. (2006) Association between carotid plaque characteristics and subsequent ischemic cerebrovascular events: a prospective assessment with MRI--initial results. Stroke, 37(3):818-823.

153. Cappendijk VC, Cleutjens KBJM, Kessels AGH, et al. (2005) Assessment of Human Atherosclerotic Carotid Plaque Components with Multisequence MR Imaging: Initial Experience. Radiology, 234(2):487-492.

154. Moody AR, Murphy RE, Morgan PS, et al. (2003) Characterization of complicated carotid plaque with magnetic resonance direct thrombus

imaging in patients with cerebral ischemia. Circulation, 107(24):3047-3052.

155. Chu B, Kampschulte A, Ferguson MS, et al. (2004) Hemorrhage in the Atherosclerotic Carotid Plaque: A High-Resolution MRI Study. Stroke, 35(5):1079-1084.

156. Murphy RE, Moody AR, Morgan PS, et al. (2003) Prevalence of complicated carotid atheroma as detected by magnetic resonance direct thrombus imaging in patients with suspected carotid artery stenosis and previous acute cerebral ischemia. Circulation, 107(24):3053-3058.

157. Saam T, Cai J, Ma L, et al. (2006) Comparison of symptomatic and asymptomatic atherosclerotic carotid plaque features with in vivo MR imaging. Radiology, 240(2):464-472.

158. Altaf N, Daniels L, Morgan PS, et al. (2008) Detection of intraplaque hemorrhage by magnetic resonance imaging in symptomatic patients with mild to moderate carotid stenosis predicts recurrent neurological events. J Vasc Surg, 47(2):337-342.

159. Singh N, Moody AR, Gladstone DJ, et al. (2009) Moderate Carotid Artery Stenosis: MR Imaging–depicted Intraplaque Hemorrhage Predicts Risk of Cerebrovascular Ischemic Events in Asymptomatic Men1. Radiology, 252(2):502-508.

160. Takaya N, Yuan C, Chu B, et al. (2005) Presence of intraplaque hemorrhage stimulates progression of carotid atherosclerotic plaques: a high-resolution magnetic resonance imaging study. Circulation, 111(21):2768-2775.

161. Parmar JP, Rogers WJ, Mugler JP, et al. (2010) Magnetic Resonance Imaging of Carotid Atherosclerotic Plaque in Clinically Suspected Acute Transient Ischemic Attack and Acute Ischemic Stroke / Clinical Perspective. Circulation, 122(20):2031-2038.

162. JM UK-I, Tang TY, Patterson A, et al. (2008) Characterisation of carotid atheroma in symptomatic and asymptomatic patients using high resolution MRI. J Neurol Neurosurg Psychiatry, 79(8):905-912.

163. Yuan C, Kerwin WS, Ferguson MS, et al. (2002) Contrast-enhanced high resolution MRI for atherosclerotic carotid artery tissue characterization. J Magn Reson Imaging, 15(1):62-67.

164. Wasserman BA, Smith WI, Trout HH, Cannon RO, Balaban RS, Arai AE (2002) Carotid Artery Atherosclerosis: In Vivo Morphologic Characterization with Gadolinium-enhanced Double-oblique MR Imaging—Initial Results. Radiology, 223(2):566-573.

165. Balu N, Yarnykh VL, Scholnick J, Chu B, Yuan C, Hayes C (2009) Improvements in carotid plaque imaging using a new eight-element phased array coil at 3T. J Magn Reson Imaging, 30(5):1209-1214.

166. Yarnykh VL, Terashima M, Hayes CE, et al. (2006) Multicontrast black-blood MRI of carotid arteries: comparison between 1.5 and 3 tesla magnetic field strengths. J Magn Reson Imaging, 23(5):691-698.

167. Syed M, Oshinski J, Kitchen C, Ali A, Charnigo R, Quyyumi A (2009) Variability of carotid artery measurements on 3-Tesla MRI and its impact on sample size calculation for clinical research. The International Journal of Cardiovascular Imaging (formerly Cardiac Imaging), 25(6):581-589.

168. Alizadeh Dehnavi R, Doornbos J, Tamsma JT, et al. (2007) Assessment of the carotid artery by MRI at 3T: a study on reproducibility. J Magn Reson Imaging, 25(5):1035-1043.

169. Li F, Yarnykh VL, Hatsukami TS, et al. (2010) Scan-rescan reproducibility of carotid atherosclerotic plaque morphology and tissue composition measurements using multicontrast MRI at 3T. J Magn Reson Imaging, 31(1):168-176.

170. Wasserman BA, Astor BC, Sharrett AR, Swingen C, Catellier D (2010) MRI measurements of carotid plaque in the atherosclerosis risk in communities (ARIC) study: Methods, reliability and descriptive statistics. J Magn Reson Imaging, 31(2):406-415.

171. Touze E, Toussaint JF, Coste J, et al. (2007) Reproducibility of high-resolution MRI for the identification and the quantification of carotid atherosclerotic plaque components: consequences for prognosis studies and therapeutic trials. Stroke, 38(6):1812-1819.

172. Sadat U, Weerakkody RA, Bowden DJ, et al. (2009) Utility of high resolution MR imaging to assess carotid plaque morphology: A comparison of acute symptomatic, recently symptomatic and asymptomatic patients with carotid artery disease. Atherosclerosis, 207(2):434-439.

173. Kerwin WS, Oikawa M, Yuan C, Jarvik GP, Hatsukami TS (2008) MR imaging of adventitial vasa vasorum in carotid atherosclerosis. Magn Reson Med, 59(3):507-514.

174. Lombardo A, Rizzello V, Natale L, et al. (2009) Magnetic resonance imaging of carotid plaque inflammation in acute coronary syndromes: a sign of multisite plaque activation. Int J Cardiol, 136(1):103-105.

175. Leiner T, Gerretsen S, Botnar R, et al. (2005) Magnetic resonance imaging of atherosclerosis. Eur Radiol, 15(6):1087-1099.

176. Yoo B, Pagel MD (2008) An overview of responsive MRI contrast agents for molecular imaging. Front Biosci, 13:1733-1752.

177. Kooi ME, Cappendijk VC, Cleutjens KB, et al. (2003) Accumulation of ultrasmall superparamagnetic particles of iron oxide in human atherosclerotic plaques can be detected by in vivo magnetic resonance imaging. Circulation, 107(19):2453-2458.

178. Trivedi RA, Mallawarachi C, JM UK-I, et al. (2006) Identifying inflamed carotid plaques using in vivo USPIO-enhanced MR imaging to label plaque macrophages. Arterioscler Thromb Vasc Biol, 26(7):1601-1606.

179. Howarth SP, Tang TY, Trivedi R, et al. (2009) Utility of USPIO-enhanced MR imaging to identify inflammation and the fibrous cap: a comparison of symptomatic and asymptomatic individuals. Eur J Radiol, 70(3):555-560.

180. Tang TY, Howarth SP, Miller SR, et al. (2009) The ATHEROMA (Atorvastatin Therapy: Effects on Reduction of Macrophage Activity) Study. Evaluation using ultrasmall superparamagnetic iron oxide-enhanced magnetic resonance imaging in carotid disease. J Am Coll Cardiol, 53(22):2039-2050.

181. Sirol M, Itskovich VV, Mani V, et al. (2004) Lipid-rich atherosclerotic plaques detected by gadofluorine-enhanced in vivo magnetic resonance imaging. Circulation, 109(23):2890-2896.

182. Ouimet T, Lancelot E, Hyafil F, et al. (2012) Molecular and Cellular Targets of the MRI Contrast Agent P947 for Atherosclerosis Imaging. Molecular Pharmaceutics, 9(4):850-861.

183. Boussel L, Arora S, Rapp J, et al. (2009) Atherosclerotic plaque progression in carotid arteries: monitoring with high-spatial-resolution MR imaging--multicenter trial. Radiology, 252(3):789-796.

184. Underhill HR, Yuan C, Zhao XQ, et al. (2008) Effect of rosuvastatin therapy on carotid plaque morphology and composition in moderately hypercholesterolemic patients: a high-resolution magnetic resonance imaging trial. Am Heart J, 155(3):584 e581-588.

185. Wang Q, Wang Y, Cai J, Cai Y, Ma L, Xu X (2010) Differences of signal evolution of intraplaque hemorrhage and associated stenosis between symptomatic and asymptomatic atherosclerotic carotid arteries: an in vivo high-resolution magnetic resonance imaging follow-up study. The International Journal of Cardiovascular Imaging (formerly Cardiac Imaging), 26(0):323-332.

186. Underhill HR, Hatsukami TS, Cai J, et al. (2010) A Noninvasive Imaging Approach to Assess Plaque Severity: The Carotid Atherosclerosis Score. American Journal of Neuroradiology, 31(6):1068-1075.

187. Noguchi T, Yamada N, Higashi M, Goto Y, Naito H (2011) High-Intensity Signals in Carotid Plaques on T1-Weighted Magnetic Resonance Imaging Predict Coronary Events in Patients With Coronary Artery Disease. J Am Coll Cardiol, 58(4):416-422.

188. Kwee RM, van Oostenbrugge RJ, Prins MH, et al. (2010) Symptomatic Patients With Mild and Moderate Carotid Stenosis. Stroke, 41(7):1389-1393.

189. Esposito L, Saam T, Heider P, et al. (2010) MRI plaque imaging reveals high-risk carotid plaques especially in diabetic patients irrespective of the degree of stenosis. BMC Medical Imaging, 10(1):27.

190. Virani SS, Catellier DJ, Pompeii LA, et al. (2011) Relation of cholesterol and lipoprotein parameters with carotid artery plaque characteristics: The Atherosclerosis Risk in Communities (ARIC) carotid MRI study. Atherosclerosis, 219(2):596-602.

191. Saam T, Raya JG, Cyran CC, et al. (2009) High resolution carotid black-blood 3T MR with parallel imaging and dedicated 4-channel surface coils. J Cardiovasc Magn Reson, 11:41.

192. Bornstedt A, Bernhardt P, Hombach V, et al. (2008) Local excitation black blood imaging at 3T: application to the carotid artery wall. Magn Reson Med, 59(5):1207-1211.

193. Dong L, Wang J, Yarnykh VL, et al. (2010) Efficient flow suppressed MRI improves interscan reproducibility of carotid atherosclerosis plaque burden measurements. J Magn Reson Imaging, 32(2):452-458.

194. Ota H, Yarnykh VL, Ferguson MS, et al. (2010) Carotid Intraplaque Hemorrhage Imaging at 3.0-T MR Imaging: Comparison of the Diagnostic Performance of Three T1-weighted Sequences1. Radiology, 254(2):551-563.

195. Rothwell PM, Eliasziw M, Gutnikov SA, et al. (2003) Analysis of pooled data from the randomised controlled trials of endarterectomy for symptomatic carotid stenosis. Lancet, 361(9352):107-116.

196. Tawakol A, Migrino RQ, Bashian GG, et al. (2006) In Vivo 18F-Fluorodeoxyglucose Positron Emission Tomography Imaging Provides a Noninvasive Measure of Carotid Plaque Inflammation in Patients. J Am Coll Cardiol, 48(9):1818-1824.

197. Kerwin WS, O'Brien KD, Ferguson MS, Polissar N, Hatsukami TS, Yuan C (2006) Inflammation in carotid atherosclerotic plaque: a dynamic contrast-enhanced MR imaging study. Radiology, 241(2):459-468.

198. Allen JD, Ham KL, Dumont DM, Sileshi B, Trahey GE, Dahl JJ (2011) The development and potential of acoustic radiation force impulse (ARFI) imaging for carotid artery plaque characterization. Vasc Med, 16(4):302-311.

199. de Korte CL, Sierevogel MJ, Mastik F, et al. (2002) Identification of Atherosclerotic Plaque Components With Intravascular Ultrasound Elastography In Vivo. Circulation, 105(14):1627-1630.

200. Baldewsing RA, Danilouchkine MG, Mastik F, Schaar JA, Serruys PW, van der Steen AF (2008) An inverse method for imaging the local elasticity of atherosclerotic coronary plaques. IEEE transactions on information technology in biomedicine : a publication of the IEEE Engineering in Medicine and Biology Society, 12(3):277-289.

201. Le Floc'h S, Ohayon J, Tracqui P, et al. (2009) Vulnerable atherosclerotic plaque elasticity reconstruction based on a segmentation-driven optimization procedure using strain measurements: theoretical framework. IEEE Trans Med Imaging, 28(7):1126-1137.

202. Selvin E, Erlinger TP (2004) Prevalence of and risk factors for peripheral arterial disease in the United States: results from the National Health and Nutrition Examination Survey, 1999-2000. Circulation, 110(6):738-743.

203. Nandalur KR, Baskurt E, Hagspiel KD, Phillips CD, Kramer CM (2005) Calcified carotid atherosclerotic plaque is associated less with ischemic symptoms than is noncalcified plaque on MDCT. Am J Roentgenol, 184(1):295-298.

204. Larsson M, Kremer F, Claus P, Kuznetsova T, Brodin LA, D'Hooge J (2011) Ultrasound-based radial and longitudinal strain estimation of the carotid artery: a feasibility study. IEEE Trans Ultrason Ferroelectr Freq Control, 58(10):2244-2251.

Section IV

Appendices

Appendix 1: NIH Stroke Scale

NIH STROKE SCALE

Patient Identification. ___ ___-___ ___ ___-___ ___ ___

Pt. Date of Birth ___ ___/___ ___/___ ___

Hospital _____(___ ___-___ ___)

Date of Exam ___ ___/___ ___/___ ___

Interval: [ ] Baseline [ ] 2 hours post treatment [ ] 24 hours post onset of symptoms ±20 minutes [ ] 7-10 days
[ ] 3 months [ ] Other _____(___ ___)

Time: ___ ___:___ ___ [ ]am [ ]pm

Person Administering Scale _____

Administer stroke scale items in the order listed. Record performance in each category after each subscale exam. Do not go back and change scores. Follow directions provided for each exam technique. Scores should reflect what the patient does, not what the clinician thinks the patient can do. The clinician should record answers while administering the exam and work quickly. Except where indicated, the patient should not be coached (i.e., repeated requests to patient to make a special effort).

Instructions	Scale Definition	Score
1a. Level of Consciousness: The investigator must choose a response if a full evaluation is prevented by such obstacles as an endotracheal tube, language barrier, orotracheal trauma/bandages. A 3 is scored only if the patient makes no movement (other than reflexive posturing) in response to noxious stimulation.	0 = **Alert;** keenly responsive. 1 = **Not alert**; but arousable by minor stimulation to obey, answer, or respond. 2 = **Not alert**; requires repeated stimulation to attend, or is obtunded and requires strong or painful stimulation to make movements (not stereotyped). 3 = Responds only with reflex motor or autonomic effects or totally unresponsive, flaccid, and areflexic.	_____
1b. LOC Questions: The patient is asked the month and his/her age. The answer must be correct - there is no partial credit for being close. Aphasic and stuporous patients who do not comprehend the questions will score 2. Patients unable to speak because of endotracheal intubation, orotracheal trauma, severe dysarthria from any cause, language barrier, or any other problem not secondary to aphasia are given a 1. It is important that only the initial answer be graded and that the examiner not "help" the patient with verbal or non-verbal cues.	0 = **Answers** both questions correctly. 1 = **Answers** one question correctly. 2 = **Answers** neither question correctly.	_____
1c. LOC Commands: The patient is asked to open and close the eyes and then to grip and release the non-paretic hand. Substitute another one step command if the hands cannot be used. Credit is given if an unequivocal attempt is made but not completed due to weakness. If the patient does not respond to command, the task should be demonstrated to him or her (pantomime), and the result scored (i.e., follows none, one or two commands). Patients with trauma, amputation, or other physical impediments should be given suitable one-step commands. Only the first attempt is scored.	0 = **Performs** both tasks correctly. 1 = **Performs** one task correctly. 2 = **Performs** neither task correctly.	_____
2. Best Gaze: Only horizontal eye movements will be tested. Voluntary or reflexive (oculocephalic) eye movements will be scored, but caloric testing is not done. If the patient has a conjugate deviation of the eyes that can be overcome by voluntary or reflexive activity, the score will be 1. If a patient has an isolated peripheral nerve paresis (CN III, IV or VI), score a 1. Gaze is testable in all aphasic patients. Patients with ocular trauma, bandages, pre-existing blindness, or other disorder of visual acuity or fields should be tested with reflexive movements, and a choice made by the investigator. Establishing eye contact and then moving about the patient from side to side will occasionally clarify the presence of a partial gaze palsy.	0 = **Normal.** 1 = **Partial gaze palsy;** gaze is abnormal in one or both eyes, but forced deviation or total gaze paresis is not present. 2 = **Forced deviation,** or total gaze paresis not overcome by the oculocephalic maneuver.	_____

NIH STROKE SCALE

Patient Identification. ___ ___-___ ___ ___-___ ___ ___

Pt. Date of Birth ___ ___/___ ___/___ ___

Hospital _____(___ ___-___ ___)

Date of Exam ___ ___/___ ___/___ ___

Interval: [ ] Baseline [ ] 2 hours post treatment [ ] 24 hours post onset of symptoms ±20 minutes [ ] 7-10 days
[ ] 3 months [ ] Other _____(___ ___)

3. Visual: Visual fields (upper and lower quadrants) are tested by confrontation, using finger counting or visual threat, as appropriate. Patients may be encouraged, but if they look at the side of the moving fingers appropriately, this can be scored as normal. If there is unilateral blindness or enucleation, visual fields in the remaining eye are scored. Score 1 only if a clear-cut asymmetry, including quadrantanopia, is found. If patient is blind from any cause, score 3. Double simultaneous stimulation is performed at this point. If there is extinction, patient receives a 1, and the results are used to respond to item 11.	0 = **No visual loss.** 1 = **Partial hemianopia.** 2 = **Complete hemianopia.** 3 = **Bilateral hemianopia** (blind including cortical blindness).	_____
4. Facial Palsy: Ask – or use pantomime to encourage – the patient to showteeth or raise eyebrows and close eyes. Score symmetry of grimace in response to noxious stimuli in the poorly responsive or non-comprehending patient. If facial trauma/bandages, orotracheal tube, tape or other physical barriers obscure the face, these should be removed to the extent possible.	0 = **Normal** symmetrical movements. 1 = **Minor paralysis** (flattened nasolabial fold, asymmetry on smiling). 2 = **Partial paralysis** (total or near-total paralysis of lower face). 3 = **Complete paralysis** of one or both sides (absence of facial movement in the upper and lower face).	_____
5. Motor Arm: The limb is placed in the appropriate position: extend the arms (palms down) 90 degrees (if sitting) or 45 degrees (if supine). Drift is scored if the arm falls before 10 seconds. The aphasic patient is encouraged using urgency in the voice and pantomime, but not noxious stimulation. Each limb is tested in turn, beginning with the non-paretic arm. Only in the case of amputation or joint fusion at the shoulder, the examiner should record the score as untestable (UN), and clearly write the explanation for this choice.	0 = **No drift;** limb holds 90 (or 45) degrees for full 10 seconds. 1 = **Drift;** limb holds 90 (or 45) degrees, but drifts down before full 10 seconds; does not hit bed or other support. 2 = **Some effort against gravity;** limb cannot get to or maintain (if cued) 90 (or 45) degrees, drifts down to bed, but has some effort against gravity. 3 = **No effort against gravity;** limb falls. 4 = **No movement.** UN = **Amputation** or joint fusion, explain: _____ **5a. Left Arm** **5b. Right Arm**	_____ _____
6. Motor Leg: The limb is placed in the appropriate position: hold the leg at 30 degrees (always tested supine). Drift is scored if the leg falls before 5 seconds. The aphasic patient is encouraged using urgency in the voice and pantomime, but not noxious stimulation. Each limb is tested in turn, beginning with the non-paretic leg. Only in the case of amputation or joint fusion at the hip, the examiner should record the score as untestable (UN), and clearly write the explanation for this choice.	0 = **No drift;** leg holds 30-degree position for full 5 seconds. 1 = **Drift;** leg falls by the end of the 5-second period but does not hit bed. 2 = **Some effort against gravity;** leg falls to bed by 5 seconds, but has some effort against gravity. 3 = **No effort against gravity;** leg falls to bed immediately. 4 = **No movement.** UN = **Amputation** or joint fusion, explain: _____ **6a. Left Leg** **6b. Right Leg**	_____

NIH STROKE SCALE

Patient Identification. ___ ___-___ ___ ___-___ ___ ___

Pt. Date of Birth ___ ___/___ ___/___ ___

Hospital _____(___ ___-___ ___)

Date of Exam ___ ___/___ ___/___ ___

Interval: [ ] Baseline [ ] 2 hours post treatment [ ] 24 hours post onset of symptoms ±20 minutes [ ] 7-10 days [ ] 3 months [ ] Other _____(___ ___)

7. Limb Ataxia: This item is aimed at finding evidence of a unilateral cerebellar lesion. Test with eyes open. In case of visual defect, ensure testing is done in intact visual field. The finger-nose-finger and heel-shin tests are performed on both sides, and ataxia is scored only if present out of proportion to weakness. Ataxia is absent in the patient who cannot understand or is paralyzed. Only in the case of amputation or joint fusion, the examiner should record the score as untestable (UN), and clearly write the explanation for this choice. In case of blindness, test by having the patient touch nose from extended arm position.	0 = **Absent.** 1 = **Present in one limb.** 2 = **Present in two limbs.** UN = **Amputation** or joint fusion, explain: _____	_____
8. Sensory: Sensation or grimace to pinprick when tested, or withdrawal from noxious stimulus in the obtunded or aphasic patient. Only sensory loss attributed to stroke is scored as abnormal and the examiner should test as many body areas (arms [not hands], legs, trunk, face) as needed to accurately check for hemisensory loss. A score of 2, "severe or total sensory loss," should only be given when a severe or total loss of sensation can be clearly demonstrated. Stuporous and aphasic patients will, therefore, probably score 1 or 0. The patient with brainstem stroke who has bilateral loss of sensation is scored 2. If the patient does not respond and is quadriplegic, score 2. Patients in a coma (item 1a=3) are automatically given a 2 on this item.	0 = **Normal;** no sensory loss. 1 = **Mild-to-moderate sensory loss;** patient feels pinprick is less sharp or is dull on the affected side; or there is a loss of superficial pain with pinprick, but patient is aware of being touched. 2 = **Severe to total sensory loss;** patient is not aware of being touched in the face, arm, and leg.	_____
9. Best Language: A great deal of information about comprehension will be obtained during the preceding sections of the examination. For this scale item, the patient is asked to describe what is happening in the attached picture, to name the items on the attached naming sheet and to read from the attached list of sentences. Comprehension is judged from responses here, as well as to all of the commands in the preceding general neurological exam. If visual loss interferes with the tests, ask the patient to identify objects placed in the hand, repeat, and produce speech. The intubated patient should be asked to write. The patient in a coma (item 1a=3) will automatically score 3 on this item. The examiner must choose a score for the patient with stupor or limited cooperation, but a score of 3 should be used only if the patient is mute and follows no one-step commands.	0 = **No aphasia;** normal. 1 = **Mild-to-moderate aphasia;** some obvious loss of fluency or facility of comprehension, without significant limitation on ideas expressed or form of expression. Reduction of speech and/or comprehension, however, makes conversation about provided materials difficult or impossible. For example, in conversation about provided materials, examiner can identify picture or naming card content from patient's response. 2 = **Severe aphasia;** all communication is through fragmentary expression; great need for inference, questioning, and guessing by the listener. Range of information that can be exchanged is limited; listener carries burden of communication. Examiner cannot identify materials provided from patient response. 3 = **Mute, global aphasia;** no usable speech or auditory comprehension.	_____
10. Dysarthria: If patient is thought to be normal, an adequate sample of speech must be obtained by asking patient to read or repeat words from the attached list. If the patient has severe aphasia, the clarity of articulation of spontaneous speech can be rated. Only if the patient is intubated or has other physical barriers to producing speech, the examiner should record the score as untestable (UN), and clearly write an explanation for this choice. Do not tell the patient why he or she is being tested.	0 = **Normal.** 1 = **Mild-to-moderate dysarthria;** patient slurs at least some words and, at worst, can be understood with some difficulty. 2 = **Severe dysarthria;** patient's speech is so slurred as to be unintelligible in the absence of or out of proportion to any dysphasia, or is mute/anarthric. UN = **Intubated** or other physical barrier, explain: _____	_____

NIH STROKE SCALE

Patient Identification. ___ ___-___ ___ ___-___ ___ ___

Pt. Date of Birth ___ ___/___ ___/___ ___

Hospital _____(___ ___-___ ___)

Date of Exam ___ ___/___ ___/___ ___

Interval: [ ] Baseline [ ] 2 hours post treatment [ ] 24 hours post onset of symptoms ±20 minutes [ ] 7-10 days
[ ] 3 months [ ] Other _____(___ ___)

11. Extinction and Inattention (formerly Neglect): Sufficient information to identify neglect may be obtained during the prior testing. If the patient has a severe visual loss preventing visual double simultaneous stimulation, and the cutaneous stimuli are normal, the score is normal. If the patient has aphasia but does appear to attend to both sides, the score is normal. The presence of visual spatial neglect or anosagnosia may also be taken as evidence of abnormality. Since the abnormality is scored only if present, the item is never untestable.	0 = **No abnormality.** 1 = **Visual, tactile, auditory, spatial, or personal inattention** or extinction to bilateral simultaneous stimulation in one ofthe sensory modalities. 2 = **Profound herni-inattention or extinction to more than one modality;** does not recognize own hand or orients to only one side of space.	_____

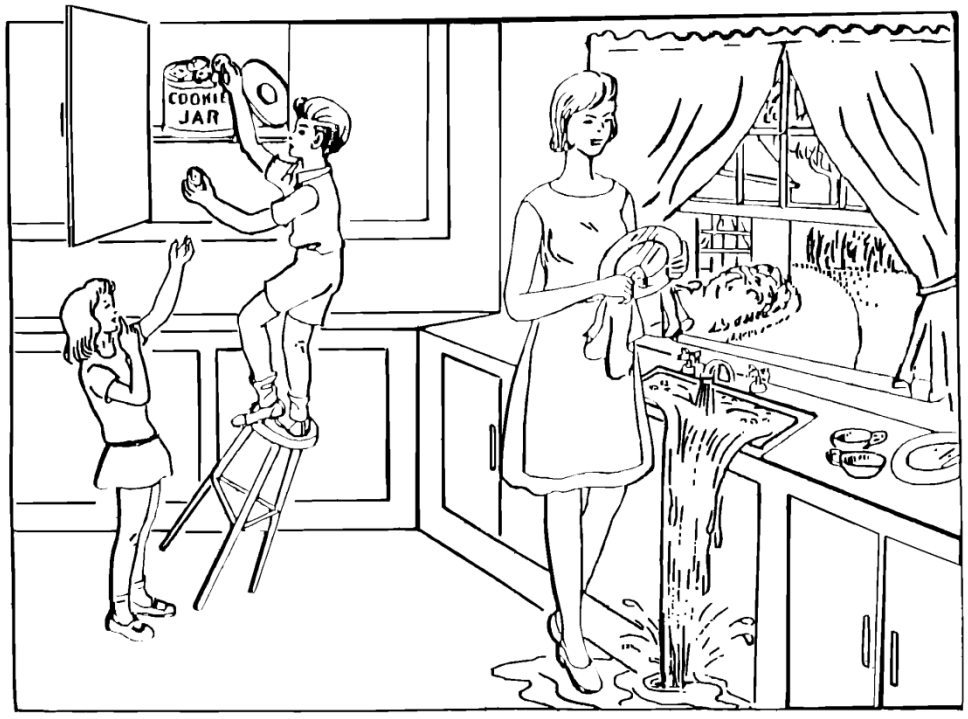

_____

_____

You know how.

Down to earth.

I got home from work.

Near the table in the dining room.

They heard him speak on the radio last night.

MAMA

TIP – TOP

FIFTY – FIFTY

THANKS

HUCKLEBERRY

BASEBALL PLAYER

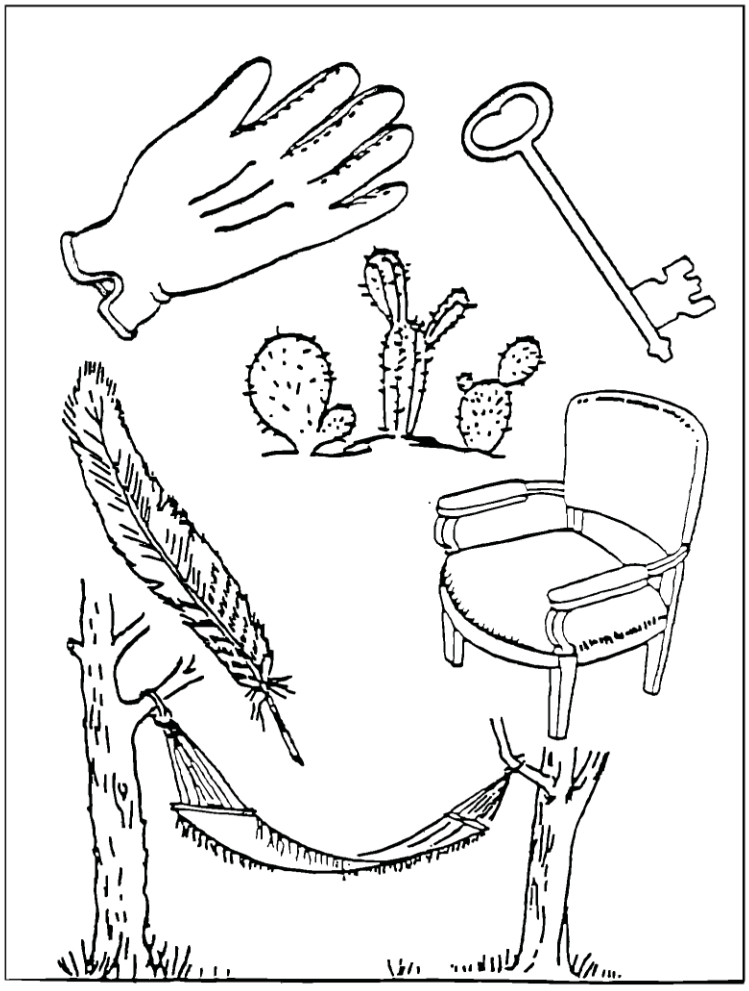

Appendix 2: Modified Rankin Scale

Modified RANKIN scale:

0 ☐ Asymptomatic
1 ☐ Non-disabling symptoms which do not interfere with lifestyle.
2 ☐ Minor disability-symptoms which lead to some restriction in lifestyle but do not interfere with the patients capacity to look after themselves.
3 ☐ Moderate disability-symptoms which significantly interfere with lifestyle or prevent totally independent existence, but able to walk without assistance.
4 ☐ Moderately severe disability-symptoms which clearly prevent independent existence. Unable to walk without assistance but does not need constant attention day and night.
5 ☐ Severely disabled-totally dependent requiring constant attention day and night.

Is any disability rated above caused by medical condition/s other than stroke

Yes ☐ No ☐

If yes, give details _____

French translation of Modified RANKIN scale:

0 ☐ Asymptomatique
1 ☐ Symptômes non-invalidantes qui n'interfèrent pas avec le style de vie du patient
2 ☐ Symptômes invalidantes mineurs qui limitent le patient mais n'interfèrent pas dans la capacité du patient de s'occuper de lui-même
3 ☐ Symptômes invalidantes modérés qui limitent significativement le style de vie du patient ou qui empêchent une indépendance totale mais le patient est capable de marcher sans aide.
4 ☐ Symptômes invalidantes modérément sévères qui empêchent l'indépendance totale même si le patient n'a pas besoin d'une attention continue jour et nuit. Le patient est incapable de marcher sans aide.
5 ☐ Handicap sévère - dépendance continue jour et nuit.
6 ☐ Décès

Est-ce que l'échelle d'évaluation est due à une condition autre que l'AVC?
Oui ☐ Non ☐
Si oui, préciser _____

Appendix 3: Follow-up Questionnaires and Forms

ÉLASTOGRAPHIE VASCULAIRE NON-INTRUSIVE : ÉTUDE D'EFFICACITÉ ET ANALYSE PRÉLIMINAIRE DE LA VULNÉRABILITÉ DE LA PLAQUE CAROTIDIENNE (NIVE II)

QUESTIONNAIRE ET FORMULAIRE STANDARDISÉ DE SUIVI AUX **PATIENTS ASYMPTOMATIQUES (i.e. CLINIQUEMENT NON-VULNÉRABLES)** CHAQUE 6 MOIS APRES L'ÉLASTOGRAPHIE ULTRASONORE

Instructions (à faire à chaque 6 mois):
Étape 1 : Compléter le tableau A de la fiche d'identification du patient classifié initialement « non-vulnérable » (voir annexe)
Étape 2 : Étudier le dossier hospitalier du patient pour compléter le formulaire/questionnaire ci-dessous
Étape 3 : Entrevue téléphonique avec le patient pour compléter ce même questionnaire
Étape 4 : Compléter le tableau B de suivi de la fiche d'identification du patient initialement « non-vulnérable » (voir annexe)
Étape 5 : Entrée de données à partir des tableaux A et B

DÉBUT DU FORMULAIRE ET QUESTIONNAIRE :

Date de l'examen du dossier : _____

Date de l'entrevue avec le patient : _____

1. Avez-vous eu une endartérectomie carotidienne? OUI [ ] NON [ ]
   - Si NON, pourquoi?
     i. [ ] Annulée car _____
     _____
     _____
     ii. [ ] Prévue pour le_____
     _____
     _____
     iii. [ ] Pas d'indication_____
     _____
     _____

2. Selon la réponse en 2., demander l'une ou l'autre de ces questions :
   a. « Avez-vous eu un ACV ou une ICT **entre l'échographie** (nommer la date de l'élasto) **et votre chirurgie?** » OUI [ ] NON [ ]

   ou

   b. « Avez-vous eu un ACV ou une ICT **après l'échographie** (nommer la date de l'élasto)?» OUI [ ] NON [ ]

   - Si NON, passer à la question 5.
   - Si OUI, passer à la question 4.
3. Avez-vous consulté dans un hôpital pour cet(s) événement(s)? OUI [ ] NON [ ]
   - Si NON, passer à la question 5.
   - Si OUI, répondre aux questions suivantes :
     a) Combien d'événements?_____
     b) Quelle(s) date(s)?_____
     c) Dans quel(s) hôpital(aux)?_____
     d) Le diagnostic exact? (ACV ou ICT ou thrombose asymptomatique ou ACV asymptomatique de novo selon imagerie)
     e) Examens Radiologiques :

EXAMEN	DATE	DIAGNOSTIC
ECHO/DOPPLER cou		
ANGIOGRAPHIE		
CT-ANGIO		
MR-ANGIO (pas celui de l'étude)		
CT CERVEAU		
IRM CERVEAU		
Échographie cardiaque		

     f) La cause de l'événement (encercler):
        - [ ] Embolie d'origine cardiaque (FA, valvulopathie, insuff ♥, …)
        - [ ] Thrombo-embolie (carotide interne, siphon carotidien, artères vertébrales, tronc basilaire, origine de l'a. sylvienne (=MCA))
        - [ ] Thrombose localisée à la carotide (non-embolique)
        - [ ] Infarctus lacunaire (diagnostic d'exclusion)

- [ ] Autre (dissection, inflammatoire, infectieux, post-radiothérapie, hématologique, néo solide, hypercoagulabilité, iatrogénique médicamenteux, vasospastique sur drogue, métabolique,…)

  _____

  _____

- [ ] Inconnue (vérifier les facteurs de risque suivants)

HTA [ ]	Tabac [ ]	Hypercholestérolémie [ ]	Diabète [ ]
ROH [ ] (>3 verres/jour)	Migraine [ ]	Contraception orale [ ]	Obésité/sédentarité [ ]

g) les symptômes précis? (cocher dans le tableau suivant) (symptômes **<u>doivent</u>** être : **apparition soudaine+déficit focalisé+rapidement maximal+durée au moins 1 minute ± amélioration progressive**)
   - En gris : symptômes non reliés à l'artère carotidienne interne
   - Noter côté (gauche ou droit) <u>du symptôme</u>, pas de la localisation
   - Noter côté gauche ou droit lorsqu'applicable, sinon préciser autre localisation ou information si cela peut aider au diagnostic eg. Convulsion généralisée vs. focale

Symptôme/déficit (encercler le symptôme)	**Gauche** [√]	**Droite** [√]	**Durée** (minutes)	**Évolution** (permanent ou temporaire)
Convulsion (cause peut être ischémie aigue ou chronique cérébrale, hémorragie cérébrale)				
Changement soudain de l'état mental ➢ Confusion, delirium ➢ Stupeur ou coma o (causé par infarctus de l'hémisphère ou infarctus du tronc cérébral ou hémorragie cérébrale)				
Hémiparésie/faiblesse soudaine ➢ Faciale ➢ Dysphagie ➢ Membre supérieur ➢ Membre inférieur ➢ dérobement des jambes				
Perte hémisensorielle soudaine ➢ Ouïe				

➢ Visuelle « voile noir » (probablement hémianopie) ➢ Visuelle monoculaire (amaurose fugace) ➢ Diplopie soudaine ➢ Membre supérieur ➢ Membre inferieur Paresthésies (douleurs en chocs, fourmillements au niveau du corps)				
Aphasie soudaine ➢ Incohérence verbale ➢ Incapable de vocaliser ➢ Difficulté de compréhension				
Dysarthrie ("slurred speech" i.e. difficulté d'articulation)				
Ataxie (maladresse (=clumsiness), difficulté de coordination, de marche, de contrôle des mouvements) ➢ Du tronc ➢ Des membres				
Vertige, trouble de l'équilibre, céphalée postérieure ➢ Lipothymie/tête légère, tinnitus (ACV peu probable) ➢ Associé à dysarthrie, diplopie, ataxie (ACV du tronc)				
Syndrome de Gertsmann (acalculie, agraphie, agnosie doigts et perte discrimination gauche/droite)				
Syndrome d'Anton-Babinski (« Contralateral Neglect Syndrome ») : négligence du trouble, de l'hémicorps, de l'hémichamp visuel (néglige souvent le côté gauche)				
Céphalée sévère, dlr nuque, perte de conscience, vomissement (ces symptômes suggèrent hémorragie intracérébrale)				
Autres symptômes pertinents				

h) <u>En résumé :</u>

(cochez et indiquer le **territoire + côté du territoire G ou D,** p.ex. : ACV Sylvien gauche causé par embolie cardiaque selon dossier hospitalier):

- [ ] **Selon le dossier HND**, le nouveau territoire intracrânien ischémique est :

  _____
  _____
  _____
  Et la cause est :
  _____
  _____

- [ ] **Le patient connaît** le nouveau territoire intracrânien ischémique, c'est :

  _____
  _____
  _____
  Et la cause est :
  _____
  _____

- [ ] **Selon les symptômes du tableau g) rapportés par le patient**, le médecin complétant ce questionnaire peut présumer que le nouveau territoire intracrânien ischémique est :

  _____
  _____
  _____
  Et la cause est :
  _____
  _____
  _____

4. « Auriez-vous eu des symptômes parmi les suivants depuis votre échographie avec nous le (nommer la date de l'élasto)? » (symptômes **doivent** être : **apparition soudaine+déficit focalisé+rapidement maximal+durée au moins 1 minute ± amélioration progressive**)
   - Veuillez passer au tableau de la question 4.g) (compléter si il y a lieu)

     a) **Si vous avez eu des symptômes**, combien de fois sont-ils survenus depuis l'échographie? _____
        - Quelle(s) date(s)?

          _____
          _____

        - **Selon les symptômes du tableau g) rapportés par le patient**, le médecin complétant ce questionnaire peut présumer que le nouveau territoire intracrânien

ischémique est :
_____
_____
_____
Et la cause est :
_____
_____
_____

b) **Si le patient n'a eu aucun des symptômes** ci-haut, donc le patient est toujours asymptomatique et dans le groupe clinique « non-vulnérable », procéder comme ceci:

- **Patient n'est pas prévu pour une endartérectomie :**
  Répéter ce questionnaire dans 6 mois

- **Patient a eu l'endartérectomie pour la carotide étudiée :**
  Passer à la question 5 et cesser le suivi pour l'artère carotidienne opérée après la fin du questionnaire

- **Patient attend une endartérectomie :**
  Répéter ce questionnaire peu après la chirurgie si prévue à une certaine date ou dans 6 mois (prendre la date la plus proche)

5. Avez-vous eu une complication **durant et immédiatement après** votre endartérectomie carotidienne?
   - OUI [ ] NON [ ]
   - Si OUI, nommer les complications avec dates:
     _____
     _____
     _____
     _____
   - Date de l'endartérectomie _____
   - Quelle carotide opérée (D ou G)? _____
   - Avez-vous eu ACV ou ICT comme complication immédiate de la chirurgie? OUI [ ] NON [ ]
     i. Si OUI, quelle date? _____
     ii. Quel territoire ischémique intracrânien (D ou G)?
     _____
     _____
     _____

FICHE D'IDENTIFICATION DU PATIENT INITIALEMENT CLASSÉ CLINIQUEMENT NON-VULNÉRABLE

TABLEAUX A ET B

Tableau A : Informations au moment de l'inclusion (jour d'élasto ou IRM) du patient initialement non-vulnérable		
CAROTIDE étudiée par NIVE	**GAUCHE [ ]**	**DROITE [ ]**
CAROTIDE étudiée par IRM	**GAUCHE [ ]**	**DROITE [ ]**
ÉTUDE dans lesquelles éligible (NIVE I, II, et/ou BRACCO ou exclu) **Si une carotide exclue, indiquer raison et barrer la colonne**		
Groupe d'âge (entourer)	**40-49** **50-59** **60-69** **70-85**	**40-49** **50-59** **60-69** **70-85**
% sténose (indiquer par quel examen)		
Date d'acquisition élastographie (si patient uniquement dans BRACCO, date de l'IRM)		

Tableau B : Informations du suivi du patient initialement non-vulnérable					
Date d'obtention de l'information: _____					
√	**Événement**	**Date(s)**	**Territoire cerveau affecté**	**Cause : carotide gauche ou droite ou autre cause**	
	ACV ou ICT symptomatique				
		Date de l'examen diagnostic	**Territoire cerveau affecté**	**IRM ou CT**	**Cause**
	ACV ou ICT silencieux				
		Date de l'examen diagnostic	**Carotide gauche ou droite?**	**CTA, MRA ou Echo-Doppler**	
	Thrombose carotidienne asymptomatique				
		Date de procédure	**Carotide gauche ou droite?**	**ACV ou ICT immédiat?**	
	Endartérectomie (ou stent)				
Conclusion : [ ] Patient cliniquement non-vulnérable			**[ ] Patient cliniquement vulnérable**		
Suivi : [ ] n'est plus nécessaire			**[ ] À prévoir le _____**		